UNIVERSITÀ DEGLI STUDI DI MESSINA

DOTTORATO DI RICERCA

Ingegneria e Chimica dei Materiali e delle Costruzioni

Ciclo XXXI

Settore Scientifico Disciplinare, SSD: CHIM/07

Sustainable conversion of biomass derived cellulose by using heterogeneous palladium based catalysts

Dottoranda:
Bianca Gumina

Relatore:
Chiar.mo Prof. Signorino Galvagno

Correlatori:
Dr. Claudia Espro
Dr. Francesco Mauriello

Anno Accademico 2017/2018

A Rosetta e Olga

Prega come se tutto dipendesse da Dio e
lavora come se tutto dipendesse da te.
S. Ignazio da Loyola

Index

Abstract

4. STUDY OF MODEL MOLECULES: HYDROGENOLYSIS OF POLYOLS

5. CONVERSION OF CELLULOSE

6. CONVERSION OF CELLULOSE USING *H*-DONOR MOLECULES

7. FINAL CONCLUSION 137

OTHER ACTIVITIES

Abstract

This doctoral work is focused on the sustainable valorization of cellulose and its derivable molecules, through the application of the hydrogenolysis technology, by using heterogeneous Pd-based catalysts, in order to achieve products with high-added values, such as chemicals and fuels. In particular, the study of hydrogenolysis has been conceived with a bottom-up approach starting from polyols, namely sorbitol (C_6) and shorter polyols (C_5-C_2), to approach finally the cellulose, with the aim to unravel the reactivity and selectivity, and to understand the mechanism of reactions involved.

This study is mainly devoted toward the investigation of the bimetallic co-precipitated Pd/Fe_3O_4 catalyst, therefore its textural and structural characteristics have been deeply elucidated through several characterization techniques (XRD, TEM, H_2-TPR, XPS and EXAFS), in order to highlight the key factors that determine its unique catalytic performances observed. A comparison of the performance of the bimetallic Pd/Fe_3O_4 catalyst and that of the commercial Pd/C was also performed. The importance of the mechanical pretreatment of cellulose (e.g. ball milling) and the role of water in its hydrogenolysis were also assessed.

The last part of this doctoral study was dedicated to the investigation of hydrogen donor (H-donor) molecules, such as limonene and 2-propanol, studying the conversion of cellulose, by using the bimetallic Pd/Fe_3O_4 catalyst. These reactions were performed in presence and in absence of water, in order to understand its role.

Chapter 1

INTRODUCTION

1.1. Sustainable production of chemicals from lignocellulosic biomass

The increasing interest in producing fuels and chemicals from biomasses is mainly derived from the rapid growth of the worldwide energy demand. Furthermore, two oil crises within the 20th century, the gradual depletion of oil and gas resources, combined with an increased demand for energy and the global warming are forcing the scientific community to investigate new, sustainable, cost efficient and renewable substitutes to fossil fuels.

To replace effectively fossil-derived fuels and chemicals, the resources must be renewable, of sufficient abundance and not in competition with agricultural land and food production. For all these reasons, the most promising sustainable source of organic carbon is the biomass from plants, since it is abundant, inexpensive, renewable, and CO_2-neutral feedstock. The definition of biomass consists in the biodegradable fraction of products, wastes and residues from biological origin, from agriculture (including vegetal and animal substances), from forestry, as well as the biodegradable fraction of industrial and municipal waste [1]. Moreover, biomass has the big advantage to be available all over the world (not being located in specific geographical territories, like fossil fuels), representing a strategic point not only to achieve a safe energy supply, but also to promote local economies. The valorization of renewable materials represent an effective way to limit excessive carbon dioxide release in the Earth atmosphere. Many potential

building blocks and fine chemistry intermediates can be produced by biomass conversion.

In particular, nowadays, the worldwide attention is focusing on the use of lignocellulosic biomasses (also known as biomass of 2nd generation), exclusively derived from residues or waste, inedible raw materials and collected from non-cultivable lands. Indeed, the lignocellulosic biomass is readily available from various waste streams, including agriculture, forestry and paper industry and is produced in large quantities ($170-200 \times 10^9$ t/year) worldwide [2]. Therefore, lignocellulosic biomasses play a particularly crucial role being ethically sustainable and not in competition with edible biomasses. For these precious reasons, at present, strong efforts are focused on the development of successful lignocelluloses-based technologies for the production of biofuels and bio-chemicals.

Lignocellulosics have a complex "chemical-architecture" [3] and are mainly composed of cellulose, hemicellulose and lignin (Figure 1.1).
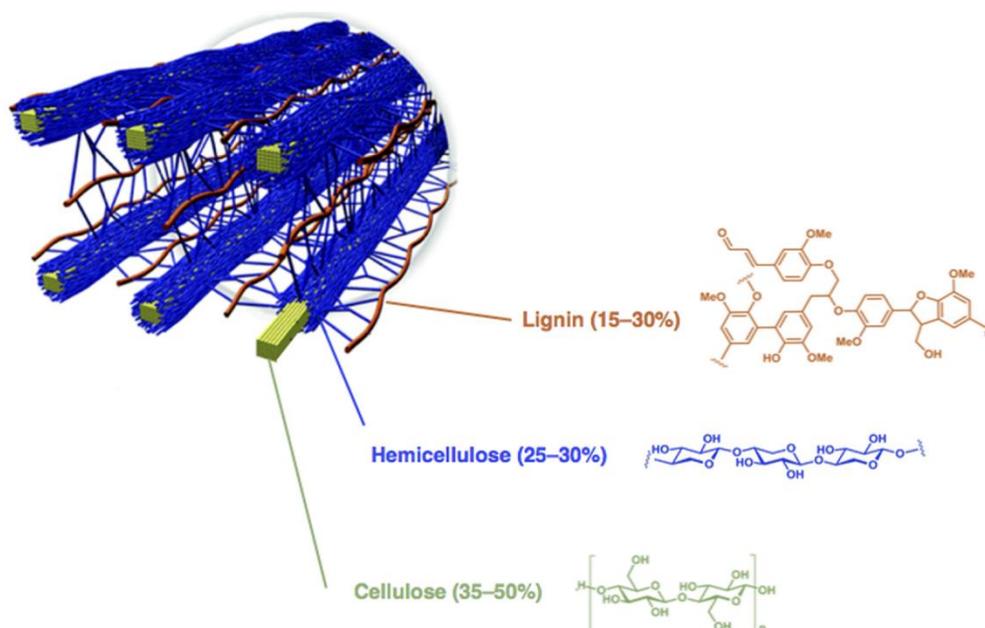
Figure 1.1 Chemical structure of lignocellulosic material and its constituents: cellulose, hemicellulose, lignin [4].

The three main constituents of lignocellulosics can be transformed into biomass-derived platform chemicals with varying compositions and

functionalities. A variety of chemical routes and industrial processes have been explored to valorize lignocellulosic biomasses [5-15]. Monosaccharides and phenolic compounds are obtained from a low-cost biogenic feedstock, even though their fractionation, depolymerization and chemical upgrading can be rather complex and cost-intensive [16]. A non-exhaustive representation of the most important lignocellulosic-derivable molecules for chemical industry are reported in Figure 1.2.
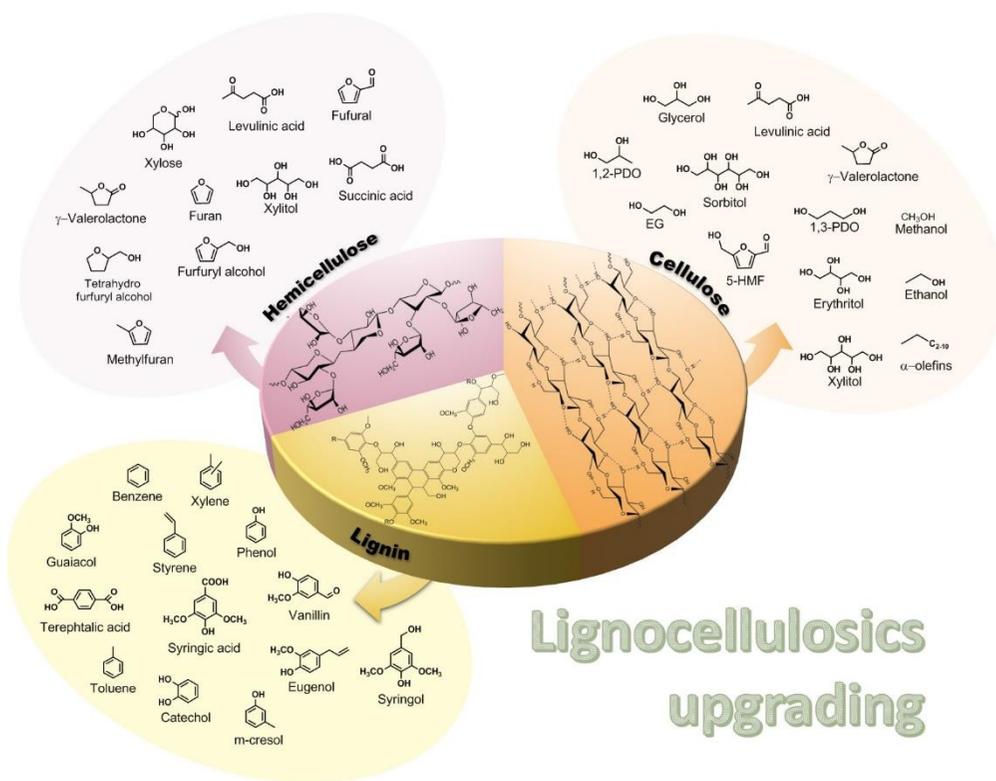
Figure 1.2 Chemical structure of cellulose, hemicellulose, lignin, and related derivable molecules [17].

Cellulose, the largest single component of lignocellulosic biomasses, is a polymer characterized by glucosidic units, with an average molecular weight of around 100,000 [3]. The glucose units are bonded through β-glycosidic linkages at the positions 1 and 4. The β-1,4- glycosidic linkages leads to side-by-side disposition of the pyranose rings in long chains, forming an intense intramolecular hydrogen bonding between the groups nearby the glycosidic

bond; this feature maintains the structure of cellulose as a "planar sheet", which can be packed as well through hydrogen bonds and a large number of Van der Waals weak interactions (Figure 1.3). In this arrangement, most chemical functions of cellulose are not accessible to enzymes, chemicals and solvents [18-20]. Cellulose is not digestible by humans, making its utilization in the chemical manufacture irrelevant for the human food supply. Therefore, the conversion of cellulose into added-value chemicals and/or fuel components is one of the core technologies in the modern bio-refinery [21-24]. The first step for cellulose valorization is based on its depolymerisation into oligomers and glucose followed by several type of catalytic reactions (hydrogenation, oxidations, esterification, etc.) for the manufacture of a pool of chemicals such as C_6–C_2 polyols, levulinic acid, hydroxymethylfurfural (HMF), among others ([21-25] and "references within"). Polyols, with their peculiar chemical properties, represent an important resource for production of several building-block chemicals. Indeed, sorbitol (C_6 polyol), xylitol (C_5 polyol) and glycerol (C_3 polyol) are included in the list of 12 potential biomass-derived platform chemicals [26]. Moreover, among the family of biomass derived polyols, glycerol (C_3 polyol) has become a primary building block being the main by-product in the biodiesel production [27-34].
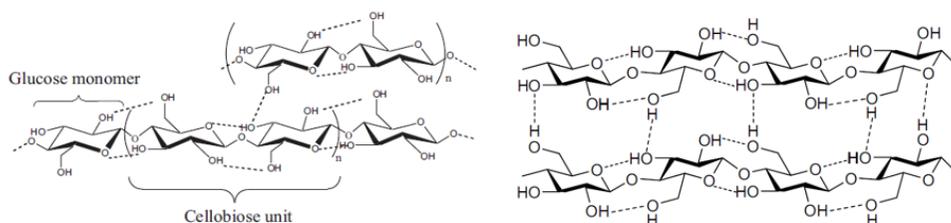
Figure 1.3 Chemical structure of cellulose.

Hemicellulose, unlike cellulose, has a heterogeneous chemical structure of pentoses, hexoses and sugar acids. Hardwood hemicelluloses is chiefly composed by xylans whereas softwood hemicellulose mainly consists of glucomannans (Figure 1.4) [35-36]. Hemicellulose can be easily hydrolyzed into its sugar constituents by chemical or enzymatic processes [37-39]. The chemical hydrolysis of hemicelluloses into xylose and arabinose is generally afforded in high yields and low costs. Xylose, in particular, is largely used in modern biorefineries to produce furfural (2-furaldehyde) through several homogeneous and heterogeneous catalytic processes [40]. Furfural, with a

4

world production of about 200,000 tonnes per year, is the key precursor of important building blocks such as furfuryl alcohol, 2-methylfuran, 2-methyltetrahydrofuran and levulinic acid [41–43].
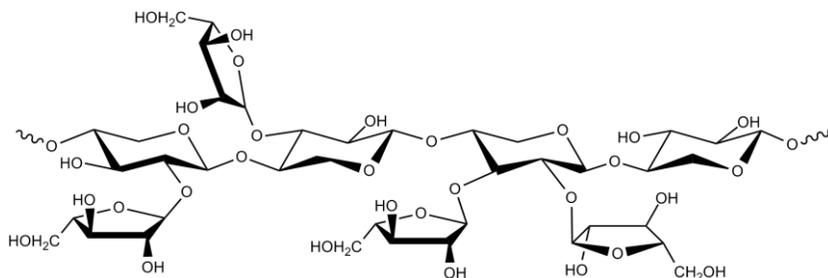
Figure 1.4 Chemical structure of hemicellulose.

Lignin is unique among other biomass components, being characterized by an aromatic sub-structure with a large amount of etheric C–O bonds (Figure 1.5) [3]. The native constituents of lignin are therefore of particular interest for a lignocellulosic biorefinery aimed to the sustainable production of green aromatic compounds. At present, industrial processes are limited to vanillin and "kraft lignin" (about 60 kt/year) manufacture but, the research on the sustainable production of chemicals from lignin has developed rapidly in the last years [44–48]. To this regard, one of the major challenges is the low cost-effective catalytic depolymerization of lignin preserving its aromatic nature [49–61].
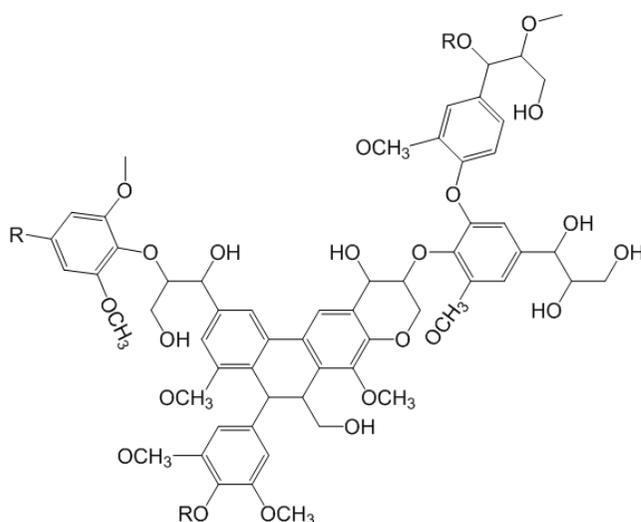
Figure 1.5 Chemical structure of lignin.

1.2. Deoxygenative technologies: Hydrogenolysis, CTH and APR

Biomass-derived polyols are characterized by a higher O/C ratio with respect to fossil-derived feedstocks, because, in their structure, every carbon atom is linked to a hydroxyl group. Therefore, deoxygenative technologies could face the need of the effective reduction of the oxygen content allowing the production of new high added value chemicals ready to be integrated into the modern market chain [62,63].

Hydrogenolysis processes, among several technologies, have gained a lot of attention since these allow the breaking of carbon-carbon and/or carbon-oxygen bonds in the presence of a hydrogen source [63–65]. One of the main drawbacks in hydrogenolysis, also known as "hydrodeoxygenation" if referred to the C–O bond breaking, is concerning the hydrogen management due to the poor solubility of molecular H_2 that leads to a considerable safety hazard. Moreover, hydrogen supply and related purchase, transport and storage costs need to be considered.

Alternatively to classic hydrogenolysis/hydrodeoxygenation processes, which generally require high pressure of molecular hydrogen, catalytic transfer hydrogenolysis (CTH) reactions by means of simple alcohols (2-propanol, methanol and ethanol) and other hydrogen donor (H-donor) molecules (hydrazine, tetralin, formic acid, cyclohexene, etc.) have been generally proposed as an efficient alternative to the direct use of H_2 in the course of the last decade [66-69]. Since their introduction in 1903 when Knoevenagel revealed the disproportionation of dimethyl-1,4-dihydroterephthalate promoted by palladium black catalysts [70], CTH reactions are getting increasing attention improving the sustainability and economics of hydrogenation reactions in modern green chemistry since: (i) they do not require hazardous pressurized molecular hydrogen; (ii) the hydrogen donors are generally readily available, inexpensive, obtainable from renewable resources and easy to handle and (iii) they generally produce valuable by-products (i.e. oxidized alcohol products). Moreover, CTH has been successfully adopted in reducing the oxygen content in biomass-derived feedstocks [69].

Another efficient route to obtain the hydrogen necessary for the cleavage of C–C and C–O bonds stems also directly from biomass-derived molecules and by the aqueous phase reforming (APR) process [71-82]. The APR process presents many advantages than conventional steam reforming reactions

because it occurs, under mild conditions, in liquid phase and in a single reactor. The APR process converts starting substrates into hydrogen, through the breaking of C–C, C–H and O–H bonds and the subsequent water gas shift (WGS) reaction. In order to maximize the hydrogen production, a good APR catalyst needs to show significant activity in the C–C bond breaking and in the WGS reaction, but poor activity towards the C–O bond cleavage and methanation reaction.

1.3. Valorization of cellulose and polyols through hydrogenolytic technologies

1.3.1 Hydrogenolysis

The hydrogenolysis process consists in the reductive breaking of C-C and C-O bonds (in the case of cellulosic compounds) by means of hydrogen. This technology offers a promising potential to overcome the available technologies and to reach the need of the future refinery concept.

The hydrogenolysis of cellulose was reported for the first time in 1925, when a dry distillation of cellulosic materials both in presence and in absence of a metal catalyst, at high temperatures and hydrogen pressures was performed [83]. In absence of catalyst a relevant formation of charcoal was observed, instead, in presence of a Ni-based catalyst, a distillate (composed of organic acids, ketones, alcohols, phenols and furans) yield higher than 80% was obtained.

An increasing research followed, with the aim to improve the yield in hydrocarbons, in milder operating conditions, using a different feedstock, and a great attention was paid on the composition of the catalyst. Several works were focused on the conversion of municipal wastes, sewage sludge and newspapers. In some cases also continuous pilot plants were developed [84-86]. In 1983 Johnson Matthey patented a production of fuel oil starting from municipal and agricultural wastes, using ruthenium and copper based catalysts [87].

Since the beginning, studies on the hydrogenolysis of biomass-based materials demonstrated the relevant potential to obtain fuels and chemicals starting from renewable sources. Already in 1944 Berl highlighted the

fundamental importance to develop a method to synthesize fuels from biomass [88]. In our days, the need of catalytic processes for biomass conversion is renewed and it is becoming urgent.

Beyond the conversion of the biomass in liquid fuels, it is also fundamental the hydrogenation of cellulose applied to the production of polyols (e.g. sorbitol, xylitol, erythritol, glycerol, 1,2-propanediol and ethylene glycol). For example, 1,2-propanediol and ethylene glycol are traditional products on large scale obtained from petrochemical industry. Also in these cases, the early applications, usually based on copper or nickel catalysts, showed the potential of cellulose for the production of short chain polyols [89,90].

In order to utilize efficiently the cellulose, it is necessary to perform effectively the hydrolysis, which is the first step to breakdown its polymeric structure in order to obtain monomeric products (e.g. glucose, sorbitol). Indeed the thermally and chemically stable structure of the cellulose is hard to be deconstructed. However, the hydrolysis is typically favored by the addition of acid substances or by the water *auto*-protolysis, promoted at high reaction temperatures [91,92].

Efficient catalysts for the hydrogenolysis of cellulose, should be able to promote both the initial hydrolysis into monomeric glucose and the following cascade reactions that lead to short chain polyols, being able to suppress the formation of side products, such as humins. So far, the catalysts studied most extensively for the hydrogenolysis of the cellulose, were nickel- and copper-based catalysts, nonetheless a great variety of other catalysts have been tested. However, the attention was mainly focused on the first reported catalysts because they are well known metals and able to catalyze the hydrogenation of glucose to sorbitol and the hydrogenolysis of glycerol [65,93].

The conversion of cellulose into hexitols may take place through two different mechanisms: the Eley-Rideal, where the hydrogenation of the carbonyl (*un*-adsorbed) occurs by the interaction with a metal-hydride surface, or the Langmuir-Hinshelwood, in which the carbonyl adsorbed on a vacant site interacts with a metal-hydride surface [65]. Typically, at temperatures higher than 200°C the hydrogenolysis reaction leads to formation of gaseous products and short chain polyols, indicating a great involvement of C-C bond cleavages. Short- chain polyols are commonly

obtained through decarbonylation, retro-aldol, retro-Michael and retro-Claisen reactions. Whereas, the C-O bond cleavage is commonly considered to proceed through dehydration followed by keto-enol tautomerization and hydrogenation, leading to dehydroxylation products.

Catalysts based on noble metals, exhibiting significant activity and high selectivity, are efficient towards the promotion of hydrogenation reactions and, for this reason, have been extensively investigated.

Fukuoka and co-workers investigated the conversion of cellulose in presence of platinum-based catalysts supported on several silico-alluminated oxides, such as γ-Al_2O_3, SiO_2-Al_2O_3 and HUSY zeolite, compared to Ru supported on HUSY. After 24 h of reaction at 190°C, with an initial pressure of 50bar of hydrogen. A 30% yield of sorbitol was obtained over all catalytic systems [94,95].

The hydrogenolysis of cellulose into polyols promoted by the Ru/C catalyst and reversibly formed acids, was reported by Luo et al. [96]. At 245°C, using an initial pressure of 60 bar of hydrogen, within 30 min of reaction, the cellulose was completely converted and a 40% yield of hexitols was reached, even though consistent side reactions occur, leading to a broad distribution of products, such as sorbitan, xylitol, erythritol, glycerol, ethylene glycol, methanol and methane. Furthermore, the formation of humins contributes to an overall low carbon efficiency of the process. The authors performed the reaction also in different solvents than water (e.g. dioxane or ethanol), where no reactivity was found, revealing the essential role of water for the conversion of cellulose [96].

Wang and co-workers report a catalytic screening of numerous metals over several supports, identifying the Ru/CNT as the catalytic system able to obtain superior yields of sorbitol, starting from un-pretreated cellulose (having 85% of crystallinity). Indeed, a 36% yield of sorbitol is obtained after 24 h of reaction at 185°C, starting with a pressure of 50 bar of hydrogen. Significant improvements can be obtained when the cellulose is pretreated: a 69% yield of sorbitol is obtained starting from a cellulose having the 33% of crystallinity, within the same operating conditions [97].

The addition of acids to the reaction is a fundamental expedient to enable the hydrolysis of cellulose in milder conditions, being usually the limiting step of the overall hydrogenolitic process. On this purpose, Palkovits and co-

workers investigated the hydrogenolysis of cellulose combining catalysts of ruthenium, platinum or palladium supported on activated carbon in presence of phosphoric or sulphuric acids. Thanks to the presence of mineral acids, a temperature of 160°C and 50 bar of initial hydrogen pressure, are enough to obtain high conversion of cellulose. Full conversion and 60% yield of C_4-C_6 sugars are also obtained in presence of Ru/C and sulphuric acid [98]. Furthermore, the same group investigated the combination of heteropoly acids (i.e. $H_3PW_{12}O_{40}$ and $H_4SiW_{12}O_{40}$) with the Ru/C catalyst, that allows to obtain 80% yield of sugar alcohols within 7 h of reaction. Interestingly, such system can be applied also to a real biomass feedstock (i.e. spruce), obtaining full conversion of cellulose and hemicellulose with a 67% yields of polyols [99].

Sels and co-workers optimized the operating conditions to obtain full conversion of ball milled cellulose and 100% selectivity into hexitols, including 85% of sorbitol and 15% of sorbitan, starting from a concentrated cellulosic feed, using a mixture of heteropoly acids and the Ru/C catalyst [100]. Furthermore, the same group investigated cesium salts of heteropoly acids combined with the Ru/C catalyst. Working in this way, higher activities were obtained and the cesium salts showed the advantage to facilitate the recycle of the acid catalysts, because they can be re-crystallized at room temperature [101]. Even more, yields up to 90% of hexitols are obtainable using traces concentration of mineral acids (35-177 ppm) coupled with ruthenium-supported on zeolites (i.e. USY and MOR) [102].

Tungstic acid combined with Ru/C catalyst was used to obtain ethylene glycol (yields up to 50%) starting from cellulose, within 30 min of reaction at 245°C and an initial pressure of 60 bar of hydrogen [103]. Even if a full conversion of cellulose can be obtained, the process suffers of low carbon efficiency, since several other products are obtained. An interesting advantage regarding the use of tungstic acid is the evidence that it is soluble in water at high temperatures (therefore the reaction is actually homogeneously catalyzed). However, at room temperature, tungstic acid is insoluble in water, facilitating its recover and reusability: more than 20 cycles of reaction were performed and a leaching of tungsten <50ppm was registered.

Wu et al. applied the sulfonic acid mesoporous silica (MCM-41) together with Ru/C, at 230°C and 60 bar of H_2, to obtain - after 40 min of reaction - propanediol and ethylene glycol as main products [104].

An innovative approach was reported by Rinaldi, which combines the mechanocatalysis to the depolymerization of cellulose, followed by hydrogenolysis [105,106]. The basic concept consists in the ball milling of the cellulose in presence of low amounts of impregnated mineral acids (e.g. sulphuric acid, chloric acid), in order to promote the depolymerization of cellulose. In this way, the soluble product obtained was hydrogenated in presence of the Ru/C catalyst, obtaining up to 94% yield of hexitols and the possibility to perform up to 6 cycles of reaction. The same authors upgraded the approach using α-cellulose, beechwood, and poplar wood in Simoloyer mills operating on hectogram and kilogram scales [107]. Innovative approaches were also reported by the Fukuoka research group, where the so-called 'mix-milling' process consists in the enhancement of the solid-solid contact between cellulose and the carbon catalyst through a pretreatment [108,109]; also the realization of a carbonaceous catalyst, prepared starting from the same woody biomass substrate (Eucalyptus), was presented [110].

Contrarily to expensive and rare noble metals, base-metals are cheaper and less rare. Therefore, base metal based catalysts could be more feasible even if they show lower activity in hydrogenation reactions. In any case, such disadvantage can be overcome by adopting appropriate precautions (e.g. increasing the temperature, the quantity of catalyst or the prolongation time of the reaction).

The addition of Ni to tungsten carbide supported on activated carbon, allows to obtain a 61% yield of ethylene glycol starting from cellulose (245°C, 60 bar of H_2, 30 min) as reported by Zhang and co-workers [111]. With a similar catalyst, the conversion of corn stalk into ethylene glycol and 1,2-propanediol was reported [112]. The same authors report also the conversion of the raw wooden biomass, where a Ni-W_2C catalyst allows 75% yield of ethylene glycol from cellulose and hemicellulose (235°C, 60 bar of H_2) and 47% yield of monophenols from lignin [113]. Nickel- promoted catalysts seem to be an interesting low cost alternative to platinum- and ruthenium- based catalysts.

Bimetallic tungsten catalysts were found active for the promotion of hydrogenolysis processes. In particular, bimetallic systems of tungsten with metals of groups VII-X of the periodic table, exhibit encouraging results to produce ethylene glycol from cellulose. Among these catalysts, the Ni-W reaches a 75% yield of ethylene glycol at 245°C, 60 bar of H_2, within 30 min of reaction [114]. As cheaper alternative, also the Raney Ni and tungstic acid were investigated [115]. Nickel, combined with other metals (Rh, Ru, Pt, Pd and Ir) supported on mesoporous carbon (MC) exhibits higher yields under the same operating conditions [116].

For the conversion of microcrystalline cellulose nickel- based systems on several supports were screened. Ni/ZnO is distinguished for the possibility to reach full conversion of microcrystalline cellulose and 70% yield into alkanediols (245°C, 60 bar of H_2, 2 h) [117].

The deposition of nickel nanoparticles at the top of carbon nanofibers leads to active systems to promote the conversion of cellulose. Indeed, 92% of conversion with a 50% yield of sorbitol within 4 h of reaction at 273°C at an initial pressure of 60 bar of H_2, was obtained [118].

Copper- based catalysts were investigated by Palkovits and co-workers. Copper supported on ZnO/Al_2O_3 achievs 95% yield of products, where 67% are C_1-C_3 compounds (245°C, 50 bar of H_2, 3 h) [119].

Considerable yields to ethylene glycol (43%) and 1,2-propanediol (32%) starting from a high concentration of cellulose (15% wt) were obtained on using CuCr catalysts added with the base $Ca(OH)_2$ [120].

Being aware of the huge amount of scientific literature concerning the valorization of cellulose and its derived polyols (moreover in continuous increase), only a summary of the most significant recent works was presented.

1.3.2 Catalytic Transfer Hydrogenolysis (CTH)

1.3.2.1 Carbohydrates and Glucose

Guo and co-workers investigated how to convert biomass derived cellulose, starch and glucose into γ-valerolactone without using any external hydrogen source. Their approach is based on a first step in which the dehydration of biomass carbohydrates into levulinic and formic acids occurs,

and a second step where formic acid furnishes the hydrogen necessary to the reduction of levulinic acid into γ-valerolactone [121]. In particular, the carbohydrates (microcrystalline cellulose, α-cellulose and starch) were hydrolyzed in presence of a 0.8M HCl aqueous solution at 220°C, in order to obtain levulinic acid and formic acid. In this step it is very important that the yield to formic acid is high enough (in excess or in equimolar amount with respect to levulinic acid) to enable the subsequent reduction of levulinic acid into γ-valerolactone. In this work, the recyclable and cheap RuCl$_3$/PPh$_3$/pyridine catalyst was used. In a model experiment, γ-valerolactone was produced with a yield of 48%, performed using glucose as a biomass-derived carbohydrate [121].

Another example of combined dehydration and transfer-hydrogenation to produce γ-valerolactone, starting from glucose or fructose, is given by Heeres and coworkers [122]. In this case the process was performed in water using an acid catalyst, the trifluoroacetic acid (TFA) coupled with a heterogeneous hydrogenation catalyst (Ru/C); also molecular hydrogen or formic acid were investigated as hydrogen donors [122].

Au-based catalysts were also investigated by Fan and co-workers [123]. Particularly, the Au/ZrO$_2$ catalysts show interesting results in converting efficiently glucose into levulinic acid and formic acid in high yield, 54 and 58% respectively, giving a 51% yield of γ-valerolactone and a total yield (95%) relative only to the second step of the transfer-hydrogenation. In the same conditions also cellulose, starch and fructose were converted [123].

Scholz et al. applied co-precipitated Cu-Ni-Al catalysts to the hydrogenation of glucose, by using 1,4-butanediol as hydrogen source, to obtain sorbitol. A yield of 67% to sorbitol was obtained from glucose. The catalyst remains stable within 48 h of reactivity, with the possibility be applied also to several other substrates (i.e. fructose, mannose, xylose, arabinose) to obtain the corresponding polyols [124].

Finally, there is also an example, given by Van Hengstum et al., where glucose is used as H-donor substrate [125]. An equimolar mixture of glucose and fructose was employed to obtain gluconic acid and hexitols, such as sorbitol and mannitol. Using Pt/C and Rh/C catalysts, it is possible to obtain equal amounts of gluconic acid and hexitols, operating at room temperature in an aqueous alkaline medium, under nitrogen atmosphere. The general

mechanism occurring in this reaction starts from the generation of hydrogen from the dehydrogenation of glucose; the hydrogen generated is chemisorbed on the metallic surface of the catalyst and it is subsequently consumed by the co-adsorbed fructose [125].

1.3.2.2 Cellulose

At present, the work developed by Fukuoka and coworkers is the unique example of a catalytic transfer hydrogenation process applied to cellulose, in order to obtain hexitols, such as sorbitol and mannitol, without using high pressures of molecular hydrogen but only hydrogen, produced in situ through the dehydrogenation of 2-propanol. A screening of several Ru-based catalysts was carried out, by using milled cellulose in an aqueous solution at 25% vol of 2-propanol at 190°C for 18 h [126] and it was clear that the support plays a crucial role for the reactivity of Ru-based catalysts. Indeed, the Ru/carbons appear the most reactive, particularly Ru/C-Q10, Ru/CMK-3 and Ru/AC(N) (entries 1-3, Table 1.1), show high conversion (74-81%) and high yields to sorbitol and mannitol (sum of C_6-polyols 42.5-46%). Other supports, such as Al_2O_3, TiO_2 and ZrO_2 were found inactive. Through characterization measurements, it was found that the reactivity is given by the presence of highly dispersed cationic ruthenium species, active in the transfer hydrogenation [126].

Beltramini, in collaboration with Fukuoka, continued the study concerning catalysts of Ru supported on activated carbon and applied to CTH of cellulose, with the scope to optimize the operating conditions. Reactions were performed in batch mode, overcoming the problem linked to long reaction time, carrying on the process with a continuous set-up in a fixed bed reactor [127]. First of all they studied the reactivity of glucose, obtaining 82% of conversion and 80% of yield to hexitols at 180°C and only 20 min of reaction, using water and 2-propanol in equal volume. Subsequently, the optimised conditions were applied to the transfer hydrogenation of cellulose oligomers, obtained through a milling process of crystalline cellulose impregnated with sulphuric acid. This pre-treatment was necessary, in order to facilitate the solubilization of the reacting substrate for the continuous process and to reduce the time of reaction. In this way, within 20 min of reaction at 180°C it was possible to obtain the highest yield to hexitols of 35%

(entry 5). Performing the reaction in a continuous set-up, a constant yield in hexitols of 36% constant for 12 h of reaction, with a LHSV of 4.7 h^{-1} was obtained. The mechanism that enables the hydrogen transfer from 2-propanol to glucose, appears to be the di-hydride mechanism [127].

Table 1.1 Catalytic transfer hydrogenolysis of cellulose performed in batch conditions.

Entry	Substrate[1]	Catalyst	H-donor[2]	Temp (°C)	Gas (bar)	Time (h)	Conv (%)	Yield Sorbitol (%)	Yield Mannitol (%)	Ref
1	MC	Ru/C-Q10	2-PO	190	N$_2$ (1)	18	80.2	36.8	9.0	[126]
2	MC	Ru/CMK-3	2-PO	190	N$_2$ (1)	18	81.2	35.7	9.3	[126]
3	MC	Ru/AC(N)	2-PO	190	N$_2$ (1)	18	74.4	33.5	9.0	[126]
4	Glucose	Ru/AC(N)	2-PO	180	Ar (15)	0.33	82	77.0	2.7	[127]
5	ACO	Ru/AC(N)	2-PO	180	Ar (15)	0.33	100	32.2	3.1	[127]

[1] Abbrevations: MC: milled cellulose; ACO: acidified cellulose oligomers;

[2] Abbreviations: 2-PO: 2-propanol.

1.3.2.3 Glycerol and other polyols

Glycerol, being derivable from cellulose, beyond to be a by-product in biodiesel manufacture, is a promising renewable molecule to obtain 1,2-propanediol, which is an important polymer precursor. Therefore, the conversion of glycerol into 1,2-propanediol, through the catalytic transfer hydrogenolysis becomes an interesting tool. In Table 1.2 are summarized the main results available in literature, concerning several catalytic substrates applied to the catalytic transfer hydrogenolysis (CTH) of glycerol.

The catalytic transfer hydrogenolysis of glycerol, was performed for the first time by Pietropaolo and co-workers, using 2-propanol as hydrogen donor and solvent [128]. The investigation started by using the unreduced bimetallic catalyst PdO/Fe$_2$O$_3$, that reaches complete conversion of glycerol and a high selectivity of 94% towards 1,2-propanediol, after 24 h of reaction at 180°C (entry 2). Ethanol was also used instead of 2-propanol, showing complete conversion of glycerol with a slightly lower selectivity to 1,2-propanediol (90%), at the same operating conditions (entry 1).

Shortening the reaction time to 8 h, it is still possible to obtain an almost complete conversion of glycerol (96%) and high selectivity to 1,2-propanediol

(87%), in presence of 2-propanol, by using the catalyst in its unreduced form of PdO/Fe_2O_3 (entry 3). The reactivity of this bimetallic catalyst can be further improved through a reductive pretreatment in H_2 at 200°C, that leads to the Pd/Fe_3O_4 catalyst converting completely the glycerol in 8 h and reaches a comparable selectivity into 1,2-propanediol (84%, entry 4) [128]. The same group has further investigated the Pd-based catalysts for the CTH of glycerol using 2-propanol as hydrogen source, focusing on bimetallic Pd-Co and Pd-Fe catalysts, to clarify which parameters affect the reactivity in the CTH of glycerol. Moreover, a particular attention was paid also to the method of synthesis chosen: incipient wetness impregnation (iWI) or co-precipitation (CP) [128].

Table 1.2 Catalytic transfer hydrogenolysis of glycerol to 1,2-propanediol.

Entry	Catalyst	H-donor [1]	Cat/Gly [2]	Temp (°C)	Gas (bar)	Time (h)	Conv (%)	1,2-PDO Select. (%)	Ref
1	PdO/Fe_2O_3	EtOH	0.237	180	N_2 (5)	24	100	90	[128]
2	PdO/Fe_2O_3	2-PO	0.237	180	N_2 (5)	24	100	94	[128]
3	PdO/Fe_2O_3	2-PO	0.237	180	N_2 (5)	8	96	87	[128]
4	Pd/Fe_3O_4	2-PO	0.237	180	N_2 (5)	8	100	84	[128]
5	Pd/Fe_3O_4	2-PO	0.207	180	N_2 (5)	24	100	56	[129]
6	[3] Pd/Fe_3O_4	2-PO	0.207	180	N_2 (5)	24	67	48	[129]
7	Pd/Co_3O_4	2-PO	0.207	180	N_2 (5)	24	100	64	[129]
8	[3] Pd/Co_3O_4	2-PO	0.207	180	N_2 (5)	24	38	15	[129]
9	Ni-Cu/Al_2O_3	-	0.166	220	H_2 (45)	24	70.5	66.9	[130]
10	Ni-Cu/Al_2O_3	2-PO	0.166	220	N_2 (45)	24	60.4	64.6	[130]
11	Ni-Cu/Al_2O_3	2-PO	0.166	220	N_2 (45)	10	28.2	77.4	[131]
12	Ni-Cu/Al_2O_3	MeOH	0.120	220	N_2 (45)	10	26.2	51.2	[131]
13	Ni-Cu/Al_2O_3	FA	0.120	220	N_2 (45)	10	33.5	85.9	[131]
14	Ni-Cu/Al_2O_3	FA	0.498	220	N_2 (45)	24	90	82	[132]
15	70Cu30Al	2-PO	-	220	N_2 (69)	5	69	90	[133]
16	$20Cu/ZrO_2$	FA	-	220	N_2 (5)	18	97	95	[134]

[1] Abbreviations: EtOH: ethanol; 2-PO: 2-propanol; MeOH: methanol; FA: formic acid;

[2] Ratio of Cat/Gly (g/g); [3] Catalyst prepared through the incipient wetness impregnation

Co-precipitated catalysts, both Pd/Fe$_3$O$_4$ and Pd/Co$_3$O$_4$, reached the complete conversion of glycerol and exhibited a high selectivity into 1,2-propanediol (60% ca.). Contrarily to impregnated samples, that showed a poor reactivity in CTH reaction. This difference in reactivity is ascribable to the presence of bimetallic ensembles over catalytic surfaces of co-precipitated systems that ensures a strong interaction between palladium and iron or cobalt. Bimetallic ensembles constitute the active phase responsible for the promotion of the glycerol CTH reaction. This evidence confirms that the catalytic method of preparation plays a crucial role in driving the electronic properties of the bimetallic PdM sites (M = Co or Fe). Furthermore, a tight correlation between the ability of catalysts towards the dehydrogenation of 2-propanol and the ability to perform CTH reactions was found [129].

The transfer hydrogenolysis of glycerol into 1,2-propanediol, catalyzed by bimetallic Pd/Fe$_3$O$_4$ and Pd/Co$_3$O$_4$ catalysts, enlightens a mechanism in which the glycerol (i) adsorbs over the bimetallic active sites and gives dehydration, breaking a C-OH of a primary alcoholic group, (ii) thanks to the hydrogen supplied from the 2-propanol dehydrogenation, the intermediate acetol can be hydrogenated into 1,2-propanediol (Figure 1.6) [129].
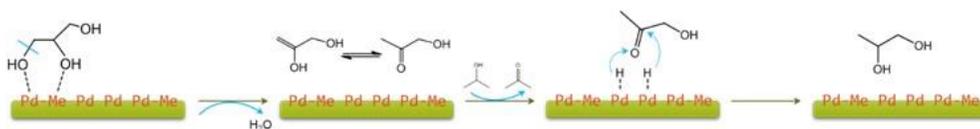
Figure 1.6 Mechanism of CTH of glycerol over Pd/Fe$_3$O$_4$ and Pd/Co$_3$O$_4$ catalysts.

Gandarias et al. have deeply studied the reactivity of bimetallic catalysts Ni-Cu/Al$_2$O$_3$, prepared through the sol-gel technique, which enables to obtain the best performances when catalysts are pretreated at 450°C [130-132]. At the beginning, authors studied the hydrogenolysis of glycerol either in presence of molecular hydrogen or in conditions in which the hydrogen is produced in situ, through the aqueous phase reforming (APR) or the catalytic transfer hydrogenolysis (CTH), performed using 2-propanol as hydrogen source [130]. They found that 2-propanol is a more effective hydrogen source than the aqueous-phase reforming, for the glycerol hydrogenolysis process. Even if the results obtained in the CTH of 2-propanol are comparable to those

obtained in presence of molecular hydrogen (entries 9-10). Two different mechanisms are involved when the hydrogenolysis of glycerol occurs in presence of molecular hydrogen or in presence of 2-propanol (Figure 1.7). Glycerol is first transformed into the intermediate 1,3-dihydroxyisopropoxide in both cases, but in the former the intermediate is first dehydrated to acetol and subsequently this is hydrogenated to give 1,2-propanediol; in the latter 1,3-dihydroxyisopropoxide is directly converted into 1,2-propanediol, whilst the acetol is obtained from 1,3-dihydroxyisopropoxide dehydration which occurs on acid sites. Moreover, the deactivation of the catalyst occurs more rapidly in the case of the presence of 2-propanol, because adjacent sites are required for the donor and the acceptor molecules during the transfer hydrogenation [130].
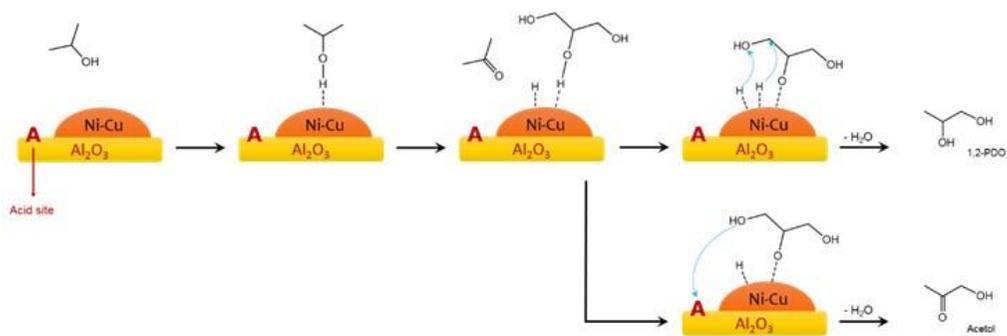
Figure 1.7 Mechanism of CTH of glycerol over Ni-Cu/Al$_2$O$_3$ catalyst.

Anyway, on changing the hydrogen donor molecule, it is possible to improve the performance of the CTH of glycerol on the bimetallic Ni-Cu/Al$_2$O$_3$ catalyst [131]. Gandarias et al. performed a study on the effect of the hydrogen donor molecule, by comparing methanol, formic acid and 2-propanol. Being aware that glycerol and the hydrogen donor molecules are in competition for the same active sites, they operated with a semi-continuous set-up in order to feed continuously the solution containing the donor molecule, changing in each test the concentration of the solution. It was found an optimum rate to feed the donor molecule, in order to maximize the selectivity into 1,2-propanediol [131]. The most significant results obtained are reported in Table 1.2 (entries 11-13). Formic acid appears to be the most

effective hydrogen donor molecule. The scale of efficiency, relative to the molecules ability, follows this order: formic acid> 2-propanol> methanol. With the aim to further improve the reactivity of the Ni-Cu/Al$_2$O$_3$ catalyst, it is necessary to add formic acid and molecular hydrogen in order to obtain a conversion of glycerol of 44% and a selectivity to 1,2-propanediol of almost 90% [131].

The kinetic study enables to understand that the hydroxyl groups of glycerol and the target product 1,2-propanediol, adsorb over the same acidic sites of the Al$_2$O$_3$ support. Therefore, to overcome this drawback, it is necessary to increase the amount of the catalyst in order to obtain high conversion (90%) and selectivity (82%), within 24 h of reaction (entry 14) [132].

Concerning the role of metallic sites, the higher prevalence of C-O bonding cleavage is given in the presence of a Cu-Ni alloy. This catalyst reduces the amount of active Ni ensembles, which are responsible for both the C-C and C-O bond cleavage, while the Cu ensembles rule mainly the C-O breaking and not the C-C one. Therefore, in presence of the reduced Ni-Cu/Al$_2$O$_3$ catalyst, the C–C bond cleavage is limited, while the activity for C–O bond cleavage is significantly promoted [132].

Rasika et al. performed a study on the dehydration and the hydrogenolysis of glycerol both in presence of water and 2-propanol, screening the reactivity of Cr-based and Cu-Al catalysts [133]. If the hydrogenolysis of glycerol is considered, the co-precipitated Cu-Al catalysts shows a better performance, particularly in presence of 2-propanol as H-donor. Indeed the 70Cu30Al catalyst reachs a 69% of conversion and 90% of selectivity in 1,2-propanediol within 5 h of reaction (entry 15). The evidence of different performances in presence of 2-propanol instead of water, indicates that the two processes are ruled by two different reaction pathways [133].

Yuan et al. investigated a series of Cu/ZrO$_2$-based catalysts, particularly the 20%Cu/ZrO$_2$, synthesized by co-precipitation, can be used to convert glycerol to 1,2-propanediol in high yields with formic acid as hydrogen source. They found that conditions to optimize the production on 1,2-propanediol, are a FA/glycerol molar ratio (1:1) and the temperature of 200°C. Both conditions enable to increase the yield to 1,2-propanediol to 94% after 18 h (entry 16) [134]. Furthermore, this kind of catalyst is also pretty stable, since

it is reusable at least five times without losing any appreciable reactivity and selectivity [134].

In conclusion it is possible to observe that the bimetallic Pd-based catalysts, particularly the Pd/Fe_3O_4, shows better performances in milder operating conditions. This is advantageous, with respect to the bimetallic PdCo catalyst, because iron oxide is preferable over cobalt oxide, being less toxic and cheaper.

In literature, some works that report the conversion of glycerol in traditional hydrogenolysis conditions (with addition of molecular hydrogen), but operating in a solvent that can donate hydrogen, like ethanol and 2-propanol are present (Table 1.3).

A bimetallic Pd-Cu/solid-base catalyst was prepared via thermal decomposition of the $Pd_xCu_{0.4}Mg_{5.6}-xAl_2(OH)_{16}CO_3$. The hydrogenolysis of glycerol is easier to be performed on bimetallic Pd-Cu/solid-base catalysts than over separated Pd and Cu systems. Performing the hydrogenolysis of glycerol on the $Pd_{0.04}Cu_{0.4}/Mg_{5.5}Al_2O_{8.5}$, at 180°C within 10 h and 20 bar of H_2, both in ethanol and methanol solutions, conversion and selectivity to 1,2-propanediol reach high values (entries 1-2) [135]. Authors suggest that such performance, better than in water, is ascribable to the less strong interaction between the ethanol and the catalyst surface, making more surface available to the conversion of glycerol [135,136]. In presence of some similar catalysts based on Rh ($Rh_{0.02}Cu_{0.4}/Mg_{5.6}Al_{1.98}O_{8.6}$), the hydrogenolysis of glycerol, in presence of ethanol, reaches high conversion and selectivity to 1,2-propanediol respectively, 91% and 99%, at 20 bar of H_2 and 180°C of temperature (entry 3). Moreover, this catalyst was found stable for five consecutive hydrogenolysis tests in ethanol, even if the conversion decreases from 91% to 57% in the third cycle and then it remains constant until the fifth cycle [137]. Similarly to Pd-Cu/solid-base catalyst, the improved performance showed in alcoholic solutions, rather than in water, was attributed to a minor interaction of the solvent with the catalytic surface [137].

Also the bimetallic Pd/Fe_3O_4 catalyst was tested for the hydrogenolysis of glycerol using 2-propanol as solvent and adopting mild operating conditions such as 180°C and only 5 bar of molecular hydrogen (entry 4) [138].

Gong et al. have found that it is possible to vehicle the selectivity of glycerol towards 1,3-propanediol using a $2Pt/_{20}WO_3/ZrO_2$ catalyst, in ethanol as solvent medium (entry 5) [139].

It should be interesting to investigate more deeply the real role of an H-donor solvent that enables to perform the hydrogenolysis of glycerol with low molecular hydrogen pressures, compared to higher pressures typically necessaries in water.

Table 1.3 Hydrogenolysis of glycerol in presence of H-donor solvents.

	Catalyst	Solvent [1]	Cat/Gly [2]	Temp (°C)	Gas (bar)	Time (h)	Conv (%)	Select. [3] (%)	Ref
1	$Pd_{0.04}Cu_{0.4}/Mg_{5.5}Al_2O_{8.5}$	MeOH	0.125	180	H_2 (20)	10	89.5	1,2-PDO (98)	[135]
2	$Pd_{0.04}Cu_{0.4}/Mg_{5.5}Al_2O_{8.5}$	EtOH	0.125	180	H_2 (20)	10	88.0	1,2-PDO (99)	[135]
3	$Rh_{0.02}Cu_{0.4}/Mg_{5.6}Al_{1.9}O_{8.6}$	EtOH	0.167	180	H_2 (20)	10	91.0	1,2-PDO (99)	[137]
4	Pd/Fe_3O_4	2-PO	0.237	180	H_2 (5)	24	100	1,2-PDO (71)	[138]
5	$2Pt/20WO_3/ZrO_2$	EtOH	0.250	170	H_2 (55)	12	45.7	1,3-PDO (21)	[139]

[1] Abbrevations: EtOH: ethanol; 2-PO: 2-propanol;

[2] Ratio of Cat/Gly (g/g);

[3] Abbreviations: 1,2-PDO: 1,2-propanediol; 1,3-PDO: 1,3-propanediol.

Another interesting route to valorize glycerol, like a potential biorefinery feedstock, is that leading to allyl alcohol by using H-donor molecules as solvent, favouring the dehydration of glycerol to acroleyn followed by reductive H-transfer to allyl alcohol (Figure 1.8).
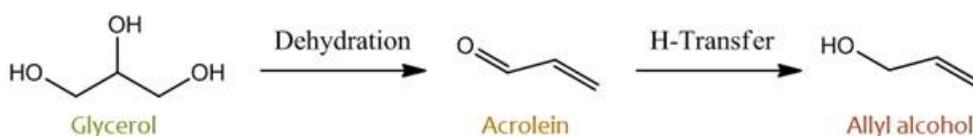

Figure 1.8 Schematic representation of the dehydration/H-transfer of glycerol into allyl alcohol.

Schüth and coworkers investigated the conversion of glycerol into allyl alcohol, through an initial dehydration to acrolein, by using iron oxide as catalyst [15]. Among the operating conditions investigated, it was found that

at 320°C it is possible to obtain an almost full conversion of glycerol and a yield to allyl alcohol of 20–25%. In particular, the selectivity in the transfer hydrogenation to allyl alcohol is close to 100%. This evidence has never been observed before, for iron oxide catalysts, scarcely considered so far in hydrogen transfer reactions. In such reactions, the hydrogen donor species could be the glycerol itself and some intermediates bearing hydroxyl groups [140].

Furthermore, Masuda and coworkers carried out the conversion of glycerol into allyl alcohol using iron oxide-based catalysts at 350°C [141]. The dehydration of glycerol takes place on acid sites of catalysts, while the allyl alcohol formation occurs through a hydrogen transfer mechanism. Several alkali metals (Na, K, Rb, and Cs) were supported on ZrO_2–FeO_X substrate and all of them gave high allyl alcohol yield suppressing glycerol dehydration due to the reduced catalyst acidic property. Particularly, the K-supported catalyst (K/ZrO_2–FeO_X) reaches an allyl alcohol yield of 27% mol. Also in this case, the hydrogen transfer mechanism seems to take place from the reaction of glycerol with hydrogen atoms derived from formic acid obtained during the reaction, or active hydrogen species produced from the decomposition of H_2O by ZrO_2. Furthermore, the addition of Al_2O_3 (K/Al_2O_3–ZrO_2–FeO_X), enables to improve the stability of the catalyst during the glycerol conversion, making the K/Al_2O_3–ZrO_2–FeO_X applicable also directly to the crude glycerol (which is the waste solution obtained from biodiesel production), reaching a yield of 29% in allyl alcohol after 4-6 h of reaction [141].

Another kind of approach was followed by Bergman and coworkers. Formic acid was applied either as acid catalyst or solvent, with the aim to deoxygenate the glycerol into an allyl compound through the mediation of formic acid (230-240°C) [142]. Using this method, it is possible to perform the conversion of the 1,2-dihydroxyl group to a carbon–carbon double bond. The same procedure was applied to erythritol, that has been converted into 2,5-dihydrofuran at 210-220°C [142]. During the dehydration step, formic acid acts as acid catalyst and in the reductive step it acts as hydrogen donor [142].

A similar approach was followed by Fristrup and co-workers [143]: two vicinal diols were reduced into an alkene group and the deoxydehydration (DODH) of glycerol and erythritol was performed with the cheap and commercially available $(NH_4)_6Mo_7O_{24} \bullet 4H_2O$ catalyst, in presence of 2-propanol, which acts as solvent and reducent agent. With this approach the

total yield of reduced species (such as alkene and alcohols) can be as high as 92%, at 240-250°C. The DODH of erythritol can reach a 39% of yield in 2,5-dihydrofuran [143].

1.3.3 Aqueous Phase Reforming (APR)

The aqueous phase reforming (APR) was reported for the first time by Dumesic and co-workers. They proposed a ravishing way to produce H_2 from oxygenated hydrocarbons using mild temperatures (200–260 °C) and pressures (20–50 bar) [71,77]. Fundamental requirements of the APR process is the production of H_2 with a low CO concentration, due to the possibility to couple the water gas shift (WGS) reaction in a single batch. A trace concentration of CO (< 500 ppm) is required to make feasible the application of the process in fuel cells. Moreover, a good catalyst of APR must not present high activity toward undesirable reactions such as methanation and Fischer-Tropsch.

In summary, the most desired metals should present a good activity toward C–C cleavage and WGS reaction and a low activity towards methanation. In agreement with these considerations, metal precious such as Pt and Pd are good candidates, but also Ni is an interesting metal, due also to its lower price, and its use in combination with Pt as bimetallic catalyst.

Numerous metal-supported catalysts have been studied for the APR process, due to the synergic effect between metal and acid/base features of the support, in order to promote different reactions. A lot of efforts have been focused on the H_2 production from methanol, ethylene glycol, glycerol, sorbitol, glucose, or cellulose on Pt, Pd, or Raney-Ni based catalysts [71-82,144-163].

Starting from cellulose a H_2 yield of ca. 27 % was obtained over the Pt/C catalyst [144]. Since satisfactory H_2 yield values are hard to achieve by using only one-component catalysts, the addition of a second metal to form PtM (M = Ni,[145-148]; Co,[148-151]; Fe,[148-152];Mn,[153]; Re[154-157]) or PdFe [148] alloys was often investigated. The formation of alloys tailors the electron density on Pt or Pd active sites [4, 164-167], improving the ability to perform the WGS reaction. The bimetallic PdFe catalysts will be discussed in the following paragraph 1.4.

Ethylene glycol at 210°C shows a TOF, in H_2 production that increases from 1.87 min^{-1} over Pt/Al_2O_3 to 5.18 over the bimetallic Pt_1Ni_1/Al_2O_3 catalyst [148].

The H_2 production from glycerol at 230°C, over Pt_1Co_5, supported on multi−walled carbon nanotubes (MWCNs), shows a time yield *per* site up of 44.4 min^{-1}, which is almost four times higher than that over single Pt atoms supported on MWCNs, while the turnover rate, in the WGS reaction, increases from 0.42 min^{-1} to 13.2 min^{-1} [150]. On the bimetallic PtRe/C catalyst, the TOF for H_2 production from glycerol was 23.3 min^{-1} at 225 °C, thirteen times higher than on the monometallic Pt/C catalyst, and also the ability to the WGS reaction increases of 65 times with the Re addition [155].

Addition of tin to the Raney-Ni catalyst, as a result of the formation of the Ni-Sn alloy and the Sn location at Ni-defect sites, significantly improves the H_2 selectivity by decreasing the rate of methane formation [77].

Another approach to improve the activity to the H_2 production is to modify the catalyst composition [158] or the support [159] with a WGS promoter, such as CeO_2, or by using the WGS promoter directly as the support, such as iron oxide [148,160]. Starting from cellulose over CeO_2 modified Raney-Ni catalyst, a H_2 yield of ca. 24% was obtained, significantly higher than that obtained over the simple Raney Ni catalyst (8%) [158].

Several supports have been tested for the APR process. A study performed by Menezes and co-workers [168] reports a screening of the support basicity, mantaining the same Pt loading. In this context, MgO and ZrO_2 show the highest hydrogen production and lower alkane yield (CH_4), due to the higher electron-donating nature of the metal and due to the basicity of the MgO support that probably is involved in the reaction mechanism. The H_2 production activity could also be promoted by CaO, $Ca(OH)_2$ or KOH [146,161-162], because bases could promote the CO_2 capture, facilitating the WGS reaction, whilst they could inhibit the methanation [146,161-162] or the dehydration pathway [155]. When Ni-based catalysts are used, alkaline conditions can improve the activity to H_2 production and also suppress Ni leaching [163].

The use of lignocellulosic fractions was also studied in the APR process.

A comparison of the three fractions obtainable from lignocellulosic biomasses (cellulose, hemicellulose, and lignin) after pretreatments in subcritical conditions, before the APR reaction, was reported by Erbatur et al. [169]. The three hydrolysate feeds over a commercial Pt/C present different behaviors. The cellulose fraction shows the highest amount of gases produced (48% more than that of hemicellulose over wheat straw), but the relative percentage of H_2 over the total gases is lower than that observed with hemicellulose. The lignin fraction does not produce hydrogen, but only CO_2 with small amounts of CH_4, while hemicellulose shows ca. 30% H_2 and 10% CH_4 in the total gas produced. Since several kinds of biomass have been studied, the differences in reactivity within the fractions analyzed were focused on the crystallinity degree. The hydrolytic pretreatment enables to reduce the crystalline index, making the fractions more available to degradation, producing a higher amount of gaseous products. The effect of the crystalline fraction over the APR reaction was analyzed more in depth by Tian et al. [170]. One of the main challenge is the acceleration of the hydrolysis step, that is highly dependent on the crystallinity of the feed. Once produced by hydrolysis, the suggested intermediate, glucose, is then readily transformed into hydrogen over a Pt/C catalyst. In order to improve this step, a combined hydrothermal-catalytic treatment accelerating the hydrolysis step of the biomass through the addition of a mineral acid to the traditional APR catalyst was proposed by Lin et al. [171].

The lignocellulosic biomass is a complex feed and the treatment needs to be developed more in depth, mainly due to the complexity of the subsequent reactions pathway, together with the hard reactivity of the feed; however, some encouraging results indicate the possibility to produce hydrogen through the APR process.

Indeed, the first pilot plant for APR, starting from glucose, was developed in 2005 by Virent Energy Systems Inc, a partner of the University of Wisconsin [172]. The project is based on the hydrogenation of glucose into sorbitol to produce a hydrogen-rich stream. At the beginning the main aim was focused on the optimization of the process in order to produce 10 kg of hydrogen *per* day, subsequently the catalyst was optimized to maintain hydrogen productivity and targets. Furthermore, Virent in the BioForming® process developed a process combining the APR technology with a modified conventional catalytic process (i.e. a petrochemical process) that can work

with a wide range of C_5 and C_6 sugars, as well as other bio-deriving feedstocks (polysaccharides, organic acids, furfural), and produces a mixture of chemical intermediates including alcohols, ketones, acids, furans, paraffins, and other oxygenated hydrocarbons. [173].

Regarding the APR reaction process, there are not many patents probably because the process is still under development and, so far, high hydrogen yields have not been obtained. In particular, the patent literature can be distinguished in (i) works concerning the reforming process alone [174-176] and (ii) more complex projects that treat rough biomasses through several steps, with APR being only one unit of the overall processes [177-178].

At present, aqueous phase reactions of polyols are studied in industries to produce fuels and chemicals [179].

Furthermore, APR processes can be included in biorefinery plants to generate *in situ* the necessary hydrogen supply (for HDT, HDO, and pyrolysis reactions), which currently comes from fossil resources.

However, several economic drawbacks need to be overcome, such as the achievement of high hydrogen yield using raw feeds, the reduction of steps regarding the feedstock pretreatment and the achievement of pure streams in order to reduce the cost of purification of the products.

Nonetheless, the encouraging results obtained and the versatility of this process which enables its application at different feedstocks without significant changes in reactivity, suggest that the APR process is a suitable alternative for the production of hydrogen and building blocks from the renewable biomass.

1.4. Upgrading of cellulose and polyols promoted by bimetallic Pd-Fe catalysts

Transition metals have been successfully used in the catalytic valorization of biomass-derived molecules. Traditionally, platinum-group metals (PGMs) are all excellent hydrogenation catalysts, widely used in industry and refineries [180-183]. Palladium has a lower cost and more abundant reserves than platinum (that is still the most widely used element in catalysis)

[184,185]. Homogeneous and heterogeneous palladium-based catalysts have found a potential application in several industrial reactions including hydrogenation, dehydrogenation, hydrogenolysis, reforming, oxidation, coupling reactions, carbonylation/decarbonylation and hydrodesulphurization [186-196]. With respect to other PGM elements, palladium is characterized by a fundamental electronic configuration unique among transition metals ($4d^{10}$, $5s^0$) [197] that can be strongly influenced by the coordination environment [167].

The modification of catalytic properties of palladium by adding a second metal can be related, from a general point of view, in terms of (i) "ligand" effects (related to the shifting of the d-band density); (ii) "ensemble" effect (a dilution of palladium surface by a relatively unreactive second co-metal); (iii) "stabilizing" effect (improving the active sites stability) [198-203]. Hence, heterogeneous catalysts based on palladium bimetallic systems have gained increasing attention for their enhanced activity and durability in different reactions. In particular, heterogeneous bimetallic Pd-Fe catalysts show an excellent performance in promoting the cleavage of C–O and C–C bonds in platform derived molecules of cellulose, hemicellulose and lignin. The main peculiarity of these bimetallic catalysts is the formation of bimetallic Pd-Fe ensembles or alloys that allows modification of the electronic density of palladium, thus promoting unexpected catalytic reactions under mild conditions.

Results obtained in important green and sustainable reactions will be presented, including: aqueous-phase reforming (APR) [148,160], hydrogenolysis [138,204-208] and catalytic transfer hydrogenolysis (CTH) [128-129] of C_6–C_2 polyols. All these reactions will be discussed in details with the aim to show the unicity of heterogeneous Pd-Fe catalysts that are suitable for a wide reductive valorization processes of all constituent components of lignocellulosic biomasses having the potential to be successfully used in modern biorefineries to produce simple bulk compounds.

Cellulose deriving polyols are characterized by the highest O/C ratio than other biomass-derived molecules and typical chemical commodities and fuels available in the industrial market. Therefore, the main issue consists in reducing the oxygen content through deoxygenative and CTH/APR processes [62, 130, 209-212].

Ethylene glycol [210] (EG, C_2 polyol) is the simplest basic unit of polyols and can be used as representative molecule for larger polyols and sugars molecules to exploit the selective cleavage of C–C, C–H, O–H and C–O bonds. Currently, ethylene glycol is mainly produced *via* ethylene obtained by cracking of fossil raw materials, but can be also easily obtained from the direct catalytic conversion of the cellulosic biomass [211,212]. Bond energies of both C–C and C–OH bonds are almost the same (ΔH_{C-C} 83 kcal·mol⁻¹ and ΔH_{C-O} 86 kcal·mol⁻¹) [213,214]. Therefore, when reactions are performed under drastic operating conditions, it is less likely to achieve a higher selectivity. If hydrogenolysis breaks selectively C–C bond, methanol will be the favorite reaction product; on the contrary, the breaking of the C–O bond will generate ethanol, that can be further converted into CO_2 or CH_4 (Figure 1.9) [4].
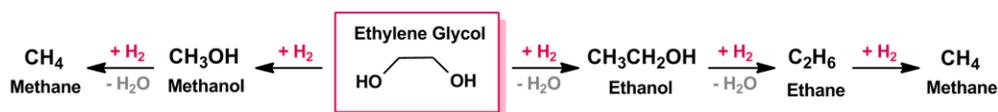
Figure 1.9 Hydrogenolysis of ethylene glycol through C-C or C-O bond rupture.

Tsang and co-workers successfully used the co-precipitated Pd/Fe₂O₃ catalyst for methanol production starting from ethylene glycol [204]. The peculiar reactivity of the catalyst, after reduction, stems from the strong metal-support interaction exerted through the extremely small PdFe clusters. Hydrogenolysis of ethylene glycol, on the 5% Pd/Fe₂O₃ catalyst at 195°C and 20 bar of hydrogen, affords high selectivity to a methanol and ethanol mixture. Other metal particles (Ru) on different oxide supports (ZnO, Ga₂O₃, CeO₂ and Al₂O₃) were also tested: the only combination for a good methanol production was found to be Pd and iron oxide (Figure 1.10).
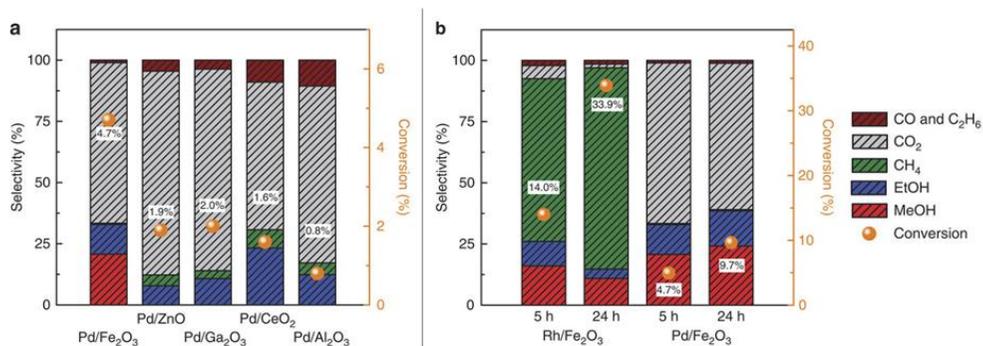
Figure 1.10 Hydrogenolysis of ethylene glycol carried out over 5% Pd supported on different oxides (a) and over 5% Pd and 5% Rh supported on iron oxide (b) [Adapted from Ref. 204].

Bimetallic PdM (M= Fe, Co, Zn) samples were investigated in the hydrogenolysis of ethylene glycol to explore the effect of the d-band filling parameter on the cleavage of C–O and C–C bonds [206]. As illustrated in Figure 1.11, experimental results show a significant decrease of the selectivity to methanol from 50% with the PdFe sample to 19% with the PdZn system. On the contrary, the selectivity to ethanol increases on passing from a value of 3% to 24%.
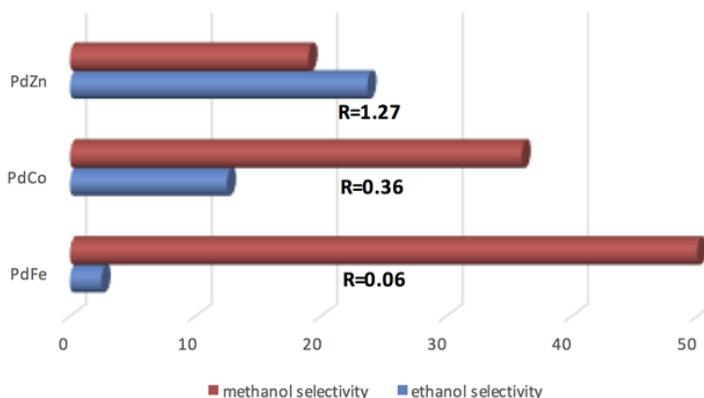
Figure 1.11 Hydrogenolysis of ethylene glycol promoted by PdFe, PdCo and PdZn catalysts. Operating conditions: 5% wt EG aqueous solution, initial pressure of H_2: 50 bar, at 250°C for 24 h of reaction [Adapted from Ref. 206].

A series of heterogeneous Pd-Fe catalysts blended with different concentration of Zn (II) were also prepared and tested in the ethylene glycol hydrogenolysis [205]. A significant selectivity toward the C–C bond cleavage was registered, related to the increased amount of neighbor Fe atoms in the PdFe nanoclusters (Figure 1.12). Furthermore, the C–C bond breaking ability increases almost linearly with the concentration of Fe(0) present in the catalytic system.
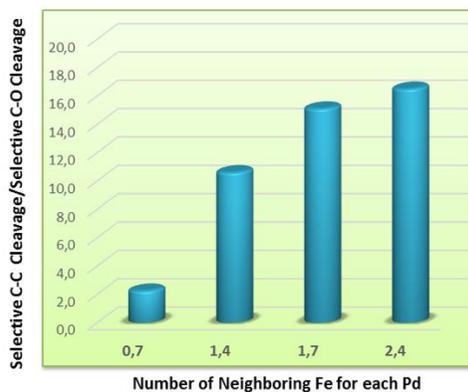
Figure 1.12 Relationship between the selectivity in C-C bond cleavage obtained in hydrogenolysis of ethylene glycol and the Fe content in PdFe catalyst [Adapted from Ref. 205].

Dumesic and co-workers were pioneers in developing the aqueous-phase reforming (APR) process from oxygenated molecules [72-82]. Bimetallic Pd-Fe catalytic systems were investigated for APR of ethylene glycol [76]. Authors highlight the promoting effect of iron in the APR process, obtaining a significant improvement in the TOF of the H_2 production, with the 6% Pd/Fe_2O_3 sample, that is considered the most promising catalytic system [76].

The real potential of Pd/Fe_3O_4 in the APR of biomass-derived oxygenated molecules was sustained and confirmed also by Qiao [160]. Pd-based catalysts were prepared by incipient wetness impregnation (IWi) over different metal oxide supports (Fe_2O_3, Cr_2O_3, NiO, Al_2O_3, ZrO_2). Pd/Fe_2O_3 catalyst appears as the most suitable IWi catalyst for its superior activity, selectivity and stability in the APR of ethylene glycol. Moreover, the Pd/Fe_3O_4 catalyst — prepared through co-precipitation— shows a superior performance than those obtained with the impregnated Pd/Fe_2O_3 sample, while the H_2 selectivity remains on

the same order of magnitude (94%), confirming the importance of the preparation method used [160].

Glycerol (Gly, C_3 polyol), the main by-product obtained from the biodiesel production, is gaining importance as bio-feedstock to produce chemicals, because of the growing worldwide expansion of biofuels [27-29]. An attractive valorization route is the selective hydrogenolysis of glycerol because it is a clean and economically competitive process that allows production of different valuable chemicals such as 1,2-propanediol (1,2-PDO), 1,3-propanediol (1,3-PDO), ethylene glycol (EG) and C_1–C_3 alcohols [30]. Great efforts have been focused on its conversion into 1,2-propanediol that is widely used in the manufacture of pharmaceuticals, cosmetics, food products, polyester resins and functional fluids. Moreover, glycerol can be used as starting substrate for the sustainable production of renewable hydrogen through the APR process. The performance of bimetallic PdFe catalysts on glycerol hydrogenolysis was recently investigated to ascertain the morphological effect of the iron oxide support (rod-like and plate-like) on the catalyst activity [207]. Pd–plate-like iron oxide catalysts show higher activity than Pd-rod-like samples with the glycerol conversion/1,2-PDO production increasing with the reduction temperature (200–300 °C) [215-216]. The higher activity, shown by the Pd-plate-like iron oxide catalyst, was correlated to a higher amount of active sites at the interface [217-218]. Moreover, CO_2-TPD measurements reveal an exact correlation between the catalytic activity and the number of basic sites (oxygen vacancies) present on the catalytic surface [219,220].

Hence, the activity of the Pd-plate-like iron oxide in glycerol hydrogenolysis was blamed to increase when the amount of surface oxygen vacancies grows up, due to the (001) polar surface, highlighting that the bifunctional metal-oxide interfacial catalysis could be conditioned by the shape of the support [207].

Glycerol hydrogenolysis over co-precipitated PdFe bimetallic catalysts with and without the addition of Zn (II), were investigated by Tsang and co-workers to elucidate the effect exerted by the addition of a second co-metal, that facilitate the reduction of Fe ions into metallic iron [205]. The hydrogenolysis carried out with an aqueous solution of glycerol (1 wt %) at 250°C for 120 h with an H_2 initial pressure of 50 bar, shows complete conversion of glycerol over reduced PdFe catalysts, both in presence and in

absence of Zn(II). The PdFe catalyst added with Zn(II) shows a different distribution of products in liquid phase with 1,2-propanediol (ca. 32%) and ethanol (ca. 32%) as main products. This result highlights that PdFe catalysts are more selective in the C–C bond cleavage than in the C–O bond breaking, when the Fe(0) content in the bimetallic nanoparticles increases through the addition of Zn(II). The increase of the Fe atom content influences the electronic structure of Pd, causing a shift of the d-band center position to a lower value. Consequently, the C–O cleavage becomes more difficult causing a gradual depletion of the electron filling in the d-band. The effect is that the back donation from the d-band of palladium to the π^* anti-bonding C–O orbital is reduced. Conversely, the lower d-band electron density strengths the Pd-C bond formation. Coupling both factors, a higher specificity to the C–C selectivity over the C–O cleavage is to be expected [205].

The effective feasibility of the selective catalytic transfer hydrogenolysis of glycerol into 1,2-propanediol, promoted by the PdFe catalyst, was demonstrated for the first time by Pietropaolo and co-workers[128]. Reactions were performed under inert atmosphere in absence of added hydrogen and it was ascertained that the transfer of hydrogen occurs from the alcoholic solvent (2-propanol or ethanol) to the glycerol, through the dehydrogenation of the solvent. Glycerol hydrogenolysis reactions were carried out within 24 h in an autoclave charged with 5 bar of inert gas, using PdO/Fe_2O_3 unreduced catalyst and a glycerol (12% wt) solution in 2-propanol (or ethanol). The glycerol reaches the complete conversion (84%–100%) in the temperature range of 150–180°C, showing a remarkable selectivity to 1,2-propanediol (91%–94%), followed by a minor amount of ethylene glycol. Acetone was also detected in liquid phase, being produced from the 2-propanol dehydrogenation. The presence of 1-hydroxyacetone (AC) is an important intermediate, that enables to maximize the selectivity to 1,2-propanediol and it is detected in reactions carried out in a shorter time than 24 h.

Glycerol CTH reactions under mild conditions (180°C, 5 bar of N_2), in 2-propanol used as solvent, were deeply investigated to understand the different reactivity obtained from co-precipitated and impregnated PdFe catalysts [129]. Impregnated samples (Pd/Fe_2O_3 and Pd/Fe_3O_4) result considerably less active than the analogous co-precipitated, and 1-hydroxyacetone is detected as the prevalent product, followed by 1,2-propanediol and ethylene glycol in small percentages. An interesting

correlation between the amount of acetone measured and the glycerol conversion was also experimentally verified. A reaction mechanism of glycerol in CTH condition was also proposed. The first step involves the glycerol chemisorptions on metal sites. The following C–OH cleavage occurs through a SN1 mechanism with an internal re-arrangement into acetol. Finally, the transfer hydrogenation of acetol to 1,2-propanediol occurs directly from 2-propanol through the H-species obtained from its dehydrogenation [129].

The main results discussed for hydrogenolysis, APR and CTH reactions of glycerol are reported in Table 1.4.

Table 1.4 Catalytic conversion of glycerol in hydrogenolysis, APR and CTH conditions over PdFe catalysts.

Catalyst	Solvent	H-source	Temp [°C]	Time [h]	Conv [%]	Main Prod [%] [4]	Ref
Zn-Pd/Fe$_3$O$_4$ [1]	H$_2$O	H$_2$ (50 bar)	250	120	100	1,2-PDO (33%), EtOH (32%)	[205]
Pd/Fe$_3$O$_4$ [1]	H$_2$O	H$_2$ (50 bar)	250	120	100	1,2-PDO(33%)	[205]
PdO/Fe$_2$O$_3$ [1]	2-PO [3]	2-PO (5bar)	180	24	100	1,2-PDO (94%)	[128]
Pd/Fe$_3$O$_4$ [1]	2-PO	2-PO (5bar)	180	24	100	1,2-PDO (56%)	[129]
Pd/Fe$_3$O$_4$ [2]	2-PO	2-PO (5bar)	180	24	66.5	1,2-PDO (48%)	[129]
Pd/Fe$_2$O$_3$ [2]	2-PO	2-PO (5bar)	180	24	44.0	AC (58%)	[129]

[1] Catalyst prepared by co-precipitation;

[2] Catalyst prepared by incipient wetness impregnation;

[3] 2-PO: 2-propanol;

[4] 1,2-PDO: 1,2-propanediol; EtOH: ethanol; AC: 1-hydroxyacetone.

Considerable research interest has been directed towards sorbitol (Sorb, C$_6$ polyol) hydrogenolysis, because it allows the production of fundamental chemical intermediates [65,221–223].

The overall reaction pathway of sorbitol hydrodeoxygenation is reported in Figure 1.13 [224]. The sorbitol conversion mainly exhibits four key reactions: hydrogenation, dehydration, retro-aldol condensation and decarbonylation [225]. Sorbitol could be dehydrated to cyclic products such as 1,4-sorbitan and isosorbide. The latter leads to 1,2,6-hexanetriol (1,2,6-HXT)

through hydrogenolysis and dehydration/hydrogenation reactions. 1,2,6-Hexanetriol is a valuable intermediate because, through dehydration/decarbonylation reactions, affords lighter alcohols and polyols; alternatively, it could be dehydrated and hydrogenated to hexanol. Hexanols can be converted into alkanes, like n-pentane and n-hexane through dehydrogenation/decarbonylation or dehydration/hydrogenation, respectively.

Most of the C_4 and C_5 oxygenates are obtained by decarbonylation reactions and can be converted into alkanes (n-butane and n-pentane) or into shorter oxygenates and alkanes through decarbonylation reactions. The retro-aldol condensation of sorbitol leads to C_2 and C_3 alcohols and polyols that are further converted into alcohols or alkanes by dehydration and hydrogenation reactions [225].

As a whole, the conversion of sorbitol mainly involves (i) the cleavage of the C–OH group through dehydrogenation/decarbonylation; (ii) the C–C bond breaking by retro-aldol condensation or (iii) the C–H and C–OH cleavage through the dehydration/hydrogenation route.
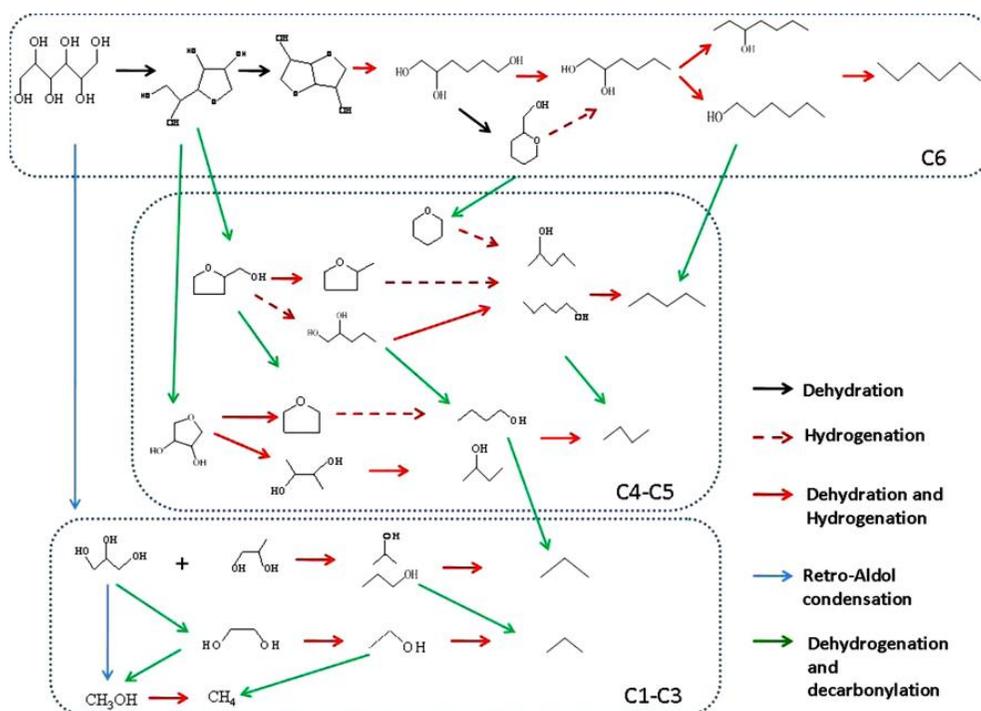
Figure 1.13 Reaction network in hydrodeoxygenation of sorbitol [226].

Dumesic and co-workers demonstrated, for the first time, that sorbitol can be hydrodeoxygenated into alkanes over a series of noble metals loaded over solid acid catalysts [72,73]. Zr-P is a promising solid-acid support for the HDO process, because it is stable in hydrothermal conditions, does not give leaching problems and it has more Brønsted acid sites than Lewis sites [227].

The addition of Fe to Pd appears a useful way to improve the catalytic activity. Indeed, the Pd_1Fe_3 sample supported on zirconia phosphate (Zr-P) shows a significant activity compared to other catalysts screened. A previous analysis shows that Fe addition to Pd plays a positive role, improving the activity up to 63 times for the hydrogenation of the carbonyl group, which is a fundamental step in HDO of biomass-derived oxygenated molecules [227-229]. As shown in Figure 1.14, the bimetallic Pd_1Fe_3/Zr-P affords the highest activity than other screened catalysts [227,230]. Authors reports the detailed product selectivity concerning 3% wt of Pd/Zr-P and Pd_1Fe_3/Zr-P catalysts, grouped by product functionality [227]. More C_1–C_4 products are formed upon adding Fe to Pd catalysts [230]. This stems from the higher amount of Fe-containing bimetallic sites [231]. Moreover, the Pd_1Fe_3/Zr-P shows a lower selectivity toward dehydration products (sorbitan and isosorbide). This means that the bimetallic catalyst promotes subsequent hydrogenolysis reactions of sorbitan and isosorbide through a series of dehydration/hydrogenation steps. Also in this case, the ability of the PdFe system to avoid undesired side reactions, such as methanation or methane reforming was confirmed. For a high conversion value (WHSV 0.16 h^{-1}) the presence of humins, derived from polymerization of isosorbide, was noticed [232].
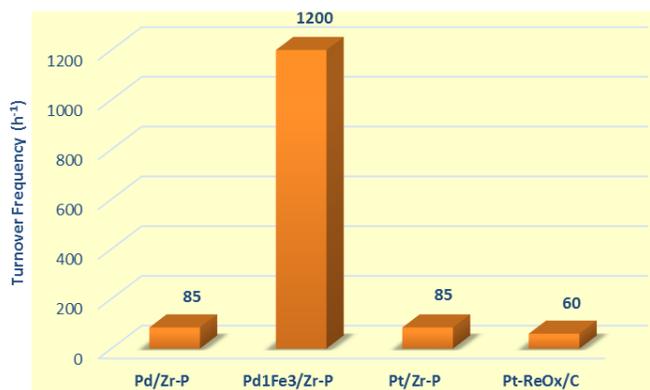
Figure 1.14 Comparison of TOF in HDO of sorbitol over Pd- and Pt-based catalysts [Adapted from Ref. 227].

In the presence of the Pd_1Fe_3/Zr-P catalyst a product mixture with an octane number (101) higher than that detected on using the Pd/Zr-P (92) is obtained. The bimetallic system is more selective in affording gasoline-range products, showing a higher yield (55%) than that of the Pd/Zr-P substrate (24%).

REFERENCES

[1] European directive 2009/28/CE.

[2] M. Pauly, K. Keegstra 'Cell-wall carbohydrates and their modification as a resource for biofuels' *Plant J.* **2008**, *54*, 559−568.

[3] H. Chen *Chemical composition and structure of natural lignocellulose. In Biotechnology of Lignocellulose: Theory and Practice* Springer Science Business Media B.V.: Dordrecht, The Netherlands, pp. 25–71, **2014**.

[4] C. Espro, B. Gumina, E. Paone, F. Mauriello 'Upgrading lignocellulosic biomasses: hydrogenolysis of platform derived molecules promoted by heterogeneous Pd-Fe catalysts' *Catalysts* **2017**, *7*, 78.

[5] C. Somerville, H. Youngs, C. Taylor, S.C. Davis, S.P. Long 'Feedstocks for lignocellulosic biofuels' *Science* **2010**, *329*, 790–792.

[6] C.O. Tuck, E. Pérez, I.T. Horváth, R.A. Sheldon, M. Poliakoff 'Valorization of biomass: Deriving more value from waste' *Science* **2012**, *337*, 695–699.

[7] K. Yan, Y. Yang, J. Chai, Y. Lu 'Catalytic reactions of gamma-valerolactone: a platform to fuels and value-added chemicals' *Appl. Catal. B Environ.* **2015**, *179*, 292–304.

[8] L. Hu, L. Lin, Z. Wu, S. Zhou, S. Liu 'Chemocatalytic hydrolysis of cellulose into glucose over solid acid catalysts' *Appl. Catal. B Environ.* **2015**, *174–175*, 225–243.

[9] L. Negahdar, I. Delidovich, R. Palkovits 'Aqueous-phase hydrolysis of cellulose and hemicelluloses over molecular acidic catalysts: Insights into the kinetics and reaction mechanism' *Appl. Catal. B Environ.* **2016**, *184*, 285–298.

[10] R.A. Sheldon 'Green and sustainable manufacture of chemicals from biomass: State of the art' *Green Chem.* **2014**, *16*, 950–963.

[11] Z. Zhang, J. Song, B. Han 'Catalytic transformation of lignocellulose into chemicals and fuel products in ionic liquids' *Chem. Rev.* **2017**, *117*, 6834–6880.

[12] C. Li, X. Zhao, A. Wang, G.H. Huber, T. Zhang 'Catalytic transformation of lignin for the production of chemicals and fuels' *Chem. Rev.* **2015**, *115*, 11559–11624.

[13] J.P. Lange 'Lignocellulose conversion: an introduction to chemistry, process and economics' *Biofuels Bioprod. Biorefin.* **2007**, *1*, 39–48.

[14] M. Stöcker 'Biofuels and biomass-to-liquid fuels in the biorefinery: Catalytic conversion of lignocellulosic biomass using porous materials' *Angew. Chem. Int. Ed.* **2008**, *47*, 9200–9211.

[15] L. Petrus, M.A. Noordermeer 'Biomass to biofuels, a chemical perspective' *Green Chem.* **2006**, *8*, 861–867.

[16] J. Artz, R. Palkovits 'Chemical building blocks from carbohydrates' *Current Opinion in Green and Sustainable Chemistry* **2018**.

[17] C. Espro, B. Gumina, T. Szumelda, E. Paone, F. Mauriello 'Catalytic transfer hydrogenolysis as an effective tool for the reductive upgrading of cellulose, hemicellulose, lignin, and their derived molecules' *Catalysts* **2018**, *8*, 313.

[18] R. Rinaldi, F. Schüth 'Design of solid catalysts for the conversion of biomass' *Energy Environ. Sci.* **2009**, *2*, 610–626.

[19] A. Cabiac, E. Guillon, F. Chambon, C. Pinel, F. Rataboul, N. Essayem 'Cellulose reactivity and glycosidic bond cleavage in aqueous phase by catalytic and non catalytic transformations' *Appl. Cat. A Gen*. **2011**, *402*, 1-10.

[20] L. Hu, L. Lin, Z. Wu, S. Zhou, S. Liu 'Chemocatalytic hydrolysis of cellulose into glucose over solid acid catalysts' *Appl. Cat. B Environ.* **2015**, *174-175*, 225-243.

[21] I. Delidovich, K. Leonhard, R. Palkovits 'Cellulose and hemicellulose valorisation: an integrated challenge of catalysis and reaction engineering' *Energy Environ. Sci.* **2014**, *7*, 2803–2830.

[22] X. Liu, X. Wang, S. Yao, Y. Jiang, J. Guan, X. Mu 'Recent advances in the production of polyols from lignocellulosic biomass and biomass-derived compounds' *RSC Adv.* **2014**, *4*, 49501–49520.

[23] W. Deng, Q. Zhang, Y. Wang 'Catalytic transformation of cellulose and its derived carbohydrates into chemicals involving C–C bond cleavage' *J. Energy Chem.* **2015**, *24*, 595–607.

[24] S. Zhao, G. Xu, C. Chang, S. Fang, Z. Liu, F. Du 'Direct conversion of carbohydrates into ethyl levulinate with potassium phosphotungstate as an efficient catalyst' *Catalysts* **2015**, *5*, 1897–1910.

[25] C. Antonetti, D. Licursi, S. Fulignati, G. Valentini, A.M. Raspolli Galletti 'New frontiers in the catalytic synthesis of levulinic acid: From sugars to raw and waste biomass as starting feedstock' *Catalysts* **2016**, *6*, 196.

[26] T. Werpy, G. Petersen, A. Aden, J. Bozell, J. Holladay, J. White, A. Manheim, D. Eliot, L. Lasure, S. Jones 'Top value added chemicals from biomass. Results of screening for potential candidates from sugars and synthesis gas' *U.S. Department of Energy: Oak Ridge*, TN, USA, **2004**.

[27] M. Pagliaro, M. Rossi *The Future of Glycerol*, 2nd ed.; Royal Society of Chemistry: Cambridge, UK, **2010**.

[28] C.H. Zhou, H. Zhao, D.S. Tong, L.M. Wu, W.H. Yu 'Recent advances in catalytic conversion of glycerol' *Catal. Rev.* **2013**, *55*, 369–453.

[29] R. Ciriminna, C. Della Pina, M. Rossi, M. Pagliaro 'Understanding the glycerol market' *Eur. J. Lipid Sci. Technol.* **2014**, *116*, 1432–1439.

[30] F. Mauriello, M.G. Musolino, R. Pietropaolo *Valorization of glycerol in propanediols production by catalytic processes: production, structure and applications in glycerol production, structure and applications*. De Santos Silva, M., Ferreira, P.C., Eds.; Nova Science Publishers: New York, NY, USA, pp. 45–76, **2012**.

[31] Z.Y. Zakaria, N.A.S. Amin, J. Linnekoski 'A perspective on catalytic conversion of glycerol to olefins' *Biomass Bioenergy* **2013**, *55*, 370–385.

[32] N.H. Tran, G.S.K. Kannangara 'Conversion of glycerol to hydrogen rich gas' *Chem. Soc. Rev.* **2013**, *42*, 9454–9479.

[33] C.H. Zhou, J.N. Beltramini, Y.X. Fan, G.Q. Lu 'Chemo-selective catalytic conversion of glycerol as a bio-renewable source to valuable commodity chemicals' *Chem. Soc. Rev.* **2008**, *37*, 527–549.

[34] Y. Nakagawa, K. Tomishige 'Heterogeneous catalysis of the glycerol hydrogenolysis' *Catal. Sci. Technol.* **2011**, *1*, 179–190.

[35] H.V. Scheller, P. Ulvskov 'Hemicelluloses' *Annu. Rev. Plant Biol.* **2010**, *61*, 263–289.

[36] Y. Huang, L. Wang, Y. Chao, D.S. Nawawi, T. Akiyama, T. Yokoyama, Y. Matsumoto 'Relationships between hemicellulose composition and lignin structure in woods' *J. Wood Chem. Technol.* **2016**, *36*, 9–15.

[37] R.F. Perez, M.A. Fraga 'Hemicellulose-derived chemicals: one-step production of furfuryl alcohol from xylose' *Green Chem.* **2014**, *16*, 3942–3950.

[38] F. Carvalheiro, L.C. Duarte, F.M. Gírio 'Hemicellulose biorefineries: a review on biomass pretreatment' *J. Sci. Ind. Res.* **2008**, *67*, 849–864.

[39] X.-J. Ji, H. Huang, Z.-K. Nie, L. Qu, Q. Xu, G.T. Tsao 'Fuels and chemicals from hemicellulose sugars' *Adv. Biochem. Eng./Biotechnol.* **2012**, *128*, 199–224.

[40] A.S. Mamman, J.-M. Lee, Y.-C. Kim, I.T. Hwang, N.J. Park, Y.K. Hwang, J.-S. Chang, J.-S. Hwang 'Furfural: hemicellulose/xylose-derived biochemical' *Biofuels Bioprod. Biorefin.* **2008**, *2*, 438–454.

[41] X. Li, P. Jia, T. Wang 'Furfural: a promising platform compound for sustainable production of C_4 and C_5 chemicals' *ACS Catal.* **2016**, *6*, 7621–7640.

[42] R. Pizzi, R.-J. Van Putten, H. Brust, S. Perathoner, G. Centi, J.C. Van der Waal 'High-throughput screening of heterogeneous catalysts for the conversion of furfural to bio-based fuel components' *Catalysts* **2015**, *5*, 2244–2257.

[43] R. Mariscal, P. Maireles-Torres, M. Ojeda, I. Sádaba, M. Lòpez Granados 'Furfural: a renewable and versatile platform molecule for the synthesis of chemicals and fuels' *Energy Environ. Sci.* **2016**, *9*, 1144–1189.

[44] C. Xu, R.A.D. Arancon, J. Labidi, R. Luque 'Lignin depolymerisation strategies: towards valuable chemicals and fuels' *Chem. Soc. Rev.* **2014**, *43*, 7485–7500.

[45] P.J. Deuss, K. Barta 'From models to lignin: transition metal catalysis for selective bond cleavage reactions' *Coord. Chem. Rev.* **2016**, *306*, 510–532.

[46] M. Zaheer, R. Kempe 'Catalytic hydrogenolysis of aryl ethers: a key step in lignin valorization to valuable chemicals' *ACS Catal.* **2015**, *5*, 1675–1684.

[47] J. Zakzeski, P.C.A. Bruijnincx, A.L. Jongerius, B.M. Weckhuysen 'The catalytic valorization of lignin for the production of renewable chemicals' *Chem. Rev.* **2010**, *110*, 3552–3599.

[48] A.M. Robinson, J.E. Hensley, J.W. Medlin 'Bifunctional catalysts for upgrading of biomass-derived oxygenates: a review' *ACS Catal.* **2016**, *6*, 5026–5043.

[49] A.G. Sergeev, J.F. Hartwig 'Selective, nickel-catalyzed hydrogenolysis of aryl ethers' *Science* **2011**, *332*, 439–443.

[50] A.G. Sergeev, J.D. Webb, J.F. Hartwig 'A heterogeneous nickel catalyst for the hydrogenolysis of aryl ethers without arene hydrogenation' *J. Am. Chem. Soc.* **2012**, *134*, 20226–20229.

[51] J. He, C. Zhao, J.A. Lercher 'Ni-catalyzed cleavage of aryl ethers in the aqueous phase' *J. Am. Chem. Soc.* **2012**, *134*, 20768–20775.

[52] J. He, L. Lu, C. Zhao, D. Mei, J.A. Lercher 'Mechanisms of catalytic cleavage of benzyl phenyl ether in aqueous and apolar phases' *J. Catal.* **2014**, *311*, 41–51.

[53] J. He, L. Lu, C. Zhao, D. Mei, J.A. Lercher 'Mechanisms of selective cleavage of C–O bonds in diaryl ethers in aqueous phase' *J. Catal.* **2014**, *309*, 280–290.

[54] X. Wang, R. Rinaldi 'A route for lignin and bio-oil conversion: Dehydroxylation of phenols into arenes by catalytic tandem reactions' *Angew. Chem. Int. Ed.* **2013**, *52*, 11499–11503.

[55] X. Wang, R. Rinaldi 'Solvent effects on the hydrogenolysis of diphenyl ether with raney nickel and their implications for the conversion of lignin' *ChemSusChem* **2012**, *5*, 1455–1466.

[56] G.S. Macala, T.D. Matson, C.L. Johnson, R.S. Lewis, A.V. Iretskii, P.C. Ford 'Hydrogen transfer from supercritical methanol over a solid base catalyst: a model for lignin depolymerization' *ChemSusChem* **2009**, *2*, 215–217.

[57] K. Barta, T.D. Matson, M.L. Fettig, S.L. Scott, A.V. Iretskii, P.C. Ford 'Catalytic disassembly of an organosolv lignin via hydrogen transfer from supercritical methanol' *Green Chem.* **2010**, *12*, 1640–1648.

[58] M.V. Galkin, S. Sawadjoon, V. Rohde, M. Dawange, J.S.M. Samec 'Mild Heterogeneous Palladium-catalyzed cleavage of β-O-40-ether linkages of lignin model compounds and native lignin in air' *ChemCatChem* **2013**, *6*,179–184.

[59] M.V. Galkin, J.S.M. Samec 'Selective route to 2-propenyl aryls directly from wood by a tandem organosolv and palladium-catalysed transfer hydrogenolysis' *ChemSusChem* **2014**, *7*, 2154–2158.

[60] M.V. Galkin, C. Dahlstrand, J. Samec 'Mild and robust redox-neutral Pd/C-catalyzed lignol β-O-4' bond cleavage through a low-energy-barrier pathway' *ChemSusChem* **2015**, *8*, 2187–2192.

[61] A. Toledano, L. Serrano, J. Labidi, A. Pineda, A.M. Balu, R. Luque 'Heterogeneously catalysed mild hydrogenolytic depolymerisation of lignin under microwave irradiation with hydrogen-donating solvents' *ChemCatChem* **2012**, *5*, 977–985.

[62] M. Schlaf 'Selective deoxygenation of sugar polyols to α, ω-diols and other oxygen content reduced materials - a new challenge to homogeneous ionic hydrogenation and hydrogenolysis catalysis' *Dalt. Trans.* **2006**, *39*, 4645–4653.

[63] S. De, B. Saha, R. Luque 'Hydrodeoxygenation processes: advances on catalytic transformations of biomass-derived platform chemicals into hydrocarbon fuels' *Bioresour. Technol.* **2015**, *178*, 108–118.

[64] G.J.S. Dawes, E.L. Scott, J. Le Nôtre, J.P.M. Sanders, J.H. Bitter 'Deoxygenation of biobased molecules by decarboxylation and decarbonylation—a review on the role of heterogeneous, homogeneous and bio-catalysis' *Green Chem.* **2015**, *17*, 3231-3250.

[65] A.M. Ruppert, K. Weinberg, R. Palkovits 'Hydrogenolysis goes bio: From carbohydrates and sugar alcohols to platform chemicals' *Angew. Chem. Int. Ed.* **2012**, *51*, 2564–2601.

[66] D. Wang, D. Astruc 'The golden age of transfer hydrogenation' *Chem. Rev.* **2015**, *115*, 6621–6686.

[67] R.A.W. Johnstone, A.H. Wilby, I.D. Entwistle 'Heterogeneous catalytic transfer hydrogenation and its relation to other methods for reduction of organic compounds' *Chem. Rev.* **1985**, *85*, 129–170.

[68] G. Brieger, T.J. Nestrick 'Catalytic transfer hydrogenation' *Chem. Rev.* **1974**, *74*, 567–580.

[69] M.J. Gilkey, B. Xu 'Heterogeneous catalytic transfer hydrogenation as an effective pathway in biomass upgrading' *ACS Catal.* **2016**, *6*, 1420–1436.

[70] E. Knoevenagel, B. Bergdolt 'Ueber das Verhalten des D2.5-Dihydroterephtalsäuredimethylesters bei höheren Temperaturen und in Gegenwart von Palladiummohr' *Eur. J. Inorg. Chem.* **1903**, *36*, 2857–2860.

[71] R.D. Cortright, R.R. Davda, J.A. Dumesic 'Hydrogen from catalytic reforming of biomass-derived hydrocarbons in liquid water' *Nature* **2002**, *418*, 964–967.

[72] R.R. Davda, J.A. Dumesic 'Catalytic reforming of oxygenated hydrocarbons for hydrogen with low levels of carbon monoxide' *Angew. Chem. Int. Ed.* **2003**, *42*, 4068–4071.

[73] J.O. Metzger 'Production of liquid hydrocarbons from biomass' *Angew. Chem. Int. Ed.* **2006**, *45*, 696–698.

[74] E.L. Kunkes, D.A. Simonetti, R.M. West, J.C. Serrano-Ruiz, C.A. Gärtner, J.A. Dumesic 'Catalytic conversion of biomass to monofunctional hydrocarbons and targeted liquid-fuel classes' *Science* **2008**, *322*, 417–421.

[75] R.R. Davda, J.W. Shabaker, G.W. Huber, R.D. Cortright, J.A. Dumesic 'Aqueous-phase reforming of ethylene glycol on silica-supported metal catalysts' *Appl. Catal. B Environ.* **2003**, *43*, 13–26.

[76] R.R. Davda, J.W. Shabaker, G.W. Huber, R.D. Cortright, J.A. Dumesic 'A review of catalytic issues and process conditions for renewable hydrogen and alkanes by aqueous-phase reforming of oxygenated hydrocarbons over supported metal catalysts' *Appl. Catal. B Environ.* **2005**, *56*, 171–186.

[77] G.W. Huber, J.W. Shabaker, J.A. Dumesic 'Raney Ni-Sn catalyst for H_2 production from biomass-derived hydrocarbons' *Science* **2003**, *300*, 2075–2077.

[78] J.W. Shabaker, R.R. Davda, G.W. Huber, R.D. Cortright, J.A. Dumesic 'Aqueous-phase reforming of methanol and ethylene glycol over alumina-supported platinum catalysts' *J. Catal.* **2003**, *215*, 344–352.

[79] J.W. Shabaker, J.A. Dumesic 'Kinetics of aqueous-phase reforming of oxygenated hydrocarbons: Pt/Al_2O_3 and Sn-modified Ni catalysts' *Ind. Eng. Chem. Res.* **2004**, *43*, 3105–3112.

[80] J.W. Shabaker, G.W. Huber, R.R. Davda, R.D. Cortright, J.A. Dumesic 'Aqueous-phase reforming of ethylene glycol over supported platinum catalysts' *Catal. Lett.* **2003**, *88*, 1–8.

[81] J.W. Shabaker, G.W. Huber, J.A. Dumesic 'Aqueous-phase reforming of oxygenated hydrocarbons over Sn-modified Ni catalysts' *J. Catal.* **2004**, *222*, 180–191.

[82] J.W. Shabaker, D.A. Simonetti, R.D. Cortright, J.A. Dumesic 'Sn-modified Ni catalysts for aqueous-phase reforming: characterization and deactivation studies' *J. Catal.* **2005**, *231*, 67–76.

[83] H.E. Fierz-David, M. Hannig 'Über die Destillation von Cellulose, Holz und ähnlichen Stoffen unter Wasserstoffdruck mit Katalysatoren' *Helv. Chim. Acta* **1925**, *8*, 900-923.

[84] H.R. Appell, I. Wender, R.D. Miller 'Conversion of urban refuse to oil' *U.S. Bureau of Mines*, Washinghton D.C., Technical Rep. 25, **1969**.

[85] J.A. Kaufman, D.V. Gupta, T.S. Szatkowski, A.H. Weiss 'Catalytic hydrogenation of solid waste carbohydrates to fuel oil' *Chem. Ing. Tech.* **1974**, *14*, 609.

[86] D.V. Gupta, W.L. Kranich, A.H. Weiss 'Catalytic hydrogenation and hydrocracking of oxygenated compounds to liquid and gaseous fuels' *Ind. Eng. Chem. Process Des. Dev.* **1976**, *15*, 256-260.

[87] G.C. Bond, A.J. Bird US Patent 4 396 786, **1983**.

[88] E. Berl 'Production of oil from plant material' *Science* **1944**, *99*, 309-312.

[89] K.L. Lautenschläger, M. Bockmühl, G. Ehrhart US Patent 1 915 431, **1933**.

[90] H.H. Gürkan US Patent 2 488 722, **1949**.

[91] L. Meiler, H. Scholler US Patent 1 641 771, **1927**.

[92] E.E. Harris, E. Beglinger Madison 'Wood Sugar Process' *Ind. Eng. Chem.* **1946**, *38*, 890-895.

[93] S. Van de Vyer, J. Geboers, P.A. Jacobs, B.F. Sels 'Recent advances in the catalytic conversion of cellulose' *ChemCatChem* **2011**, *3*, 82-94.

[94] A. Fukuoka, P.L. Dhepe 'Catalytic conversion of cellulose into sugar alcohols' *Angew. Chem. Int. Ed.* **2006**, *45*, 5161-5163.

[95] P.L. Dhepe, A. Fukuoka 'Cracking of cellulose over supported metal catalysts' *Catal. Surv. Asia* **2007**, *11*, 186-191.

[96] C. Luo, S. Wang, H. Liu 'Cellulose conversion into polyols catalyzed by reversibly formed acids and supported ruthenium clusters in hot water' *Angew. Chem. Int. Ed.* **2007**, *46*, 7636-7639.

[97] W. Deng, X. Tan, W. Fang, Q. Zhang, Y. Wang 'Conversion of cellulose into sorbitol over carbon nanotube-supported ruthenium catalyst' *Catal. Lett.* **2009**, *133*, 167.

[98] R. Palkovits, K. Tajvidi, J. Procelewska, R. Rinaldi, A.M. Ruppert 'Hydrogenolysis of cellulose combining mineral acids and hydrogenation catalysts' *Green Chem.* **2010**, *12*, 972-978.

[99] R. Palkovits, K. Tajvidi, A.M. Ruppert, J. Procelewska 'Heteropoly acids as efficient acid catalysts in the one-step conversion of cellulose to sugar alcohols' *Chem Commun.* **2011**, *47*, 576-578.

[100] J. Geboers, S. Van de Vyver, K. Carpentier, K. de Blochouse, P. Jacobs, B. Sels 'Efficient catalytic conversion of concentrated cellulose feeds to hexitols with heteropoly acids and Ru on carbon' *Chem Commun.* **2010**, *46*, 3577-3579.

[101] J. Geboers, S. Van de Vyver, K. Carpentier, P. Jacobs, B. Sels 'Hydrolytic hydrogenation of cellulose with hydrotreated caesium salts of heteropoly acids and Ru/C' *Green Chem.* **2011**, *13*, 2167-2174.

[102] J. Geboers, S. Van de Vyver, K. Carpentier, P. Jacobs, B. Sels 'Efficient hydrolytic hydrogenation of cellulose in the presence of Ru-loaded zeolites and trace amounts of mineral acid' *Chem Commun.* **2011**, *47*, 5590-5592.

[103] Z. Tai, J. Zhang, A. Wang, M. Zheng, T. Zhang 'Temperature-controlled phase-transfer catalysis for ethylene glycol production from cellulose' *Chem. Commun.* **2012**, *48*, 7052-7054.

[104] Z. Wu, S. Ge, C. Ren, M. Zhang, A. Yip, C. Xu 'Selective conversion of cellulose into bulk chemicals over Brønsted acid-promoted ruthenium catalyst: one-pot vs. sequential process' *Green Chem.* **2012**, *14*, 3336-3343.

[105]N. Meine, R. Rinaldi, F. Schüth 'Solvent-free catalytic depolymerization of cellulose to water-soluble oligosaccharides' *ChemSusChem* **2012**, *5*, 1449-1454.

[106]J. Hilgert, N. Meine, R. Rinaldi, F. Schüth 'Mechanocatalytic depolymerization of cellulose combined with hydrogenolysis as a highly efficient pathway to sugar alcohols' *Energy Environ. Sci.* **2013**, *6*, 92-96.

[107]M.D. Kaufman Rechulski, M. Käldström, U. Richter, F. Schüth, R. Rinaldi 'Mechanocatalytic depolymerization of lignocellulose performed on hectogram and kilogram scales' *Ind. Eng. Chem. Res.* **2015**, *54*, 4581–4592.

[108]M. Yabushita, H. Kobayashi, K. Hara, A. Fukuoka 'Quantitative evaluation of ball-milling effects on the hydrolysis of cellulose catalyzed by activated carbon' *Catal. Sci. Technol.* **2014**, *4*, 2312-2317.

[109]A. Shrotri, H. Kobayashi, A. Fukuoka 'Efficient catalytic conversion of cellulose to platform chemicals using mechanical treatment' *J. Jpn. Petrol Inst.* **2015**, *58*, 1-8.

[110]H. Kobayashi, H. Kaiki, A. Shrotri, K. Techikawara, A. Fukuoka 'Hydrolysis of woody biomass by a biomass-derived reusable heterogeneous catalyst' *Chem. Sci.* **2016**, *7*, 692-696.

[111]N. Ji, T. Zhang, M. Zheng, A. Wang, H. Wang, X. Wang, J.G. Chen 'Direct catalytic conversion of cellulose into ethylene glycol using nickel-promoted tungsten carbide catalysts' *Angew. Chem. Int. Ed.* **2008**, *47*, 8510-8513.

[112]J. Pang, M. Zheng, A. Wang, T. Zhang 'Catalytic hydrogenation of corn stalk to ethylene glycol and 1,2-propylene glycol' *Ind. Eng. Chem. Res.* **2011**, *50*, 6601-6608.

[113]C. Li, M. Zheng, A. Wang and T. Zhang 'One-pot catalytic hydrocracking of raw woody biomass into chemicals over supported carbide catalysts: simultaneous conversion of cellulose, hemicellulose and lignin' *Energy Environ. Sci.* **2012**, *5*, 6383-6390.

[114]M. Zheng, A. Wang, N. Ji, J. Pang, X. Wang, T. Zhang 'Transition metal–tungsten bimetallic catalysts for the conversion of cellulose into ethylene glycol' *ChemSusChem* **2010**, *3*, 63-66.

[115] Z. Tai, J. Zhang, A. Wang, J. Pang, M. Zheng, T. Zhang 'Catalytic conversion of cellulose to ethylene glycol over a low-cost binary catalyst of raney Ni and tungstic acid' *ChemSusChem* **2013**, *6*, 652-658.

[116] J. Pang, A. Wang, M. Zheng, Y. Zhang, Y. Huang, X. Chen, T. Zhang 'Catalytic conversion of cellulose to hexitols with mesoporous carbon supported Ni-based bimetallic catalysts' *Green Chem.* **2012**, *14*, 614-617.

[117] X. Wang, L. Meng, F. Wu, Y. Jiang, L. Wang and X. Mu 'Efficient conversion of microcrystalline cellulose to 1,2-alkanediols over supported Ni catalysts' *Green Chem.* **2012**, *14*, 758-765.

[118] S. Van de Vyver, J. Geboers, M. Dusselier, H. Schepers, T. Vosch, L. Zhang, G. VanTendeloo, P.A. Jacobs, B.F. Sels 'Selective bifunctional catalytic conversion of cellulose over reshaped Ni particles at the tip of carbon nanofibers' *ChemSusChem* **2010**, *3*, 698-701.

[119] K. Tajvidi, K. Pupovac, M. Kükrek, R. Palkovits 'Copper-based catalysts for efficient valorization of cellulose' *ChemSusChem* **2012**, *5*, 2139-2142.

[120] Z. Xiao, S. Jin, M. Pang, C. Liang 'Conversion of highly concentrated cellulose to 1,2-propanediol and ethylene glycol over highly efficient CuCr catalysts' *Green Chem.* **2013**, *15*, 891-895.

[121] L. Deng, J. Li, D.-M. Lai, Y. Fu, Q.-X. Guo 'Catalytic conversion of biomass-derived carbohydrates into γ-valerolactone without using an external H_2 supply' *Angew. Chem. Int. Ed.* **2009**, *48*, 6529 –6532.

[122] H. Heeres, R. Handana, D. Chunai, C.B. Rasrendra, B. Girisuta, H.J. Heeres 'Combined dehydration/(transfer)-hydrogenation of C_6-sugars (D-glucose and D-fructose) to γ-valerolactone using ruthenium catalysts' *Green Chem.* **2009**, *11*, 1247–1255

[123] X.-L. Du, L. He, S. Zhao, Y.-M. Liu, Y. Cao, H.-Y. He, K.-N. Fan 'Hydrogen-independent reductive transformation of carbohydrate biomass into γ-valerolactone and pyrrolidone derivatives with supported gold catalysts' *Angew. Chem.* **2011**, *123*, 7961–7965.

[124] D. Scholz, C. Aellig, C. Mondelli, J. Pèrez-Ramìrez 'Continuous transfer hydrogenation of sugars to alditols with bioderived donors over Cu–Ni–Al catalysts' *ChemCatChem* **2015**, *7*, 1551 – 1558.

[125]A.J. van Hengstum, A.P.G. Kieboom, H. van Bekkum 'Catalytic transfer hydrogenation of glucose-fructose syrups in alkaline solution' *Starch* **1984**, *36*, 317-320.

[126]H. Kobayashi, H. Matsuhashi, T. Komanoya, K. Hara, A. Fukuoka 'Transfer hydrogenation of cellulose to sugar alcohols over supported ruthenium catalysts' *Chem. Commun.* **2011**, *47*, 2366-2368.

[127]A. Shrotri, H. Kobayashi, A. Tanksale, A. Fukuoka, J. Beltramini 'Transfer hydrogenation of cellulose-based oligomers over carbon-supported ruthenium catalyst in a fixed-bed reactor' *ChemCatChem* **2014**, *6*, 1349-1356.

[128]M.G. Musolino, L.A. Scarpino, F. Mauriello, R. Pietropaolo 'Selective transfer hydrogenolysis of glycerol promoted by palladium catalysts in absence of hydrogen' *Green Chem.* **2009**, *11*, 1511-1513.

[129]F. Mauriello, H. Ariga, M.G. Musolino, R. Pietropaolo, S. Takakusagi, K. Asakura 'Exploring the catalytic properties of supported palladium catalysts in the transfer hydrogenolysis of glycerol' *Appl. Catal. B Environ.* **2015**, *166-167*, 121-131.

[130]I. Gandarias, P.L. Arias, J. Requies, M. El Doukkali, M.B. Güemez 'Liquid-phase glycerol hydrogenolysis to 1,2-propanediol under nitrogen pressure using 2-propanol as hydrogen source' *J. Catal.* **2011**, *282*, 237–247.

[131]I. Gandarias, P.L. Arias, S.G. Fernández, J. Requies, M. El Doukkali, M.B. Güemez 'Hydrogenolysis through catalytic transfer hydrogenation: Glycerol conversion to 1,2-propanediol' *Catal. Tod.* **2012**, *195*, 22– 31.

[132]I. Gandarias, J. Requies, P.L. Arias, U. Armbruster, A. Martin 'Liquid-phase glycerol hydrogenolysis by formic acid over Ni–Cu/Al$_2$O$_3$ catalysts' *J. Catal.* **2012**, *290*, 79–89.

[133]R.B. Mane, C.V. Rode 'Continuous dehydration and hydrogenolysis of glycerol over non-chromium copper catalyst: laboratory-scale process studies' *Org. Process Res. Dev.* **2012**, *16*, 1043–1052.

[134]J. Yuan, S. Li, L. Yu, Y. Liu, Y. Cao 'Efficient catalytic hydrogenolysis of glycerol using formic acid as hydrogen source' *Chinese J. Catal.* **2013**, *34*, 2066–2074.

[135]S. Xia, Z. Yuan, L. Wang, P. Chen, Z. Hou 'Hydrogenolysis of glycerol on bimetallic Pd-Cu/solid-base catalysts prepared via layered double hydroxides precursors' *Appl. Catal. A Gen.* **2011**, *403*, 173– 182.

[136]A. Bienholz, H. Hofmann, P. Claus 'Selective hydrogenolysis of glycerol over copper catalysts both in liquid and vapour phase: Correlation between the copper surface area and the catalyst's activity' *Appl. Catal. A: Gen.* **2011**, *391*, 153–157.

[137]S. Xia, Z. Yuan, L. Wang, P. Chen, Z. Hou 'Catalytic production of 1,2-propanediol from glycerol in bio-ethanol solvent' *Biores. Technol.* **2012**, *104*, 814–817.

[138]M.G. Musolino, L.A. Scarpino, F. Mauriello, R. Pietropaolo 'Glycerol hydrogenolysis promoted by supported palladium catalysts' *ChemSusChem* **2011**, *4*, 1143 – 1150.

[139]L. Gong, Y. Lü, Y. Ding, R. Lin, J. Li, W. Dong, T. Wang, W. Chen 'Solvent effect on selective dehydroxylation of glycerol to 1,3-propanediol over a Pt/WO$_3$/ZrO$_2$ catalyst' *Chin. J. Catal.* **2009**, *30*, 1189–1191.

[140]Y. Liu, H. Tüysü, C.-J. Jia, M. Schwickardi, R. Rinaldi, A.-H. Lu, W. Schmidt, F. Schüt 'From glycerol to allyl alcohol: iron oxide catalyzed dehydration and consecutive hydrogen transfer' *Chem. Commun.* **2010**, *46*, 1238–1240.

[141]A. Konaka, T. Tago, T. Yoshikawa, A. Nakamura, T. Masuda 'Conversion of glycerol into allyl alcohol over potassium-supported zirconia–iron oxide catalyst' *Appl. Catal. B: Envir.* **2014**, *146*, 267– 273.

[142]E. Arceo, P. Marsden, R.G. Bergman, J.A. Ellman 'An efficient didehydroxylation method for the biomass-derived polyols glycerol and erythritol. Mechanistic studies of a formic acid-mediated deoxygenation' *Chem. Commun.* **2009**, 3357–3359.

[143]J.R. Dethlefsen, D. Lupp, A. Teshome, L.B. Nielsen, P. Fristrup 'Molybdenum-catalyzed conversion of diols and biomass-derived polyols to alkenes using isopropyl alcohol as reductant and solvent' *ACS Catal.* **2015**, *5*, 3638–3647.

[144]G. Wen, Y. Xu, Z. Xu, Z. Tian 'Direct conversion of cellulose into hydrogen by aqueous-phase reforming process' *Catal. Commun.* **2010**, *11*, 522–526.

[145] M.M. Rahman, T.L. Church, M.F. Variava, A.T. Harris, A.I. Minett 'Bimetallic Pt–Ni composites on ceria-doped alumina supports as catalysts in the aqueous-phase reforming of glycerol' *RSC Adv.* **2014**, *4*, 18951–18960.

[146] C. He, J. Zheng, K. Wang, H. Lin, J.Y. Wang, Y. Yang 'Sorption enhanced aqueous phase reforming of glycerol for hydrogen production over Pt-Ni supported on multi-walled carbon nanotubes' *Appl. Catal. B Environ* **2015**, *162*, 401–411.

[147] D.J.M.D. Vlieger, B.L. Mojet, L. Lefferts, K. Seshan 'Aqueous phase reforming of ethylene glycol − Role of intermediates in catalyst performance' *J. Catal.* **2012**, *292*, 239–245.

[148] G.W. Huber, J.W. Shabaker, S.T. Evans, J.A. Dumesic 'Aqueous-phase reforming of ethylene glycol over supported Pt and Pd bimetallic catalysts' *Appl. Catal. B Environ.* **2006**, *62*, 226–235.

[149] X. Wang, N. Li, Z. Zhang, C. Wang, L.D. Pfefferle, G.L. Haller 'High-yield hydrogen production from aqueous phase reforming over single-walled carbon nanotube supported catalysts' *ACS Catal.* **2012**, *2*, 1480–1486.

[150] P.J. Dietrich, M.C. Akatay, F.G. Sollberger, E.A. Stach, J.T. Miller, W.N. Delgass, F.H. Ribeiro 'Effect of Co loading on the activity and selectivity of PtCo aqueous phase reforming catalysts' *ACS Catal.* **2014**, *4*, 480–491.

[151] X. Wang, N. Li, L.D. Pfefferle, G.L. Haller 'Pt-Co bimetallic catalyst supported on single-walled carbon nanotubes: effect of alloy formation and oxygen containing groups' *J. Phys. Chem. C* **2010**, *114*, 16996–17002.

[152] A.V.H. Soares, G. Perezc, F.B. Passos 'Alumina supported bimetallic Pt–Fe catalysts applied to glycerol hydrogenolysis and aqueous phase reforming' *Appl. Catal. B Environ* **2016**, *185*, 77–87.

[153] F. Bossola, X.I. Pereira-Hernández, C. Evangelisti, Y. Wang, V.D. Santo 'Investigation of the promoting effect of Mn on a Pt/C catalyst for the steam and aqueous phase reforming of glycerol' *J. Catal.* **2017**, *349*, 75–83.

[154] A. Ciftci, D.A.J.M. Ligthart, E.J.M. Hensen 'Aqueous phase reforming of glycerol over Re-promoted Pt and Rh catalysts' *Green Chem.* **2014**, *16*, 853–863.

[155] D.L. King, L. Zhang, G. Xia, A.M. Karim, D.J. Heldebrant, X. Wang, T. Peterson, Y. Wang 'Aqueous phase reforming of glycerol for hydrogen production over Pt–Re supported on carbon' *Appl. Catal. B Environ* **2010**, *99*, 206–213.

[156] Z. Wei, A. Karim, Y. Li, Y. Wang 'Elucidation of the roles of Re in aqueous-phase reforming of glycerol over Pt–Re/C catalysts' *ACS Catal.* **2015**, *5*, 7312–7320.

[157] A. Ciftci, D.A.J.M. Ligthart, A.O. Sen, A.J.F.V. Hoof, H. Friedrich, E.J.M. Hensen 'Pt-Re synergy in aqueous-phase reforming of glycerol and the water−gas shift reaction' *J. Catal.* **2014**, *311*, 88−101.

[158] G. Wen, C. Wang, Y. Xu, Q. Liu, H. Liu, Z. Tian 'Preparation of Ce-modified Raney Ni catalysts and their application in aqueous- phase reforming of cellulose' *Catal. Lett*. **2011**, *141*, 1851−1858.

[159] M.M. Rahman, T.L. Church, A.I. Minett, A. T. Harris, A. T. 'Effect of CeO_2 addition to Al_2O_3 supports for Pt catalysts on the aqueous phase reforming of glycerol' *ChemSusChem* **2013**, *6*, 1006−1013.

[160] J. Liu, B. Sun, J. Hu, Y. Pei, H. Li, M. Qiao 'Aqueous-phase reforming of ethylene glycol to hydrogen on Pd/Fe_3O_4 catalyst prepared by co-precipitation: Metal−support interaction and excellent intrinsic activity' *J. Catal.* **2010**, *274*, 287−295.

[161] Y. Xu, Z. Tian, G. Wen, Z. Xu, W. Qu, L. Lin 'Production of CO_x-free hydrogen by alkali enhanced hydrothermal catalytic reforming of biomass-derived alcohols' *Chem. Lett.* **2006**, *35*, 216− 217.

[162] J. Liu, X. Chu, L. Zhu, R.D. Jiye Hu, S. Xie, Y. Pei, S. Yan, M. Qiao, K. Fan 'Simultaneous aqueous-phase reforming and KOH carbonation to produce CO_x-free hydrogen in a single reactor' *ChemSusChem* **2010**, *3*, 803−806.

[163] T.V. Haasterecht, C.C.I. Ludding, K.P.D. Jong, J.H. Bitter 'Toward stable nickel catalysts for aqueous phase reforming of biomass derived feedstock under reducing and alkaline conditions' *J. Catal.* **2014**, *319*, 27−35.

[164] E. Christoffersen, P. Liu, A. Ruban, H.L. Skriver, J.K. Nørskov 'Anode materials for low-temperature fuel cells: a density functional theory study' *J. Catal.* **2001**, *199*, 123−131.

[165]J.R. Kitchin, J.K. Nørskov, M.A. Barteau, J.G. Chen 'Modification of the surface electronic and chemical properties of Pt(111) by subsurface 3d transition metals' *J. Chem. Phys.* **2004**, *120*, 10240−10246.

[166]J. Greeley, M. Mavrikakis 'Alloy catalysts designed from first principles' *Nat. Mater.* **2004**, *3*, 810−815.

[167]F. Liao, T.W.B. Lo, S.C.E. Tsang 'Recent developments in palladium-based bimetallic catalysts' *ChemCatChem* **2015**, *7*, 1998–2014.

[168] A.O. Menezes, M.T. Rodrigyes, A. Zimmaro, L.E.P. Borges, M.A. Fraga 'Production of renewable hydrogen from aqueous-phase reforming of glycerol over Pt catalysts supported on different oxides' *Renew. Energ.* **2011**, *36*, 595–599.

[169]S. Irmak, M. Kurtulus, A. Hasanoglu, O. Erbatur 'Gasification efficiencies of cellulose, hemicellulose and lignin fractions of biomass in aqueous media by using Pt on activated carbon catalyst' *Biomass Bioenergy* **2013**, *49*, 102–108.

[170]G. Wen, Y. Xu, Z. Xu, Z. Tian 'Direct conversion of cellulose into hydrogen by aqueous-phase reforming process' *Catal. Commun.* **2010**, *11*, 522–526.

[171]A.C. Chang, Y.S. Lee, K.H. Lin 'Simultaneous bio-hydrogen and reducing sugar formation by the aqueous phase biomass reforming' *Int. J. Hydrogen Energy* **2012**, *37*, 15691-15695.

[172]R.D. Cortright 'Hydrogen generation from biomass-derived carbohydrates via the aqueous phase reforming (APR) process' award number: DEFG36- 05G15046 (2005-2008), *DOE Hydrogen Program FY 2005 Progress Report*, **2005**.

[173] Virent http://www.virent.com/technology/bioforming, **2015**.

[174](a) J. Monnier, Y. Zang, A. MacFarlain WO Patent 2009/129622, **2009**; (b) J. Monnier, Y. Zang, A. MacFarlain US Patent 8 673 262 (B2), **2014**.

[175]R.D. Cortright, G.A. Dumesic US Patent 6 699 457 (B2), **2004**.

[176](a) R.D. Cortright US Patent 8 754 263 (B2), 2014. (b) R.D. Cortright WO Patent 2008/069830, **2008**.

[177]J.N. Chheda, J.B. Powell WO Patent 2012/088078 (A2), **2012**.

[178] L. Ma, T. Wang, Z. Yuan, X. Zhang, X. Zhuang, C. Wu, T. Jiang, Q. Zhang US Patent 2012/0216451 (A1), **2012**.

[179] L. Vilcocq, A. Cabiac, C. Especel, E. Guillon, D. Duprez 'Transformation of sorbitol to biofuels by heterogeneous catalysis: chemical and industrial considerations' *Oil Gas Sci. Technol.* **2013**, *68*, 841-860.

[180] P.B. Kettler 'Platinum group metals in catalysis: Fabrication of catalysts and catalyst precursors' *Org. Proc. Res. Dev.* **2003**, *7*, 342–354.

[181] P.B. Wells, A.G. Wilkinson 'Platinum group metals as heterogeneous enantioselective catalysts' *Top. Catal.* **1998**, *5*, 39–50.

[182] G.J.K. Acres 'Platinum group metal catalysis at the end of this century' *Platinum Met. Rev.* **1984**, *28*, 150–157.

[183] F. Hartley 'Chemistry of the Platinum Group Metals' 1st ed.; Elsevier Science: Central Milton Keynes, UK, **2008**.

[184] Heraeus, 'Platinum & Palladium Focus 2016' Available online: https://www.heraeus.com/media/media/group/doc_group/precious_me tals/Platinum__Palladium_Focus_2016Europe.pdf

[185] ETF Securities (US) LLC. Platinum and Palladium: Riding theWave of an Expanding AutoMarket. Available online: https://www.etfsecurities.com/Documents/PP%20Commentary%20sub mitted%20to%20ALPS.pdf

[186] A. Tungler, T. Tarnai, L. Hegediis, K. Fodor 'Palladium-mediated heterogeneous catalytic hydrogenations' *Platinum Met. Rev.* **1998**, *42*, 108–115.

[187] D. Astruc, F. Lu, J.R. Aranzaes 'Nanoparticles as recyclable catalysts: The frontier between homogeneous and heterogeneous catalysis' *Angew. Chem. Int. Ed.* **2005**, *48*, 7852–7872.

[188] A. Brennführer, H. Neumann, M. Beller 'Palladium-catalyzed carbonylation reactions of aryl halides and related compounds' *Angew. Chem. Int. Ed.* **2009**, *48*, 4114–4133.

[189] L. Yin, J. Liebscher 'Carbon-carbon coupling reactions catalyzed by heterogeneous palladium catalysts' *Chem. Rev.* **2007**, *107*, 133–173.

[190] H.-U. Blaser, C. Malan, B. Pugin, F. Spindler, H. Steiner, M. Studer 'Selective hydrogenation for fine chemicals: Recent trends and new developments' *Adv. Synth. Catal.* **2003**, *346*, 103–151.

[191] R. Grigg, S.P. Mutton 'Pd-catalysed carbonylations: Versatile technology for discovery and process chemists' *Tetrahedron* **2010**, *66*, 5515–5548.

[192] J.P. Genet, M. Savignac 'Recent developments of palladium (0) catalyzed reactions in aqueous medium' *J. Organomet. Chem.* **1999**, *576*, 305–317.

[193] X. Chen, K.M. Engle, D.-H. Wang, Y. Jin-Quan 'Palladium(II)-catalyzed C–H activation/C–C cross-coupling reactions: Versatility and practicality' *Angew. Chem. Int. Ed.* **2009**, *48*, 5094–5115.

[194] D. Astruc 'Palladium nanoparticles as efficient green homogeneous and heterogeneous carbon-carbon coupling precatalysts: A unifying view' *Inorg. Chem.* **2007**, *46*, 1884–1894.

[195] E. Antolini 'Palladium in fuel cell catalysis' *Energy Environ. Sci.* **2009**, *2*, 915–931.

[196] M. Pagliaro, V. Pandarus, R. Ciriminna, F. Béland, P.D. Carà 'Heterogeneous versus homogeneous palladium catalysts for cross-coupling reactions' *ChemCatChem* **2012**, *4*, 432–445.

[197] M. Hartings 'Reactions coupled to palladium' *Nat. Chem.* **2012**, *4*, 764.

[198] B. Coq, F. Figueras 'Bimetallic palladium catalysts: Influence of the co-metal on the catalyst performance' *J. Mol. Catal. A Chem.* **2001**, *173*, 117–134.

[199] G.C. Bond 'Metal-support and metal-additive effects in catalysis' *Platinum Met. Rev.* **1983**, *21*, 16–18.

[200] A.D. Banadaki, A. Kajbafvala 'Recent advances in facile synthesis of bimetallic nanostructures: An overview' *J. Nanomater.* **2014**, *2014*, 985948.

[201] S. De, J. Zhang, R. Luque, N. Yan 'Ni-based bimetallic heterogeneous catalysts for energy and environmental applications' *Energy Environ. Sci.* **2016**, *9*, 3314–3347.

[202] M. Sankar, N. Dimitratos, P.J. Miedziak, P.P. Wells, C.J. Kielye, G.J. Hutchings 'Designing bimetallic catalysts for a green and sustainable future' *Chem. Soc. Rev.* **2012**, *41*, 8099–8139.

[203] D.M. Alonso, S.G. Wettstein, J.A. Dumesic 'Bimetallic catalysts for upgrading of biomass to fuels and chemicals' *Chem. Soc. Rev.* **2012**, *41*, 8075–8098.

[204] C.T. Wu, K.M.K. Yu, F. Liao, N. Young, P. Nellist, A. Dent, A. Kroner, S.C.E. Tsang 'A non-syn-gas catalytic route to methanol production' *Nat. Commun.* **2012**, *3*, 1050.

[205] F. Liao, T.W.B. Lo, D. Sexton, J. Qu, C.-T. Wu, S.C.E. Tsang 'PdFe nanoparticles as selective catalysts for C–C cleavage in hydrogenolysis of vicinal diol units in biomass-derived chemicals' *Catal. Sci. Technol.* **2015**, *5*, 887–896.

[206] F. Liao, T.W.B. Lo, J. Qu, K.A. Wu, A. Dent, S.C.E. Tsang 'Tunability of catalytic properties of Pd-based catalysts by rational control of strong metal and support interaction (SMSI) for selective hydrogenolyic C–C and C–O bond cleavage of ethylene glycol units in biomass molecules' *Catal. Sci. Technol.* **2015**, *7*, 3491–3495.

[207] J. Ge, Z. Zeng, F. Liao, W. Zheng, Z. Hong, S.C.E. Tsang 'Palladium on iron oxide nanoparticles: The morphological effect of the support in glycerol hydrogenolysis' *Green Chem.* **2013**, *15*, 2064–2069.

[208] T. Jiang, Q. Huai, T. Geng, W. Ying, T. Xiao, F. Cao 'Catalytic performance of PdNi bimetallic catalyst for glycerol hydrogenolysis biomass and bioenergy' *Biomass Bioen.* **2015**, *78*, 71–79.

[209] A. Martin, U. Armbruster, I. Gandarias, P.L. Arias 'Glycerol hydrogenolysis into propanediols using in situ generated hydrogen—A critical review' *Eur. J. Lipid Sci. Technol.* **2013**, *115*, 9–27.

[210] H. Yue, Y. Zhao, X. Ma, J. Gong 'Ethylene glycol: Properties, synthesis, and applications' *Chem. Soc. Rev.* **2012**, *41*, 4218–4244.

[211] M. Zheng, J. Pang, A. Wang, T. Zhang 'One-pot catalytic conversion of cellulose to ethylene glycol and other chemicals: From fundamental discovery to potential commercialization' *Chinese J. Catal*. **2014**, *35*, 602–613.

[212] A. Wang, T. Zhang 'One-pot conversion of cellulose to ethylene glycol with multifunctional tungsten-based catalysts' *Acc. Chem. Res.* **2013**, *46*, 1377–1386.

[213] Y.R. Luo Comprehensive Handbook of Chemical Bond Energies; CRC Press: Boca Raton, FL, USA, **2007**.

[214] M. Salciccioli, W. Yu, M.A. Barteau, J.G. Chen, D.G. Vlachos 'Differentiation of O–H and C–H bond scission mechanisms of ethylene glycol on Pt and Ni/Pt using theory and isotopic labeling experiments' *J. Am. Chem. Soc*. **2011**, *133*, 7996–8004.

[215] R.A. Bennett, C.L. Pang, N. Perkins, R.D. Smith, P. Morrall, R.I. Kvon, M. Bowker 'Surface structures in the SMSI state; Pd on (1x2) reconstructed TiO$_2$(110)' *J. Phys. Chem. B* **2002**, *106*, 4688–4696.

[216] O. Dulub, W. Hebenstreit, U. Diebold 'Imaging cluster surfaces with atomic resolution: The strong metal-support interaction state of Pt supported on TiO$_2$ (110)' *Phys. Rev. Lett.* **2000**, *84*, 3646–3649.

[217] A. Alhanash, E.F. Kozhevnikova, I.V. Kozhevnikov 'Hydrogenolysis of glycerol to propanediol over Ru: polyoxometalate bifunctional catalyst' *Catal. Lett*. **2007**, *120*, 307–311.

[218] M. Balaraju, V. Rekha, P.S. Sai Prasad, R.B.N. Prasad, N. Lingaiah 'Selective hydrogenolysis of glycerol to 1,2 propanediol over Cu–ZnO catalysts' *Catal. Lett*. **2008**, *126*, 119–124.

[219] H. Hattori 'Heterogeneous basic catalysis' *Chem. Rev.* **1995**, *95*, 537–558.

[220] H. Hattori 'Solid base catalysts: Generation of basic sites and application to organic synthesis' *Appl. Cat. A Gen*. **2001**, *222*, 247–259.

[221] K.L. Deutsch, D.G Lahr, B.H. Shanks 'Probing the ruthenium-catalyzed higher polyol hydrogenolysis reaction through the use of stereoisomers' *Green Chem.* **2012**, *14*, 1635–1642.

[222] B.H. Shanks 'Conversion of biorenewable feedstocks: New challenges in heterogeneous catalysis' *Ind. Eng. Chem. Res.* **2010**, *49*, 10212–10217.

[223] D.K. Sohounloue, C. Montassier, J. Barbier 'Catalytic hydrogenolysis of sorbitol' *React. Kinet. Catal. Lett.* **1983**, *22*, 391–397.

[224] N. Li, G.W. Huber 'Aqueous-phase hydrodeoxygenation of sorbitol with Pt/SiO$_2$–Al$_2$O$_3$: Identification of reaction intermediates' *J. Catal.* **2010**, *270*, 48–59.

[225]R. Rinaldi 'Catalytic Hydrogenation for Biomass Valorization' RSC Energy and Environment Series No. 13; The Royal Society of Chemistry: London, UK, pp. 1–310, **2015**.

[226]P. Thibault, V. Elser 'X-ray diffraction microscopy' *Annu. Rev. Condens. Matter Phys.* **2010**, *1*, 237–255.

[227]J. Lee, Y.T. Kim, G.W. Huber 'Aqueous-phase hydrogenation and hydrodeoxygenation of biomass-derivedoxygenates with bimetallic catalysts' *Green Chem.* **2014**, *16*, 708–718.

[228]B.M. Moreno, N. Li, J. Lee, G.W. Huber, M.T. Klein 'Modeling aqueous-phase hydrodeoxygenation of sorbitol over Pt/SiO_2–Al_2O_3' *RSC Adv.* **2013**, *3*, 23769–23784.

[229]G.W. Huber, R.D. Cortright, J.A. Dumesic 'Renewable alkanes by aqueous-phase reforming of biomass-derived oxygenates' *Angew. Chem. Int. Ed.* **2004**, *43*, 1549–1551.

[230]Y.T. Kim, J.A. Dumesic, G.W. Huber 'Aqueous-phase hydrodeoxygenation of sorbitol: A comparative study of Pt/Zr phosphate and Pt_ReO_x/C' *J. Catal.* **2013**, *304*, 72–85.

[231]B.D. Li, J. Wang, Y.Z Yuan, H. Ariga, S. Takakusagi, K. Asakura 'Carbon nanotube-supported RuFe bimetallic nanoparticles as efficient and robust catalysts for aqueous-phase selective hydrogenolysis of glycerol to glycols' *ACS Catal.* **2011**, *1*, 1521–1528.

[232]A. Yamaguchi, N. Hiyoshi, O. Sato, M. Shirai 'Sorbitol dehydration in high temperature liquid water' *Green Chem.* **2011**, *13*, 873–881.

Chapter 2

EXPERIMENTAL

All chemicals, involved in this doctoral experimentation, were purchased and used without any further purification.

2.1. Preparation of the catalyst

The Pd/Fe_3O_4 catalyst, designed with a nominal palladium loading of 5% wt, was prepared through the co-precipitation technique. The synthesis occurs through a co-precipitation reaction from a solution containing nitrate precursors of palladium (II) and iron (III) poured into a solution of carbonates (Figure 2.1).
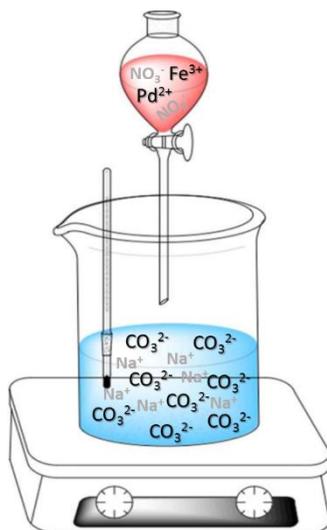
Figure 2.1 Co-precipitation of the metallic precursors within a solution of carbonates.

The obtained solid co-precipitate was washed and filtrated and then dried overnight at 120°C and, before any reaction, reduced with H_2 at 200°C.

Benchmark catalysts such as Pd/C and Fe_3O_4 were purchased from commercial sources (AlfaAesar and Sigma Aldrich) and Pd/C was used after reduction under H_2 flow at 200°C for 2 h.

2.2. Characterization techniques

Characterization techniques typically used for the textural, structural and morphological investigation of bimetallic Pd-Fe catalysts were: x-ray diffraction (XRD), transmission electron microscopy (TEM), temperature-programmed reduction (H_2-TPR), x-ray photoelectron spectroscopy (XPS) and extended x-ray absorption fine structure (EXAFS). All these techniques are widely used because they provide accurate results allowing to obtain both quantitative and qualitative results [1,2].

2.2.1. X-ray Diffraction (XRD)

X-ray diffraction (XRD) patterns were acquired at room temperature on a Philips X-Pert diffractometer by using the Ni β-filtered CuKα radiation (λ = 0.15418 nm). Analyses were registered in the 2θ range of 10–80° at a scan speed of 0.5° min^{-1}. Diffraction peaks were compared with those of standard compounds reported in the JPCDS data file.

2.2.2. Transmission Electron Microscopy (TEM)

The particle size and the relative morphology of investigated catalysts were analyzed by performing Transmission Electron Microscopy (TEM) measurements using a JEM-2100F (JEOL, Japan) operating at an acceleration voltage of 200 kV and directly interfaced with a computer controlled-CCD for real-time image processing. Particle size distributions were obtained by counting several hundred particles visible on the micrographs on each sample. From the size distribution, the average diameter was calculated by using the expression: $d_n = \Sigma n_i d_i / n_i$ (where n_i is the number of particles of diameter d_i).

2.2.3. Hydrogen Temperature Programmed Reduction (H₂-TPR)

H_2-TPR measurements were performed using a conventional TPR apparatus. The dried sample (50 mg) was heated at a linear rate of 10°C min⁻¹ from 0 to 1000°C in a 5% vol H_2/Ar mixture at a flow rate of 20 cm³ min⁻¹. The consumption of hydrogen was monitored with a thermal conductivity detector (TCD). A molecular sieve cold trap (maintained at −80°C) and a tube filled with KOH, placed before the TCD, were used to block water and CO_2, respectively. Signal calibration was done by injecting a known amount of H_2 into the carrier.

2.2.4. CO-pulse chemisorption

The active surface areas (S_{act}) were determined by CO pulse chemisorption technique using a 'Micromeritics Chemi Sorb 2750' system at room temperature. Samples were first reduced with H_2 at 25 stp ml/min using a 10°C min⁻¹ ramp up to 200°C, then cleaned with He, at 25 stp ml/min for 15 min, and finally cooled to room temperature.

CO pulses (0.64 stp ml, 5% CO/He – 1.29 μmol CO each injection) were injected until saturation. S_{act} values were calculated by assuming a CO/Pd stoichiometry of 1 and a surface area of 7.87×10^{-20} m² per Pd atom [3].

2.2.5. X-ray Photoelectron Spectroscopy (XPS)

X-ray photoelectron spectroscopy (XPS) measurements were performed on a JPS-9010MC photoelectron spectrometer using an AlK (1486.6 eV) radiation source. After the reduction treatment, samples were introduced into the XPS chamber, avoiding exposure to air. All spectra were recorded at room temperature, and the binding energies (BE) were set taking the C 1s peak at 284.6 eV as reference.

In order to obtain XPS spectra, the pressure in the analysis chamber was maintained at 5×10^{-9} mbar. The binding energies (BE) were set taking the C 1s peak at 284.6 eV as the reference. Peak deconvolution and fitting analyses were performed using the peak-fitting software "SPECSURF, JEOL" including the spin–orbit splitting and relative intensities of the spin–orbit components fixed.

Extended X-ray absorption fine structure (EXAFS) of the Pd-based catalysts have been measured at the Photon Factory of the High Energy Accelerator Research Organization - KEK (Tsukuba, Japan). Fe-K edge XANES/EXAFS spectra for the catalysts were obtained using a Si (111) two-crystal monochromator with beam line BL9A, whereas Pd K-edge spectra were obtained using a Si (311) two-crystal monochromator with beam line NW10A.

Analysis of the EXAFS data have been performed using the EXAFS analysis program, REX (Rigaku Co.).

2.3. Mechanical pretreatment of cellulose

Cellulose structure is difficult to be converted, because its robustness due to β-1,4-glycosidic linkages and *inter-* and *intra*-chain hydrogen bonds.

Therefore, pretreatments (chemical, mechanical, etc.) are useful to overcome this problem, reducing crystalline domains and increasing amorphous regions, making the cellulose more suitable to the conversion. In particular a mechanical pretreatment, instead of chemical pretreatments, avoids to use corrosive and toxic substances [4-6].
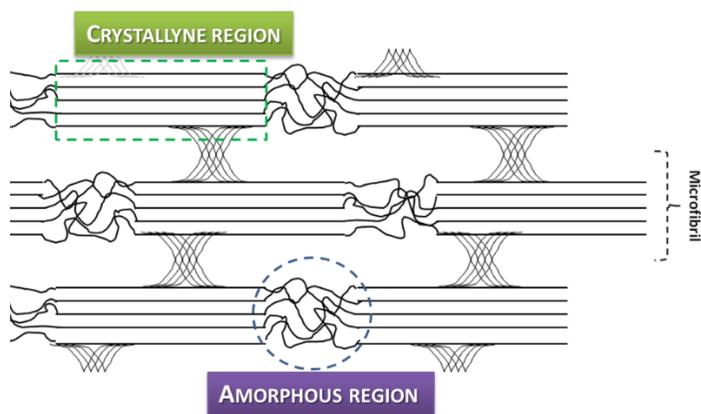
Figure 2.2 Schematic representation of cellulose regions: crystalline and amorphous

The microcrystalline cellulose (Sigma Aldrich, particle size of 51µm) was mechanically pretreated in a planetary ball milling (Mono Mill II, Fritsch) with a speed of 400 rpm for 3 h; about 10g of microcrystalline cellulose (MCC) were treated *per* run.

Microcrystalline and ball milled celluloses were characterized through XRD measurements, performed at room temperature on a Philips X-Pert diffractometer by using the Ni β-filtered Cu Kα radiation ($\lambda = 0.15418$ nm) in the 2θ range of 20–80° at a scan speed of 0.5° min^{-1}. Finally, the crystallinity index (CrI%) was estimated through the Segal method.

2.3.1. *Crystalline Index*

In order to quantify the crystallinity index (CrI %) relative to the cellulose before (MCC) and after (BMC) the mechanical pretreatment, the Segal method has been employed [7].

This method, also known as 'XRD peak height method', is useful to compare the relative differences between samples, being based on the changes in XRD patterns during the variation of crystalline domains, through the application of (e.g. mechanical) treatments.

The crystallinity index (CrI%) can be calculated through the ratio of the height of the 002 peak (I_{002}) and the height of the minimum (I_{AM}), between the 002 and the 101 peaks [7-9], represented in Figure 2.3, in agreement with the following equation:

$$CrI\ (\%) = \frac{I_{002} - I_{AM}}{I_{002}} \cdot 100$$
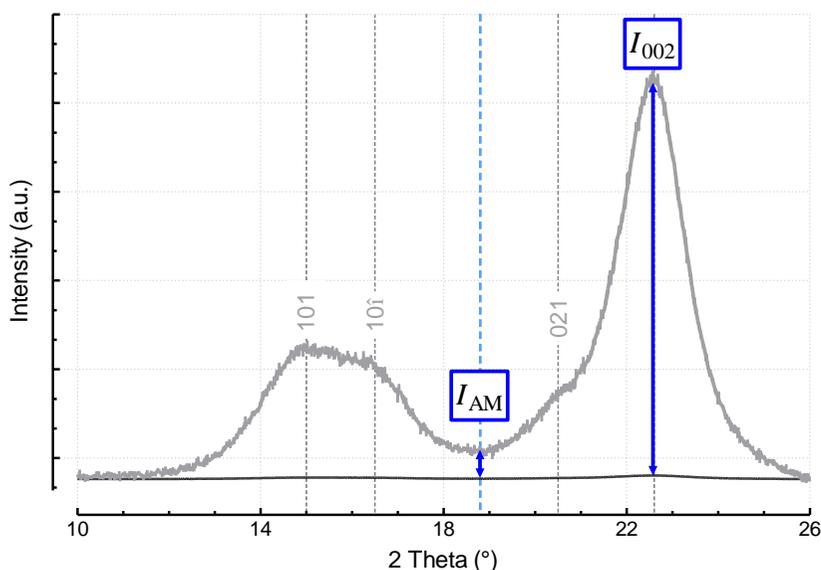
Figure 2.3 Schematic representation of the 'Segal method' applied to the quantification of the crystallinity index.

2.4. Catalytic experiments

Catalytic reactions were performed in batch conditions in a 100 ml stainless steel autoclave (Parr Instruments) at a stirring speed of 500 rpm. The vessel was charged with 40ml of aqueous suspension with 4%wt of cellulose and 0.25g of the reduced catalyst; then the reactor was purged at least two times with N_2 (99,9%). Subsequently the desired pressure (5 bar of H_2 or N_2) was reached and finally the reactor was heated at the reaction temperature (180-240°C), continuously monitored through a thermocouple fixed into the autoclave and connected to the reactor controller, within the duration of the test (up to 24h). At the end of the reaction, the system was cooled down and, when at room temperature, the pressure was released carefully and the liquid phase analyzed. In some experiments also the gas phase was analyzed.

During three years of doctoral work, it was necessary to use autoclaves having different size. Therefore, the operating conditions were properly adapted, in order to keep comparable every catalytic test.

Table 2.1 Operating conditions used when reactions were performed in a set-up of 100 mL or 75mL.

	Set-up 100mL	Set-up 75 mL
V_{LIQ}	40 mL	30 mL
V_{GAS}	60 mL	45 mL
W_{SUBSTR}	1,7 g	1.3 g
W_{CAT}	0.25g	0.19 g
V_{LIQ}/V_{GAS}	1.5	1.5
W_{CAT}/V_{LIQ}	0.00625	0.00625
W_{CAT}/W_{SUBSTR}	0.147	0.147
% W_{SUBSTR}	4%	4%

2.5. Analytical techniques applied to reactions

Products present in aqueous liquid phase, were quantified through off-line high performance liquid chromatography (HPLC) analysis.

The Shimadzu HPLC was equipped with an Aminex HPX-87-H column, following these parameters: mobile phase 5mM H_2SO_4 at a speed flow of 0,6 ml min^{-1} and oven heated at 70°C; every measurement was performed within a range of 30-60 min.

During the year of research developed at RWTH Aachen University, the following two analytical methods, applied to a similar Shimadzu HPLC apparatus, were also used:

- Phenomenex-Rezex ROA Oganic Acid H^+ (300 x 7.8mm) column maintained at 70°C, using a 0.6 ml min^{-1} flow of 5mM H_2SO_4; the duration of each analysis was 30 min;

- Organic Acid Resins column, operating at 40°C, eluted with a mobile phase of 2mM trifluoroacetic acid (TFA) at a speed flow of 1 ml min^{-1} flow; the duration of each analysis was 25 min.

The carbon content of each aqueous reaction solution, before and after every reaction, was quantified by using a total organic carbon (TOC) analyzer Shimadzu. TOC measurements are fundamental to confirm the carbon balance in the liquid phase.

Products present in the gaseous phase were analyzed through gas chromatography (GC), using an instrument (Agilent 7890A) equipped with a molecular sieve column (Supelco, Porapak Q column 80/100 mesh) and a capillary column (HP-PLOT/Q, internal diameter: 0,53 mm; length: 30 m; film thickness: 40 μm) linked with the TCD detector and a capillary column (HP-Al, internal diameter: 0.53 mm; length: 50 m; film thickness: 15 μm) connected to a FID detector.

The organic mixture relative to reactions performed starting from limonene, were analyzed through a GC (Thermo Fisher) equipped with an IVA-OV1701 column (length 50 m, internal diameter 0.25 mm and film thickness 0.25 μm), using a FID (250°C, 50Hz); Temp. 50-240°C at a speed of heating of 8°C /min and 20 min of isotherm.

2.6. Conversion, selectivity and carbon mass balance

The conversion of polyols in the liquid phase was calculated on the basis of the following equation:

$$Conversion\ [\%] = \frac{mol\ of\ reacted\ substrate}{mol\ of\ substrate\ feed} \times 100$$

When the reagent is solid, like cellulose, the conversion has been estimated through gravimetric method, in agreement with the following equation:

$$Conv._{CELL.}\ [\%] = \frac{w_{Cell}^{IN} - w_{Cell}^{OUT}}{w_{Cell}^{IN}} \times 100$$

Where w_{Cell}^{IN} indicates the weight of cellulose put at the beginning of the reaction and w_{Cell}^{OUT} is the weight of cellulose recovered at the end of the reaction.

The molar selectivity of each product detected in the liquid phase was calculated in agreement with the following equation:

$$Molar\ Selectivity\ [\%] = \frac{mol\ of\ specific\ product\ in\ Liq\ phase}{\Sigma mol\ of\ all\ products\ in\ Liq\ phase} \times 100$$

The products yield was calculated on carbon basis and defined as:

$$Product\ Yield\ [\%] = \frac{mol\ of\ specific\ product\ \times C\ atoms\ in\ specific\ product}{mol\ of\ total\ C\ atoms\ in\ substrate} \times 100$$

The carbon balance at the end of each reaction was confirmed by using a liquid total organic carbon analyzer (Shimadzu TOC-VCSH). The percentage of carbon loss has been estimated through the comparison of the carbon balance evaluated by HPLC analysis and by TOC measurements. A good agreement between the carbon balance obtained by HPLC and TOC measurements was found (carbon loss in liquid phase lower than 5%). Each measurement was repeated at least three times and every result is conveniently mediated.

The total organic carbon of the gas phase, when calculated, was estimated as the difference between the TOC measurements before and after hydrogenolysis reactions. In all experiments, the analytical results of GC analysis showed a carbon balance in gas phase higher than 95%.

REFERENCES

[1] C. Espro, B. Gumina, E. Paone, F. Mauriello 'Upgrading lignocellulosic biomasses: Hydrogenolysis of platform derived molecules promoted by heterogeneous Pd-Fe catalysts' *Catalysts* **2017**, *7*, 78.

[2] F. Liao, T.W.B. Lo, S.C.E. Tsang 'Recent developments in palladium-based bimetallic catalysts' *ChemCatChem* **2015**, *7*, 1998–2014.

[3] J. Liu, B. Sun, J. Hu, Y. Pei, H. Li, M. Qiao 'Aqueous-phase reforming of ethylene glycol to hydrogen on Pd/Fe_3O_4 catalyst prepared by co-precipitation: Metal–support interaction and excellent intrinsic activity' *J. Catal.* **2010**, *274*, 287–295.

[4] A. Shrotri, H. Kobayashi, A. Fukuoka 'Cellulose depolymerization over heterogeneous catalysts' *Acc. Chem. Res*. **2018**, *51*, 761−768.

[5] M.H.L. Silveira, A.R.C. Morais, A.M. da Costa Lopes, D.N. Olekszyszen, R. Bogel-Łukasik, J. Andreaus, L. Pereira Ramos 'Pretreatment technologies for the development of cellulosic ethanol and biorefineries' *ChemSusChem* **2015**, *8*, 3366 – 3390.

[6] A.K. Kumar, S. Sharma 'Recent updates on different methods of pretreatment of lignocellulosic feedstocks: a review' *Bioresour. Bioprocess.* **2017**, *4*, 7.

[7] L. Segal, J.J. Creely, A.E. Martin, C.M. Conrad 'An empirical method for estimating the degree of crystallinity of native cellulose using the x-ray diffractometer' *Tex. Res. J.* **1962**, *29*, 786-794.

[8] L.E. Hult, T. Iversen, J. Sugiyama 'Characterization of the supramolecular structure of cellulose in wood pulp fibers' *Cellulose* **2003**, *10*, 103-110.

[9] C.J. Garvey, I.H. Parker, G.P. Simon 'On the interpretation of X-ray diffraction powder patterns in terms of the nanostructure of cellulose I fibers' *Macromol. Chem. Phys.* **2005**, *206*, 1568-1575.

Chapter 3

CHARACTERIZATION

3.1. Physico-chemical characterization of Pd/Fe$_3$O$_4$ catalyst

The present study is focused on the application of the bimetallic Pd/Fe$_3$O$_4$ catalyst, particularly the catalyst synthesized through the co-precipitation method. Previously, also impregnated bimetallic catalysts have been investigated by our research group, but the method of impregnation allows to obtain catalysts with a structural composition that is unable to obtain significant activities, with respect to co-precipitated catalysts [1,2].

The co-precipitated Pd/Fe$_3$O$_4$ catalyst, having a nominal palladium loading of 5% wt, was prepared through the dropwise addition of a solution containing nitrate precursors of palladium (II) and iron (III) into a solution of sodium carbonate. The obtained co-precipitate was washed and filtrated, then dried overnight at 120°C and, before any reaction, reduced at 200°C under a H$_2$ flow.

X-ray fluorescence (XRF) measurements indicated 8.7% wt of palladium loading, over a BET surface area of 170 m^2/g, where 2.51 m^2/g is the active surface area, as detected through CO pulse chemisorption measurements [3].

The most common analysis techniques used so far for the characterization of bimetallic Pd-Fe catalysts were: x-ray diffraction (XRD), transmission electron microscopy (TEM), temperature-programmed reduction (H$_2$-TPR), x-ray photoelectron spectroscopy (XPS) and extended x-ray absorption fine structure (EXAFS). All these techniques are widely used because they provide accurate results allowing to obtain both quantitative and qualitative results [1, 9].

3.1.1. X-ray Diffraction (XRD)

XRD pattern of the co-precipitated Pd/Fe_3O_4 catalyst, after the reduction at 200°C under H_2 flow, reveals only reflections related to Fe_3O_4 (Figure 3.1). Typical reflections related to the cubic crystal magnetite, in agreement with JCPDS No. 82-1533, are here below reported: 30.4° (220); 35.8° (311); 43.4° (400); 54.0° (422); 57.5° (511); 63.2° (440) [5-7].
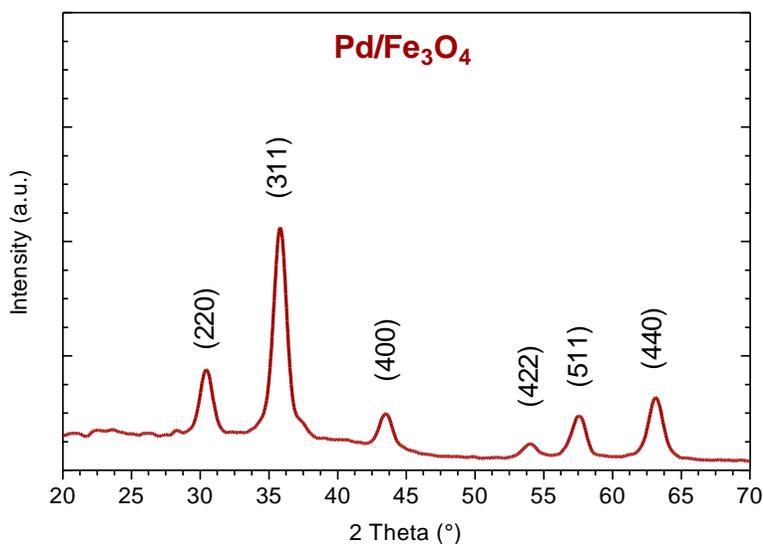
Figure 3.1 XRD pattern of the Pd/Fe_3O_4 catalyst.

The absence of the (111) reflection, related to metallic palladium, means that palladium nanoparticles are very well dispersed over the catalytic surface [1-4].

XRD patterns of co-precipitated Pd/Fe_3O_4 catalyst reduced at 100°C (a), 200°C (b) and after 12 h (c) and 24 h (d) of reactions are reported in Figure 3.2. Profiles (a) and (b) show only characteristic reflections of Fe_3O_4, indicating that the catalyst is under the reduced form already when the reduction is performed at 100°C [3].

The absence of the reflection at the 2θ degree ca. 40.1°, related to the metallic palladium (111) plane, indicates that the palladium particles are under the XRD revelation limit (<2.5 nm) and are highly dispersed on the magnetite surface, as confirmed by TEM measurements.

XRD patterns of catalysts recovered after reactions are shown in profiles (c) and (d). Also after 24 h of reaction there are no modifications of the Fe_3O_4 support structure, whilst the increase of the diffraction peak ascribed to the plane (111) of the metallic palladium is indicative of the presence of palladium particles agglomeration.
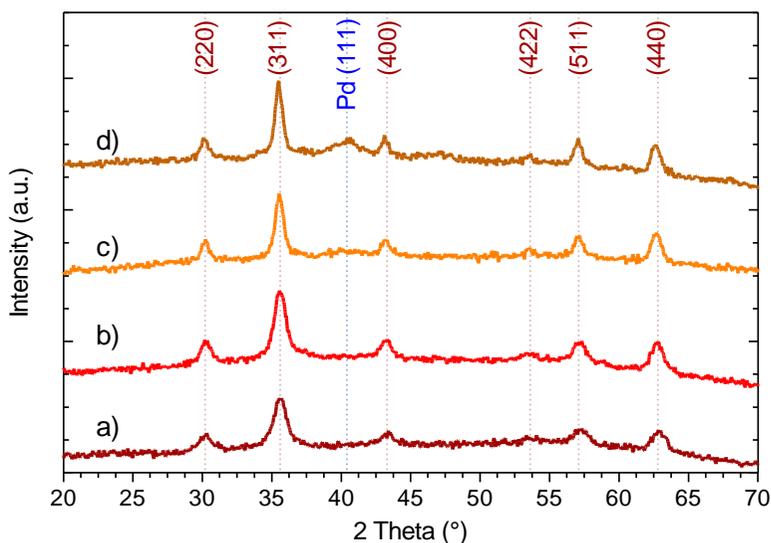
Figure 3.2 XRD patterns of Pd/Fe₃O₄ catalyst reduced at 100°C (a), reduced at 200°C (b) and after 12h (c) and 24h (d) of reaction. On the top of diffractograms corresponding faces of Fe₃O₄ (bordeaux) and metallic palladium (blue) are reported.

3.1.2.   *Transmission Electron Microscopy (TEM)*

TEM images of the co-precipitated Pd/Fe₃O₄ catalyst at magnification of 50 and 5 nm and relative particle size distribution are reported in Figure 3.3. The Pd/Fe₃O₄ catalyst exhibits a predominance of nanometric palladium particles, within the range of 1.2 and 3.5 nm, and a pretty narrow size distribution. Indeed, a bimodal distribution with a majority of particles of 1.2 nm diameter, followed by a second population of slightly larger palladium particles, with 2.3 nm average diameter, was found [1-4].

These results are in agreement with XRD measurements, in which the absence of the diffraction line related to metallic palladium, suggests the presence of highly dispersed palladium particles, which should be extremely

small, being the conventional limit of XRD instruments for the detection of supported nanoparticles usually of 2-2.5 nm.

Furthermore, similar results of reduced palladium on iron oxide catalyst were reported also by Tsang and palladium particles sized in the range of ca. 0.5 – 2.5 nm of diameter were found [8].
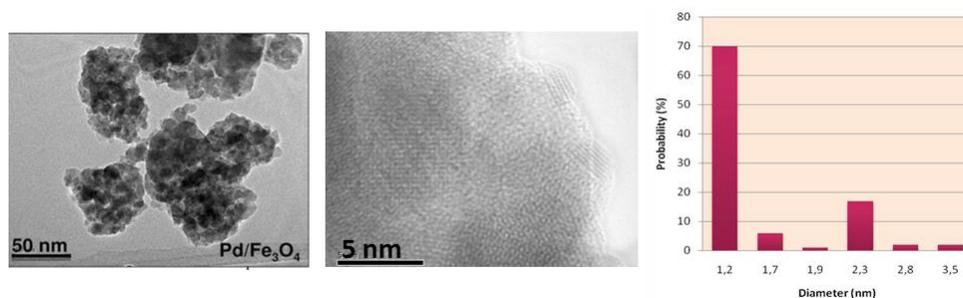
Figure 3.3 TEM images of Pd/Fe₃O₄ catalyst at magnification of 50 and 5 nm and relative particle size distribution.

3.1.3. *Hydrogen Temperature Programmed Reduction (H₂-TPR)*

The H₂-TPR profile of the unreduced co-precipitated Pd/Fe₂O₃ catalyst shows a main area of only one intense peak of reduction at low temperature, starting at 44°C and centered at ca. 80°C, that includes reductions of either $Pd^{+2} \rightarrow Pd^{0}$ and $Fe^{+3} \rightarrow Fe_3O_4$, as determined by the calculation of the hydrogen consumption [1-4].
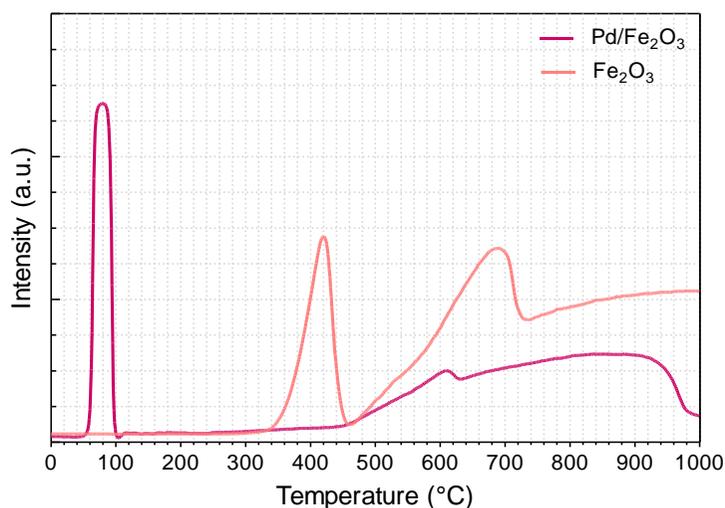
Figure 3.4 H₂-TPR profiles of Pd/Fe₂O₃ catalyst (violet) and pure Fe₂O₃ (pink).

The H_2-TPR profile of the unreduced pure Fe_2O_3 catalyst is also included, in order to compare the reductive profile of the bimetallic catalyst (Figure 3.4). For the pure iron oxide (Fe_2O_3), the reduction starts at significantly higher temperatures (ca. 320°C) and the profile presents two main peaks: the first centered at ca. 420°C that belongs to the reduction of $Fe^{+3} \rightarrow Fe_3O_4$, whilst the second is centered at ca. 690°C due to the following reduction of $Fe_3O_4 \rightarrow FeO$.

Through the comparison of H_2-TPR profiles of the unreduced bimetallic catalyst (Pd/Fe_2O_3) and the pure oxide (Fe_2O_3) the promoting effect played by the palladium nanoparticles on the iron oxide support, which is indicative of a strong metal-support interaction (SMSI) [1-4, 9], results very clear.

Furthermore, the low temperature at which is placed the main reduction peak of the unreduced bimetallic catalyst (Pd/Fe_2O_3), entirely below 100°C, is in agreement with the XRD pattern of the bimetallic catalyst reduced at 100°C (profile (a) in Figure 3.2), that shows signals only referred to the magnetite structure [3-4].

If these evidences are not enough, other authors, so far, reported similar results relative to co-precipitated Pd/Fe_3O_4 catalysts, where the method used to synthesize the material plays a fundamental role on the properties observed; in particular all authors reach the same conclusion regarding the effectiveness of palladium nanoparticles in promoting the reduction of hematite into magnetite [1, 8-12].

3.1.4. *X-ray Photoelectron Spectroscopy (XPS)*

The comparison of X-ray photoelectron spectroscopy (XPS) spectra of reduced and unreduced Pd/Fe_xO_y samples leads to confirm the presence of only Fe_3O_4 over the reduced catalyst (as previously shown through XRD patterns, Figures 3.1 and 3.2). This evidence was ascertained because of the absence of the satellite peak at 718.5 eV. This indicates that the Fe_2O_3 structure over the reduced surface is totally absent (Table 3.1).

Furthermore, after the reducing treatment, the shift of ca. 0.5 eV of the Pd $3d_{5/2}$ binding energy to higher values, than that observed for metallic palladium, indicates the presence of partial positively charged metal Pd species ($Pd^{\delta+}$) (Table 3.1 and Figure 3.5).

This evidence is attributed to alloy formation for bimetallic supported Pd catalysts [2,3].

Table 3.1 Binding Energy values of Pd $3d_{5/2}$, Fe $2p_{3/2}$ and Fe $2p_{3/2}$ sat., and O 1s for *un*-reduced (Pd/Fe_2O_3) and reduced (Pd/Fe_3O_4) bimetallic catalysts.

Catalyst	Binding Energy (eV)			
	Pd $3d_{5/2}$	Fe $2p_{3/2}$	Fe $2p_{3/2}$ sat.	O 1s
Pd/Fe_2O_3	336.2	710.9	718.5	530.2
Pd/Fe_3O_4	335.2	710.7	-	530.2
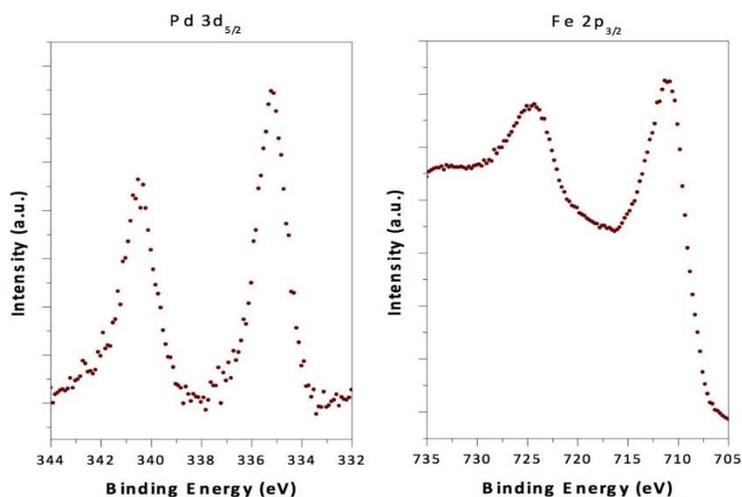
Figure 3.5 XPS Pd $3d_{5/2}$ and Fe $2p_{3/2}$ graphs of the reduced Pd/Fe_3O_4 catalyst.

3.1.5. *Extended X-ray Absorption Fine Structure (EXAFS)*

Extended X-ray absorption fine structure (EXAFS) is a technique able to provide valuable information about the structure of metal alloys, since it gives information about the local structure around Pd, the Pd–support oxide interaction and/or the Pd bimetal nanoparticle formation [13-15].

EXAFS characterization of different Pd/Fe$_x$O$_y$ catalysts has been deeply investigated by several research groups and the results have been summarized in a review dedicated to Pd/Fe$_x$O$_y$ catalysts [1].

The results, obtained through EXAFS investigations performed over bimetallic Pd/Fe$_3$O$_4$ and monometallic Pd/C (used as the benchmark Pd-based catalyst) catalysts, are reported here below in Table 3.2.

Results reveal that some iron particles are alloyed into the palladium nanoparticles forming Pd–Fe bimetallic ensembles, being the Pd-Fe bond length shorter than that of Pd-Pd bonds (Table 3.2). These findings indicate that on the Pd/Fe reduced catalyst strong interactions between the palladium nanoparticles and the iron oxide support are present [1-3].

Table 3.2 EXAFS characterization at the Pd K-edge for Pd/Fe and Pd/C catalysts.

Catalyst	Scattering pair	CN [a]	Bond Length (Å)	R-factor (%)	Ef [b] (eV)	DW factor [c]	K-range
Pd/Fe	Pd-Pd	1.9	2.66	1.6	-7.4	7.3	2-12
	Pd-Fe	1.0	2.59			5.1	
Pd/C	Pd-Pd	8.0	2.73	2.6	-7.6	6.1	2-17

[a]   CN = coordination number;

[b]   Ef = Energy of fluorescent x-ray

[c]   DW factor: Debye-Waller factor ($\sigma^2 \cdot 10^{-3}$ Å^2).

3.2. Conclusions

The surface of the co-precipitated Pd/Fe_3O_4 catalyst is characterized by the presence of highly dispersed palladium nanoparticles, as shown by X-ray diffraction (XRD) and transmission electron microscopy (TEM) techniques.

Furthermore, TEM characterizations allowed to measure the average size of the particles and the relative particle size distribution that reveal a majority of particles of 1.2 nm diameter.

H_2-TPR measurements indicate the presence of only one intense peak at low temperature, entirely placed at T<100°C, whose area includes the reduction of both palladium and iron cations species, confirming the existence of a strong metal-support interaction (SMSI) and highlighting the promoter effect played by palladium in the reduction of iron oxide from hematite into magnetite.

XPS investigations on the reduced Pd/Fe_3O_4 catalyst confirm the presence of intimate interactions between palladium nanoparticles and the iron oxide support.

Finally, EXAFS measurements confirm the presence of Pd-Fe bimetallic ensembles on the surface of the reduced Pd/Fe_3O_4 catalyst.

REFERENCES

[1] C. Espro, B. Gumina, E. Paone, F. Mauriello 'Upgrading lignocellulosic biomasses: Hydrogenolysis of platform derived molecules promoted by heterogeneous Pd-Fe catalysts' *Catalysts* **2017**, *7*, 78.

[2] F. Mauriello, H. Ariga, M.G. Musolino, R. Pietropaolo, S. Takakusagi, K. Asakura 'Exploring the catalytic properties of supported palladium catalysts in the transfer hydrogenolysis of glycerol' *Appl. Catal. B: Environ.* **2015**, *166–167*, 121–131.

[3] F. Mauriello, A. Vinci, C. Espro, B. Gumina, M.G. Musolino, R. Pietropaolo 'Hydrogenolysis vs. aqueous phase reforming (APR) of glycerol promoted by a heterogeneous Pd/Fe catalyst' *Catal. Sci. Technol.* **2015**, *5*, 4466-4473.

[4] B. Gumina, F. Mauriello, R. Pietropaolo, S. Galvagno, C. Espro 'Hydrogenolysis of sorbitol into valuable C_3-C_2 alcohols at low H_2 pressure promoted by the heterogeneous Pd/Fe_3O_4 catalyst' *Mol. Catal.* **2018**, *446*, 152-160.

[5] J. Sun, S. Zhou, P. Hou, Y. Yang, J. Weng, X. Li, M. Li 'Synthesis and characterization of biocompatible Fe_3O_4 nanoparticles' *J Biomed Mater Res A* **2007**, *80A*, 333-341.

[6] H. Itoh, T. Sugimoto 'Systematic control of size, shape, structure, and magnetic properties of uniform magnetite and maghemite particles' *J. Colloid Interface Sci.* **2003**, *265*, 283–295.

[7] W. Voit, D.K. Kim, W. Zapka, M. Muhammed, K.V. Rao 'Magnetic behavior of coated superparamagnetic iron oxide nanoparticles in ferrofluids' *Mater Res Soc* **2001**, *676*, 781–786.

[8] C.-T. Wu, K.M.K. Yu, F. Liao, N. Young, P. Nellist, A. Dent, A. Kroner, S.C.E. Tsang 'A non-syn-gas catalytic route to methanol production' *Nat. Commun.* **2012**, *3*, 1050 (1-8).

[9] F. Liao, T.W.B. Lo, S.C.E. Tsang 'Recent developments in palladium-based bimetallic catalysts' *ChemCatChem* **2015**, *7*, 1998–2014.

[10] J. Liu, B. Sun, J. Hu, Y. Pei, H. Li, M. Qiao 'Aqueous-phase reforming of ethylene glycol to hydrogen on Pd/Fe_3O_4 catalyst prepared by co-

precipitation: Metal–support interaction and excellent intrinsic activity' *J. Catal.* **2010**, *274*, 287–295.

[11] D. Scholz, C. Aellig, I. Hermans 'Catalytic transfer hydrogenation /hydrogenolysis for reductive upgrading of furfural and 5-(hydroxymethyl) furfural' *ChemSusChem* **2014**, *7*, 268–275.

[12] A.J.R. Hensley, Y. Hong, R. Zhang, H. Zhang, J. Sun, Y. Wang, J.S. McEwen 'Enhanced Fe_2O_3 reducibility via surface modification with Pd: characterizing the synergy within Pd/Fe catalysts for hydrodeoxygenation reactions' *ACSCatal.* **2014**, *4*, 3381–3392.

[13] L.R. Sharpe, W.R. Heineman, R.C Elder 'EXAFS spectro-electrochemistry' *Chem. Rev.* **1990**, *90*, 705–722.

[14] A. Gaur, B.D. Shrivastava, H.L. Nigam X-ray 'Absorption fine structure (XAFS) spectroscopy—A review' *Proc. Indian Natl. Sci. Acad.* **2013**, *79*, 921–966.

[15] K. Asakura 'Recent developments in the in situ XAFS and related work for the characterization of catalysts in Japan' *Catal. Surv. Asia* **2003**, *7*, 177–182.

Chapter 4

STUDY OF MODEL MOLECULES: HYDROGENOLYSIS OF POLYOLS

4.0. Overview of the approach
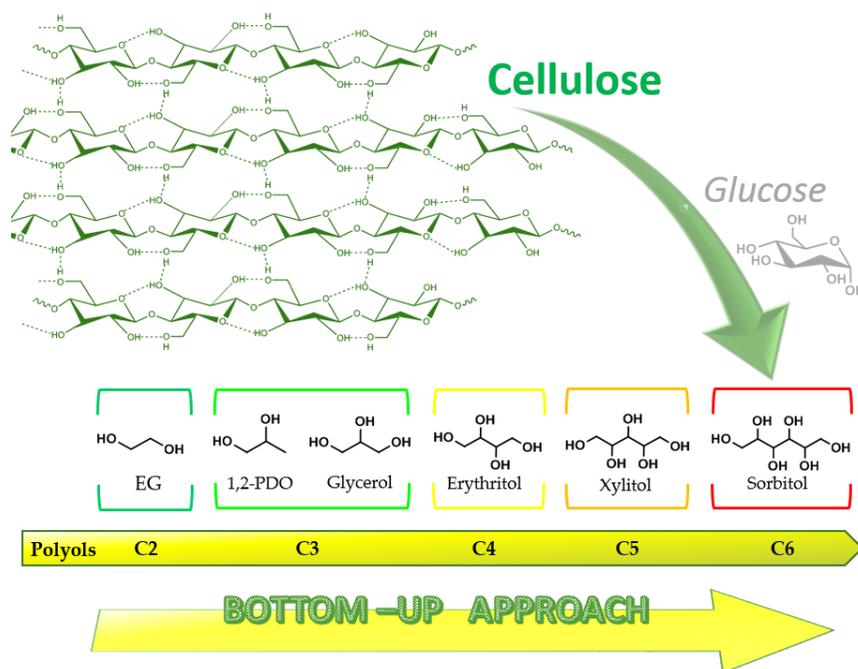
Figure 4.0 Schematic representation of the approach followed to investigate the performance of the Pd/Fe₃O₄ catalyst for the valorization of polyols, before to investigate directly the polymer cellulose.

Before to start the detailed description of the reaction pattern involved in the hydrogenolysis of polyols promoted by the co-precipitated Pd/Fe$_3$O$_4$ catalyst, it is important to spend few words to explain the approach followed during this investigation.

The first part of this research was focused on the study of the hydrogenolysis of polyols, starting from polyols with short carbon chain before the investigation of polyols with longer carbon chain, in particular the C$_6$ polyol sorbitol. This approach enables to facilitate the comprehension of the mechanism of reaction given by the co-precipitated Pd/Fe$_3$O$_4$ catalyst.

Only after the clarification of the overall reactions pathways followed by using the title catalyst, it was possible to shift the attention on the polymer cellulose, described in the subsequent chapter of this thesis.

4.1. Polyols C$_3$-C$_2$

The experimental investigation, at the beginning, was focused on biomass-derived polyols having the shortest carbon chain (C$_3$ – C$_2$), such as glycerol, 1,2-propanediol and ethylene glycol.

Glycerol (C$_3$ polyol, Gly) is a valuable feedstock, being the main by-product in bio-diesel production, cheaply available in increasing amounts [1]. Furthermore, the selective hydrogenolysis of glycerol leads to 1,2-propanediol (C$_3$ diol, 1,2-PDO), which is a useful feedstock in several industrial fields [2]. Ethylene glycol (C$_2$ polyol, EG) is the shortest polyol, typically used as antifreeze agent and as precursor of valuable polyesters (polyethylene terephthalate (PET) and polyethylene-naphthalate (PEN)) [3].

4.1.1.   Hydrogenolysis reactions

In Table 4.1 the results obtained by the hydrogenolysis of glycerol, 1,2-propanediol and ethylene glycol, within the range of temperature investigated (180-240°C), using a very low initial H$_2$ pressure (5 bar) are summarized.

Using glycerol as starting substrate, 1,2-propanediol (1,2-PDO) is the main reaction product at the lowest temperature (180°C) investigated, indicating that the Pd/Fe$_3$O$_4$ catalyst prefers the C–O bond cleavage rather

than the C–C bond breaking. Upon increasing the reaction temperature, a higher glycerol conversion accompanied by a lower selectivity towards 1,2-propanediol together with an increased amount of ethanol, methanol, 1-propanol and 2-propanol is observed. It is worth noting that the amount of ethanol reaches a maximum of 70.5% in the liquid phase products at 240°C, indicating that, at higher temperatures, the Pd/Fe$_3$O$_4$ catalyst also activates consistently the C–C bond breaking.

Table 4.1 Conversion of C$_3$-C$_2$ polyols promoted by the Pd/Fe$_3$O$_4$ catalyst in presence of molecular hydrogen.

Operating Conditions: 40 ml of aqueous solution with 4% wt of polyol, 0.25g of Pd/Fe$_3$O$_4$ catalyst, initial pressure of H$_2$: 5 bar, 180-240°C, 24 h of reaction, within an autoclave of 100mL.

Entry	Temp. [°C]	Conv. [%]	C$_{Liq}$ Ph. [%]	Molar Selectivity [%]				
				C3 1,2-PDO	POs	C2 EG	EtOH	C1 MeOH
Glycerol	180	92.4	78.6	77.1	0.2	15.0	7.7	0.0
Glycerol	210	100.0	67.6	57.7	1.7	9.7	27.2	3.7
Glycerol	240	100.0	57.2	9.3	10.1	0.5	70.5	9.6
1,2-PDO	180	14.2	98.6	-	5.3	0.0	94.7	0.0
1,2-PDO	210	61.5	72.2	-	6.1	0.0	93.9	0.0
1,2-PDO	240	78.7	67.7	-	8.6	0.0	90.0	1.4
EG	180	11.0	91.6	-	-	-	50.1	49.9
EG	210	31.7	72.7	-	-	-	43.4	56.6
EG	240	72.1	51.7	-	-	-	28.2	71.8

Abbreviations: 1,2-PDO = 1,2-Propanediol; POs: Propanols (1-propanol and 2-propanol); EG: Ethylene Glycol; EtOH: Ethanol; MeOH: Methanol.

Note: (-) means that such product is not considerable for the reaction considered, while (0.0) means that such product has not been detected.

1,2-Propanediol was also tested as starting reagent, in the same operating conditions, in the presence of molecular hydrogen (Table 4.1). Ethanol was found to be the main product, obtained with higher selectivity (90-94.7%) at every temperature investigated.

All these results suggest that ethanol found at higher reaction temperatures, arises mainly from the dehydrogenation/decarbonylation of 1,2-propanediol.

Having identified 180°C as the best reaction temperature in order to obtain 1,2-propanediol from glycerol, the hydrogenolysis of glycerol at different reaction times (Table 4.2) was investigated. As expected, the glycerol conversion increases when the reaction time passes from 6 to 24 hours.

Table 4.2 Conversion of glycerol promoted by the Pd/Fe_3O_4 catalysts in presence of molecular hydrogen, at different reaction times.

Operating Conditions: 40 ml of aqueous solution with 4% wt of glycerol, 0.25g of Pd/Fe_3O_4 catalysts, initial pressure of H_2: 5 bar, 180°C, 6-24 h of reaction, within an autoclave of 100mL.

Entry	Time [h]	Conv. [%]	C_{Liq} Ph. [%]	C3 1,2-PDO	POs	C2 EG	EtOH	C1 MeOH
								Molar Selectivity [%]
Glycerol	6	**60.9**	81.1	78.6	0.0	16.0	4.2	1.2
Glycerol	12	**78.2**	79.8	78.1	0.0	16.0	4.9	1.0
Glycerol	24	**100.0**	57.2	9.3	10.1	0.5	70.5	9.6

Abbreviations: 1,2-PDO = 1,2-Propanediol; POs: Propanols (1-propanol and 2-propanol); EG: Ethylene Glycol; EtOH: Ethanol; MeOH: Methanol.

The pressure effect was also investigated upon increasing the initial hydrogen pressure from 5 to 20 bar, at 180°C. It was observed a decrease in glycerol conversion as well as a lower 1,2-propanediol selectivity (Figure 4.1). Such a conversion decrease, on increasing the hydrogen pressure, in other hydrogenolysis reactions carried out over heterogeneous palladium systems, was ascribed to the competitive adsorption of the substrate and H_2 on the catalyst surface [4].

The recycle of the Pd/Fe_3O_4 catalyst at 180°C in the presence of H_2, was performed after washing the sample with pure water and a lower conversion, as expected, was observed (Figure 4.2). However, the selectivity did not change appreciably, as already reported in the past, and in experiments performed using 2-propanol as solvent [5]. The Pd/Fe_3O_4 catalyst was also

tested at higher glycerol concentrations (20% wt of glycerol solution, 1g of reduced Pd/Fe$_3$O$_4$ catalyst, initial pressure of H$_2$: 20 bar, 24 hours of reaction): the selectivity towards 1,2-propanediol (83,9%), ethylene glycol (11,2%), ethanol (4,2%) and propanols (0,7%) was detected with a glycerol conversion of 83,9%.
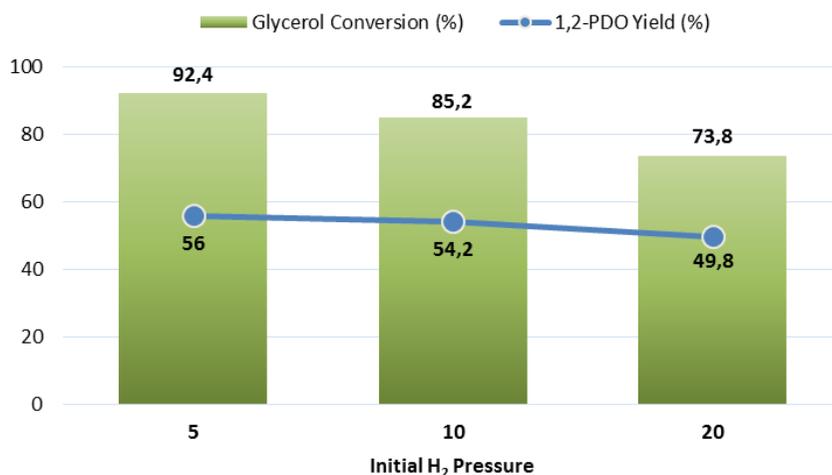
Figure 4.1   Initial H$_2$ pressure effect on the glycerol conversion (%) and 1,2-propanediol yield (%) in the reaction performed with the reduced Pd/Fe$_3$O$_4$ catalyst.
Operating Conditions: 40 ml of aqueous solution with 4% wt of glycerol, 0.25g of Pd/Fe$_3$O$_4$ catalyst, initial pressure of H$_2$: 5-20 bar, 180°C, 24 h of reaction, within an autoclave of 100mL.

Finally, the reactivity of ethylene glycol hydrogenolysis (Table 4.1), in presence of the Pd/Fe$_3$O$_4$ catalyst, shows a pretty equimolar selectivity into methanol and ethanol at 180°C and, when the temperature increases, the main product becomes methanol. Reactions starting from ethylene glycol proceed more slowly with respect to glycerol, at every temperature investigated. At 180°C, the Pd/Fe$_3$O$_4$ catalyst equally cleaves the C–C and the C–O bonds of EG, allowing the production of methanol and ethanol in comparable yields. Upon raising the reaction temperature, an enhanced performance of Pd/Fe$_3$O$_4$ catalyst to C–C bond breaking is noticed.

The presence of added H$_2$ in the catalytic test does not allow a truthful quantitative analysis of gas phase products. However, in the temperature

range investigated (180–240°C) a qualitative analysis reveals the main presence of CO_2 accompanied by a very low amount of alkanes.
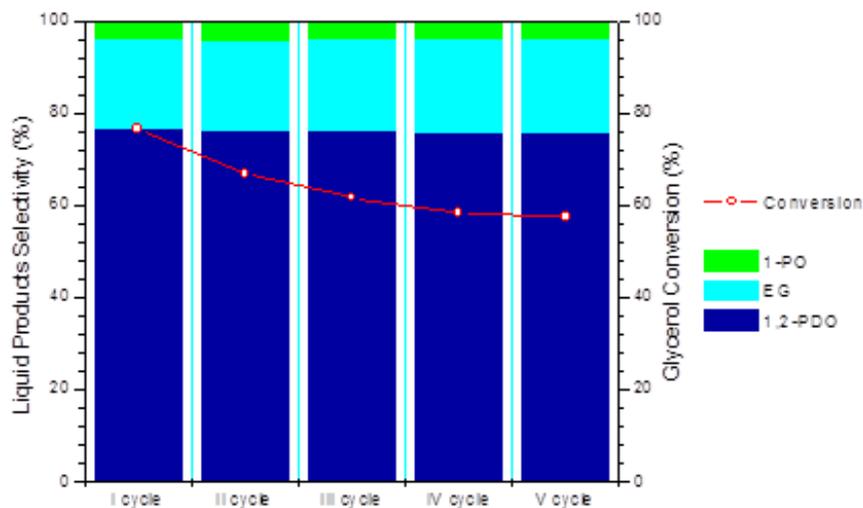
Figure 4.2 Recycle of the Pd/Fe_3O_4 catalyst in the glycerol hydrogenolysis (in presence of molecular H_2).
Operating Conditions: 40 ml of aqueous solution with 4% wt of glycerol, 0.25g of Pd/Fe_3O_4 catalyst, initial pressure of H_2: 5 bar, 180°C, 24 h of reaction, within an autoclave of 100mL.

4.1.2. *Reactions without molecular H₂: under inert atmosphere*

Since glycerol is considered an interesting feedstock to produce bio – hydrogen, the feasibility to produce hydrogen from glycerol through the aqueous-phase reforming process promoted by the Pd/Fe_3O_4 catalyst was investigated [6-8].

In Table 4.3 and 4.4 results obtained by reactions carried out under inert atmosphere (aqueous phase reforming (APR) conditions), the distributions of products in liquid and gas phases, respectively, are reported.

Upon increasing the temperature from 180 to 210 and 240°C, glycerol is fully converted with a higher production of gas phase products and at 240°C a H_2 selectivity of 80.5% in gas phase products is reached.

The liquid phase product distribution for the APR of glycerol at 180°C, includes mainly 1,2-propanediol, ethylene glycol, and methanol. In the gas phase, H_2 is the main product (73.4%) together with CO_2 (26.1%) and a negligible amount (0.5%) of light alkanes (methane, ethane and propane) are observed. The hydrogen necessary for the hydrogenolysis reaction derives from the aqueous phase reforming of glycerol itself as well as from the water gas shift (WGS) process.

Table 4.3 Conversion of glycerol and ethylene glycol promoted by the Pd/Fe$_3$O$_4$ under inert atmosphere. Liquid phase composition. *Operating Conditions:* 40 ml of aqueous solution with 4% wt of polyol, 0.25g of Pd/Fe$_3$O$_4$ catalyst, initial pressure of N$_2$: 5 bar, 180-240°C, 24 h of reaction, within an autoclave of 100mL.

Entry	Temp. [°C]	Conv. [%]	C_{Liq} Ph. [%]	Molar Selectivity [%]				
				C3		C2		C1
				1,2-PDO	POs	EG	EtOH	MeOH
Glycerol	**180**	**9.8**	76.8	72.8	3.5	12.2	1.0	10.5
Glycerol	**210**	**100**	64.7	42.9	5.2	6.3	36.6	9.0
Glycerol	**240**	**100**	41.9	9.4	8.7	0.2	73.0	8.7
EG	**180**	**13.3**	89.8	-	-	-	39.7	60.3
EG	**210**	**34.5**	73.5	-	-	-	26.7	73.3
EG	**240**	**66.2**	50.9	-	-	-	23.4	76.6

Abbreviations: 1,2-PDO = 1,2-Propanediol; POs: Propanols (1-propanol and 2-propanol); EG: Ethylene Glycol; EtOH: Ethanol; MeOH: Methanol.

Note: (-) means that such product is not considerable for the reaction considered, while (0.0) means that such product has not been detected.

Significant changes in the liquid phase product composition are also detected. As expected, the amount of 1,2-propanediol decreases while a higher selectivity to ethanol and propanols is observed. Similarly, the ethylene glycol selectivity drops from 12.2% at 180°C to 6.3% at 210°C and to 0.2% at 240°C as a result of the further dehydrogenation and hydrogenolysis processes.

Table 4.4 Conversion of glycerol and ethylene glycol promoted by the Pd/Fe₃O₄ under inert atmosphere. Gas phase composition. *Operating Conditions:* 40 ml of aqueous solution with 4% wt of polyol, 0.25g of Pd/Fe₃O₄ catalyst, initial pressure of N_2: 5 bar, 180-240°C, 24 h of reaction, within an autoclave of 100mL.

Entry	Temp. [°C]	Conv. [%]	C$_{Gas}$ Ph. [%]	Molar Selectivity [%]		
				H$_2$	CO$_2$	Alkanes
Glycerol	**180**	**9.8**	23.2	73.4	26.1	0.5
Glycerol	**210**	**100**	35.3	77.8	20.8	1.4
Glycerol	**240**	**100**	58.1	80.3	17.5	2.2
EG	**180**	**13.3**	10.2	81.7	18.3	0.0
EG	**210**	**34.5**	26.5	81.6	18.4	0.0
EG	**240**	**66.2**	49.1	81.2	18.8	0.0

It is important to highlight that CO is never detected, which is indicative of a worthy activity of the bimetallic Pd/Fe₃O₄ catalyst toward the water gas shift reaction.

Typical operating conditions in APR processes are characterized by the presence of higher pressures, in order to maintain water in the liquid state. The operating conditions, described in this work, use very low initial pressure. However, in the temperature range investigated, the amount of water in the vapor state should be very low (below 3% at 240°C) allowing to investigate the C–C bond breaking under reaction conditions very close to those usually adopted for APR reactions.

A combination of APR and *in situ* hydrogenolysis reactions of ethylene glycol is also observed. In line with the reactions carried out in the presence of added H₂, a lower conversion of ethylene glycol, with respect to glycerol, is achieved within the temperature range of 180–240°C. The liquid phase analysis shows methanol (C–C bond breaking) as the main reaction product and the selectivity to ethanol (C–O bond cleavage) gets lower as the temperature increases. Gas phase products are characterized by a good H₂ production and an insignificant amount of alkanes.

4.1.3. *Discovering the reaction mechanism: Hydrogenolysis vs. APR*

The results of the glycerol conversion at 180°C in the presence of molecular H_2 over the Pd/Fe_3O_4 catalyst are in agreement with those obtained before, by other members of our group, when 2-propanol was used as the solvent and hydroxyacetone (AC) was identified as a reaction intermediate during the 1,2-propanediol formation [5, 9]. The main difference lies in the higher fraction of ethylene glycol and ethanol detected in water and not observed in 2-propanol where a good selectivity to 1-propanol was also found (Figure 4.3).
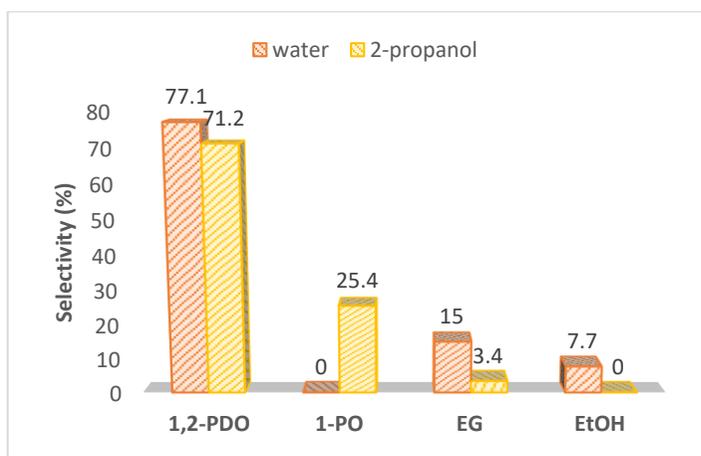
Figure 4.3 Glycerol hydrogenolysis promoted by the Pd/Fe_3O_4 catalyst in presence of added H_2 (5 bar), by using water (conversion = 92,4%) or 2-propanol (conversion = 100%) as reaction solvent. Distribution of products in liquid phase.

Therefore, it can be stated that in glycerol hydrogenolysis, it is undesirable to use water as a reaction medium in order to drive the equilibrium to propanol formation.

Cross-check experiments, under both reaction conditions used in this study (H_2 or N_2) and within the temperature range investigated (180–240°C), show that pure Fe_3O_4 does not give any glycerol conversion, suggesting that the presence of palladium is an essential prerequisite for C–O and C–C bond breaking.

In agreement with the catalytic results, the conversion of glycerol promoted by the bimetallic Pd/Fe_3O_4 catalyst can follow two distinctive routes for the 1,2-propanediol and ethylene glycol formation (Figure 4.4).
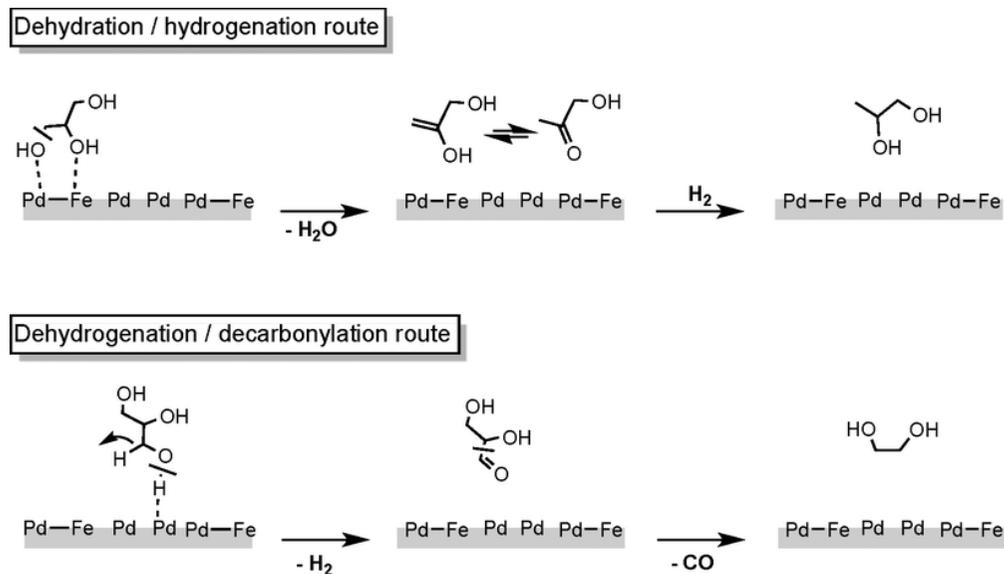
Figure 4.4 Initial steps in glycerol conversion, both in presence and in absence of molecular H_2: the dehydration/hydrogenation and the dehydrogenation/decarbonylation routes.

The adsorption of two adjacent alcoholic groups of glycerol on Pd and Fe sites with a subsequent C–OH breaking promoted by palladium, is the first step in the reaction pathway that leads to 1,2-propanediol. The unstable enol is then rearranged to hydroxyacetone (AC), which is finally hydrogenated into 1,2-propanediol [9]. On the other hand, glycerol conversion toward ethylene glycol proceeds via a previous dissociation of primary alcoholic groups followed by the C–H bond breaking. The ensuing glyceraldehyde undergoes a final C–CO breaking leading to ethylene glycol and CO formation. Other possible alternative processes, such as the one affording dihydroxyacetone (derived from the dehydrogenation of the secondary alcoholic group), have been discarded since such pretty stable compound has never been detected.

Data reported in Tables 4.3 and 4.4 concerning reactions carried out under inert conditions show that, together with H_2, CO_2 and a small amount of

alkanes, liquid phase products are formed. The presence of hydrogenolysis products implies that the *in situ* produced H_2 participates directly in the hydrogenation of the intermediates produced from the dehydration route.

Therefore, it can be affirmed that hydrogenolysis and APR are competitive processes (hydrogenolysis vs. APR) and that the dehydration and dehydrogenation reactions are key elementary steps in the conversion of glycerol both in the presence and in absence of added H_2.

In the presence of H_2 or under inert atmosphere, at 180°C, the Pd/Fe_3O_4 catalyst allows the conversion of glycerol to 1,2-propanediol in a good yield showing an enhanced ability toward the C–O bond cleavage. Conversely, at higher reaction temperatures, dehydrogenation reactions prevail and the dehydration/ hydrogenation steps become less important, even when 1,2-propanediol is used as the starting substrate (Table 4.1). To this regard, the research group of Tsang has also recently observed the higher ability of the co-precipitated Pd/Fe_3O_4 catalyst (prepared by an analogous synthetic procedure) in the selective C–C bond breaking of biomass derived polyols at a high reaction temperature (250°C) [10]. Accordingly, a recent report clearly shows that reaction temperatures lower than 180°C are more advantageous to the production of propanols from 1,2-propanediol [11]. The temperature dependence of the reaction pathway's selectivity can be related to the different bond energies involved in the alternative processes [12]. The dehydration/ hydrogenation route implies the initial C–OH cleavage of the primary alcoholic group ($E_{C-OH} \cong 80$ kcal mol^{-1}) [12] followed by the rearrangement of the unstable enol to hydroxyacetone which is finally hydrogenated to 1,2-propanediol [9]. Conversely, the dehydrogenation /decarbonylation route involves the prior O–H breaking ($E_{O-H} \cong 104$ kcal mol^{-1}) [11] followed by the β C–H (with respect to oxygen) elimination and by the consequent C–CO rupture [13-14]. Moreover, since a negligible amount of methanol was detected in the reactions carried out by using 1,2-propanediol as the starting substrate it can be confirmed that the rupture of the O–H bond is a fundamental prerequisite for C–C cleavage. Similar conclusions have been also proposed by Lercher and co-workers that suggest a reaction network consisting of parallel routes, including dehydrogenation and dehydration as the primary steps in the hydrodeoxygenation and APR of C_3 alcohols and polyols [15-16].

In this regard, it is worth to underline that the C–CO bond energy value is about 83 kcal mol^{-1}, quite proximate to that of an internal C–C bond ($E_{C–C} \cong$ 85 kcal mol^{-1}) [12]. Therefore, C–CO is cleaved preferentially with respect to the direct breaking of the C–C bond since (i) the terminal C=O group does not undergo steric hindrance and easily interacts with the catalyst metal surface and (ii) its removal is helped by the simultaneous aldehydic C–H ($\cong$95 kcal mol^{-1}) bond breaking promoted by metal particles. Accordingly, on the basis of theoretical studies, it has been reported that the C–C bond breaking of glycerol on the Pt (111) surface has a very high barrier with respect to that of the terminal C–CO bond cleavage [17].
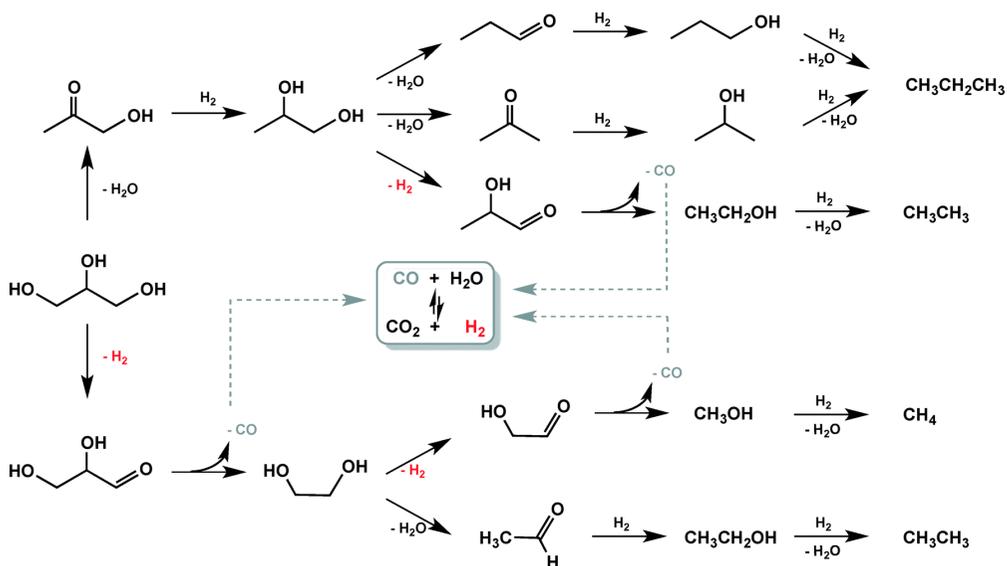
Figure 4.5 Hydrogenolysis vs. APR: overall reaction pathways for the conversion of glycerol.

An analogous competition of the dehydration/hydrogenation and dehydrogenation processes (hydrogenolysis vs. APR) occurs starting from ethylene glycol. The catalytic results at 180 and 210°C in the presence of H$_2$ show a competition between the CO–H bond cleavage and C–O bond breaking reactions (methanol and ethanol are almost equally formed) while, at 240°C, the CO–H bond scission reaction becomes more favorable with a higher production of methanol confirming the temperature dependence of the dehydration and dehydrogenation routes. Under inert conditions, methanol is the main reaction product obtained in the liquid phase as a result of the prevalence of the dehydrogenation/decarbonylation route.

Recent density functional theory (DFT) calculations, complemented with temperature-programmed desorption (TPD) experiments, demonstrate that the decomposition of ethylene glycol on Pt and Pt/Ni surfaces proceeds first through dehydrogenation to reach one of the species with a terminal CO followed by C–C bond cleavage [18]. All these results allow the overall pathways for describing the hydrogenolysis vs. APR reactions starting from glycerol to be drawn, as represented in Figure 4.5. The gas phase composition of the reactions carried out under inert atmosphere are characterized by a H_2/CO_2 ratio higher than the maximum value theoretically expected for the glycerol APR (1):

$$C_3H_8O_3 + 3H_2O \rightarrow 7H_2 + 3CO_2 \qquad\qquad (1)$$
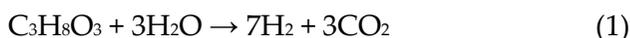
The explanation for the "apparent" anomaly is that the catalytic tests are conducted in batch mode with the gas phase products collected in a gas sampler cylinder directly connected to the autoclave reactor. The sampling system adopted allows the collection of gas-phase products at about 2/3 of the pressure measured at 25°C. Therefore, under our sampling conditions, it is necessary to take into consideration that CO_2 is much more soluble in water than H_2 ($CO_{2(sol)}/H_{2(sol)} \cong 55$). Therefore the H_2/CO_2 ratio measured is expected to be higher than predicted on the basis of reaction (1) and even higher as the final pressure (related to the reaction temperature) increases.

In accordance with all these considerations, the measured pH values of the liquid phase are 6.10, 5.90 and 5.75 for the reactions carried out respectively at 180, 210 and 240°C as expected from the weak acidity of CO_2 in water.

Analogous considerations can be referred to APR reactions of ethylene glycol.

Another very important peculiarity of the Pd/Fe_3O_4 catalyst is the absence of CO (as a gas phase product) in all experiments. The obvious implication is that the WGS equilibrium is completely shifted towards H_2 and CO_2 formation. Consequently, the Pd/Fe_3O_4 is very efficient in the WGS reaction but poorly effective as a Fisher–Tropsch or methanation catalyst.

This is easily understandable considering that both palladium and Fe_3O_4 are known to be efficient catalysts for affording WGS products. Analogous results were also obtained by Dumesic's research group showing a superior activity of the impregnated Pd/Fe_3O_4 catalyst with respect to the analogous

Pd/Fe$_2$O$_3$ in the APR of ethylene glycol as a result of the enhanced WGS reaction promoted by the synergistic effect of Pd nanoparticles and magnetite [19].

4.2. Polyols C$_6$-C$_4$

Cellulose and hemicellulose derived sorbitol (C$_6$ polyol, Sorb) and xylitol (C$_5$ polyol, Xyl) have been inserted in the list of top 12 biomass-based building blocks [4,20-21] representing key renewable resources for modern biorefineries. Sorbitol is attracting intense industrial and research interests [22-23]. At present, it is largely used in pharmaceutical, food and cosmetic industries [24]. Moreover, sorbitol has been proposed as building block for production of biofuels, chemicals [25-27] and renewable hydrogen (through the aqueous phase reforming process, APR) [25, 28-32]. Xylitol is widely applied as sweetener and inhibitor for the development of bacteria in foods [24, 33]. Erythritol (C$_4$ polyol, Eryth) is the main starting substrate for the synthesis of butanediols (BDOs), that are widely employed as precursors of polyester resins, polyurethanes and polymers such as polybutylene-terephthalate (PBT) [24,33].

4.2.1. *Hydrogenolysis of Sorbitol*

The catalytic results of the bimetallic Pd/Fe$_3$O$_4$ catalyst in the hydrogenolysis of sorbitol, compared with that of the commercial Pd/C, are reported in Table 4.5. The bimetallic Pd/Fe$_3$O$_4$ catalyst shows excellent performances affording an almost complete conversion at 180°C (91%) and a total conversion (100%) at 210°C. The distribution pattern of products, in liquid phase, changes within the temperature range investigated. Indeed, at lower temperatures (150 and 180°C) the main reaction products are xylitol (Xyl) and glycerol (Gly), followed by lower amounts of erythritol (Eryth) and ethylene glycol (EG). When the temperature increases, xylitol and glycerol are gradually converted into smaller polyols such as butanediols (BDOs = 1,2-butandiol + 1,4- butanediol + 2,3-butandiol), 1,2-propanediol (1,2-PDO), propanols (POs: 1-propanol and 2-propanol), ethylene glycol (EG) and ethanol (EtOH). It is worth noting that, as the reaction proceeds toward products having lower molecular weight, the amount of ethanol progressively increases, so that it becomes the main product, in liquid phase,

at 240°C (63.5% mol-based selectivity, 25.4% carbon based yield). On the contrary, the commercial Pd/C exhibits a significant lower activity. Indeed, at 210°C the sorbitol conversion is less than 30% and the maximum is 60% at 240°C, the highest temperature investigated. The selectivity pattern, on increasing the temperature, follows a similar trend as that reported for the Pd/Fe$_3$O$_4$ catalyst; furthermore, a much lower ethanol yield is always registered (12% carbon-based yield at 240°C).

Table 4.5 Conversion of sorbitol promoted by Pd/C and Pd/Fe$_3$O$_4$ catalysts, in presence of molecular H$_2$. Liquid phase composition. *Operating Conditions: 40 ml of aqueous solution with 4% wt of sorbitol, 0.25g of reduced catalyst, initial pressure of H$_2$: 5 bar, 180-240°C, 24 h of reaction, within an autoclave of 100mL.*

| | | | | Molar Selectivity [%] | | | | | | | | | | | |
| Cat. | Temp. | Conv. | Liq Ph. | C5 | C4 | | | | C3 | | | | C2 | | |
	[°C]	[%]	[%]	Xyl	Eryth	1,2-BDO	1,4-BDO	2,3-BDO	Gly	1,2-PDO	1-PO	2-PO	EG	EtOH	OP
Pd/Fe$_3$O$_4$	240	100.0	40.0	0.0	0.0	0.0	0.3	2.8	0.0	5.9	13.0	1.0	0.0	63.5	13.5
Pd/C	240	60.0	44.0	0.0	0.0	3.2	0.0	2.0	0.0	20.4	13.4	0.0	12.4	45.4	3.2
Pd/Fe$_3$O$_4$	210	100.0	60.0	0.0	0.0	8.4	0.0	7.4	1.2	22.0	10.0	0.0	8.1	41.3	1.6
Pd/C	210	28.0	100.0	0.0	0.0	11.4	0.0	2.1	4.3	35.0	4.2	0.0	26.1	16.9	0.0
Pd/Fe$_3$O$_4$	180	91.0	80.0	5.5	1.8	7.2	0.0	5.0	19.5	27.9	2.0	0.0	13.4	8.5	9.2
Pd/C	180	13.6	100.0	0.0	0.0	12.0	0.0	0.0	18.0	42.0	0.0	0.0	22.0	6.0	0.0
Pd/Fe$_3$O$_4$	150	17.0	100.0	33.0	7.0	0.5	0.0	0.0	35.0	10.0	0.0	0.0	8.0	0.5	6.0
Pd/C	150	<1	100.0	-	-	-	-	-	-	-	-	-	-	-	-

Abbreviations: Xyl: Xylitol; Eryth: Erythritol; 1,2-BDO: 1,2-Butanediol; 1,4-BDO:1,4-Butanediol; 2,3-BDO: 2,3-Butanediol; Gly: Glycerol; 1,2-PDO: 1,2-Propanediol; 1-PO: 1-Propanol; 2-PO: 2-propanol; EG: Ethylene glycol; EtOH: Ethanol; OP: other products.

Furthermore, pure Fe$_3$O$_4$ was tested, within the same temperature range, but no appreciable sorbitol conversion was observed.

The lack of a significant reactivity using either Pd/C or pure Fe$_3$O$_4$, confirms that the marked activity shown by the bimetallic Pd/Fe$_3$O$_4$ catalyst has to be attributed to the strong interaction between palladium and iron, as consequence of the preparation method (co-precipitation) [34, 35] in analogy with other reports attaining to C$_3$ and C$_2$ polyols.

Table 4.6 Conversion of sorbitol promoted by the Pd/Fe₃O₄ in presence of molecular H_2. Gas phase composition. *Operating Conditions:* 40 ml of aqueous solution with 4% wt of sorbitol, 0.25g of Pd/Fe₃O₄ catalyst, initial pressure of H_2: 5 bar, 180-240°C, 24 h of reaction, within an autoclave of 100mL.

Temp [°C]	Conv. [%]	Gas Ph. [%]	Molar Selectivity [%]			
			CH_4	C_2H_6	C_3H_8	CO_2
240	100.0	60.0	6.0	0.9	1.6	91.5
210	100.0	40.0	3.1	0.5	0.2	96.2
180	91.0	20.0	0.7	0.2	0.2	98.9

Gaseous products were also quantitatively analyzed, pulling out the gas phase from the reaction vessel, cooled down at room temperature, after every experiment without accounting for the amount of molecular hydrogen, added as pure reactant (5 bar at 25°C) at the start of each reaction. The amount of gas products rises on increasing the reaction temperature (180–240°C), although its composition was found quite constant, being composed by, mainly, carbon dioxide and only small amounts of alkanes (methane, ethane and propane). Gaseous compositions, detected at different temperatures, are depicted in Figure 4.6. It is worth to highlight that carbon monoxide was never detected in the gas phase, confirming that the Pd/Fe₃O₄ catalyst is also effective to promote the water gas shift reaction, as previously observed in the hydrogenolysis of glycerol and ethylene glycol, carried out under APR conditions [36].
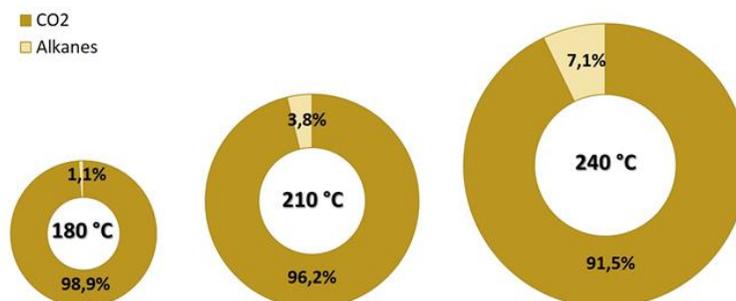
Figure 4.6 Hydrogenolysis of sorbitol: gas phase composition at 180°C (20%), 210°C (40%) and 240°C (60%) after 24h of reaction promoted by Pd/Fe₃O₄ catalyst.

Considering the 240°C value as a significant reaction temperature to maximize the ethanol production in liquid phase, sorbitol hydrogenolysis was also investigated at different reaction times (3, 6, 12 and 24 h). The sorbitol conversion was complete already after 3 h of reaction, although the ethanol selectivity in liquid phase increases as the reaction proceeds from 3 to 24 h (Figure 4.7, top). Results obtained from investigations at different reaction times at 180 and 210°C are reported in Table 4.7 and 4.8. The effect of the hydrogen pressure increase from 5 to 20 bar was also investigated. At 240°C the conversion of sorbitol remains complete; however, the decrease of ethanol selectivity in liquid phase was ascertained (Figure 4.7, bottom). A similar effect was also observed, at 180 and 210°C (Figure 4.8 and 4.9). The result suggests an inhibitory effect, due to the hydrogen pressure, on the hydrogenolysis reaction, probably ascribed to a competitive adsorption of substrate and hydrogen on the catalyst surface [19, 25, 36–47].
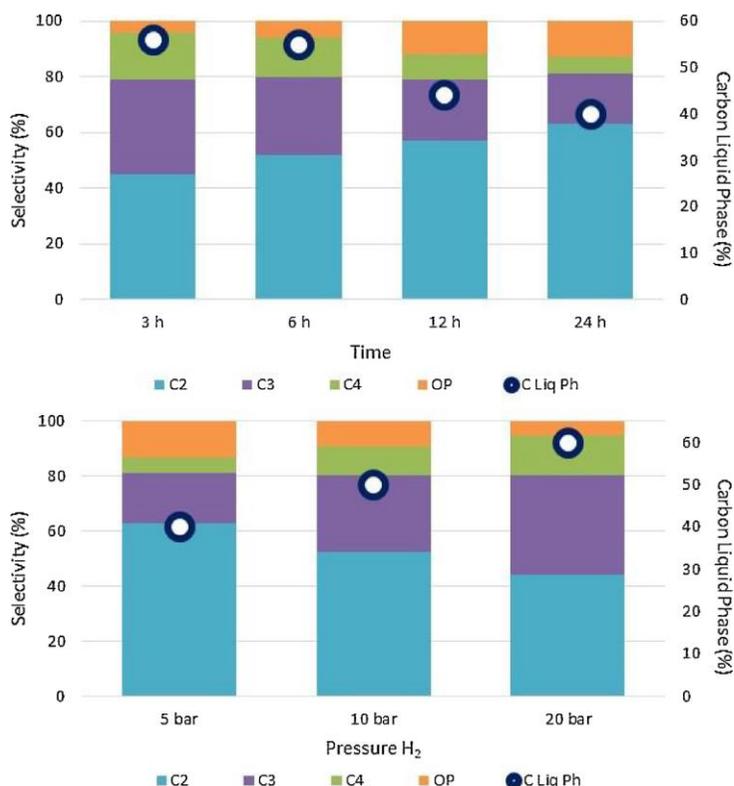
Figure 4.7 Reaction time (top) and initial H_2 pressure (bottom) effects, showed in terms of selectivity (%) and carbon liquid phase (%) obtained in the hydrogenolysis of sorbitol carried out in presence of H_2 at 240°C, with Pd/Fe$_3$O$_4$ catalyst, for 24 h of reaction.

Table 4.7 Reaction time effect (6-24h). Liquid product selectivity (% mol) in the hydrogenolysis of sorbitol carried out at 180°C. *Operating Conditions:* 40 ml of aqueous solution with 4% wt of sorbitol, 0.25g of Pd/Fe$_3$O$_4$ catalyst, initial pressure of H$_2$: 5 bar, 180°C, 6-24 h of reaction, within an autoclave of 100mL.

Time [h]	Conv [%]	Liq.Ph. [%]	C5 Xyl	C4 Eryth	1,2 -BDO	1,4 -BDO	2,3 -BDO	C3 Gly	1,2-PDO	1-PO	2-PO	C2 EG	EtOH	OP
6	56.0	95.0	14.0	4.0	6.0	0.0	3.0	27.0	20.0	2.0	0.0	11.0	5.0	8.0
12	78.0	80.0	9.6	3.0	6.5	0.0	5.5	25.6	22.5	1.0	0.0	11.2	6.2	8.9
24	91.0	80.0	5.5	1.8	7.2	0.0	5.0	19.5	27.9	2.0	0.0	13.4	8.5	9.2

(The "Molar Selectivity [%]" spans the product columns C5 through OP.)

Abbreviations: Xyl: xylitol; Eryth: erythritol; 1,2-BDO: 1,2-butanediol; 1,4-BDO: 1,4-butanediol; 2,3-BDO: 2,3-butanediol; Gly: glycerol; 1,2-PDO: 1,2-propanediol; 1-PO: 1-propanol; 2-PO: 2-propanol; EG: ethylene glycol; EtOH: ethanol; OP: other products.

Table 4.8 Reaction time effect (6-24h). Liquid product selectivity (% mol) in the hydrogenolysis of sorbitol carried out at 210°C. *Operating Conditions:* 40 ml of aqueous solution with 4% wt of sorbitol, 0.25g of Pd/Fe$_3$O$_4$ catalyst, initial pressure of H$_2$: 5 bar, 210°C, 3-24 h of reaction, within an autoclave of 100mL.

Time [h]	Conv [%]	Liq.Ph. [%]	C5 Xyl	C4 Eryth	1,2 -BDO	1,4 -BDO	2,3 -BDO	C3 Gly	1,2-PDO	1-PO	2-PO	C2 EG	EtOH	OP
3	96.7	90.0	1.9	0.0	10.3	0.0	4.3	12.7	34.8	2.8	0.0	18.0	11.7	3.5
6	100	70.0	1.8	0.0	9.3	0.0	6.1	8.0	34.5	1.7	0.0	14.4	18.2	6.0
12	100	65.0	0.0	0.0	9.0	0.0	7.4	1.3	29.1	7.2	0.0	10.3	32.2	3.5
24	100	60.0	0.0	0.0	8.4	0.0	7.4	1.2	22.0	10.0	0.0	8.1	41.3	1.6

(The "Molar Selectivity [%]" spans the product columns C5 through OP.)

Abbreviations: Xyl: xylitol; Eryth: erythritol; 1,2-BDO: 1,2-butanediol; 1,4-BDO: 1,4-butanediol; 2,3-BDO: 2,3-butanediol; Gly: glycerol; 1,2-PDO: 1,2-propanediol; 1-PO: 1-propanol; 2-PO: 2-propanol; EG: ethylene glycol; EtOH: ethanol; OP: other products
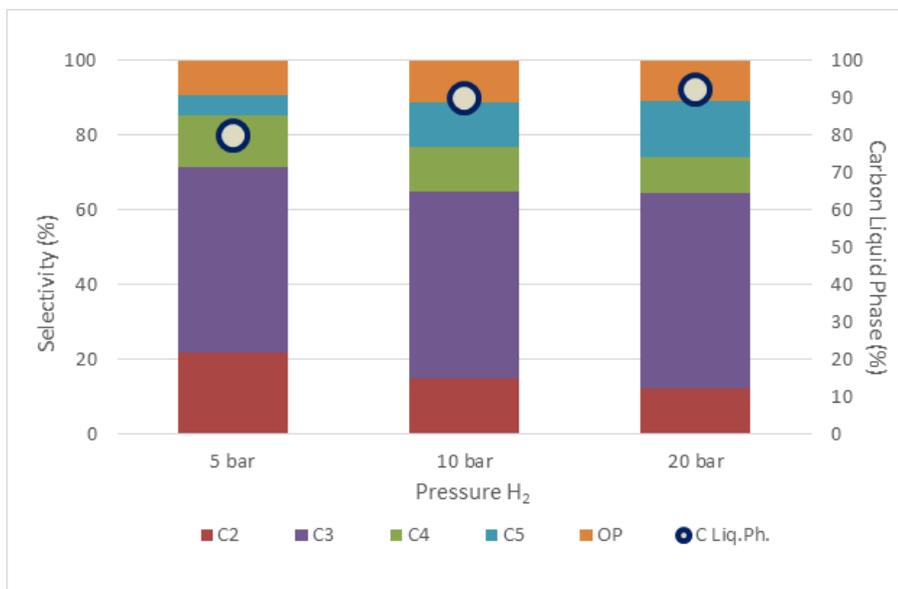
Figure 4.8 Effect of the initial H_2 pressure increase (5-20 bar) on the product distribution expressed in terms of selectivity (%) and carbon in liquid phase (%) obtained through hydrogenolysis of sorbitol carried out in presence of H_2 at 180°C, with Pd/Fe$_3$O$_4$ catalyst after 24 h of reaction.
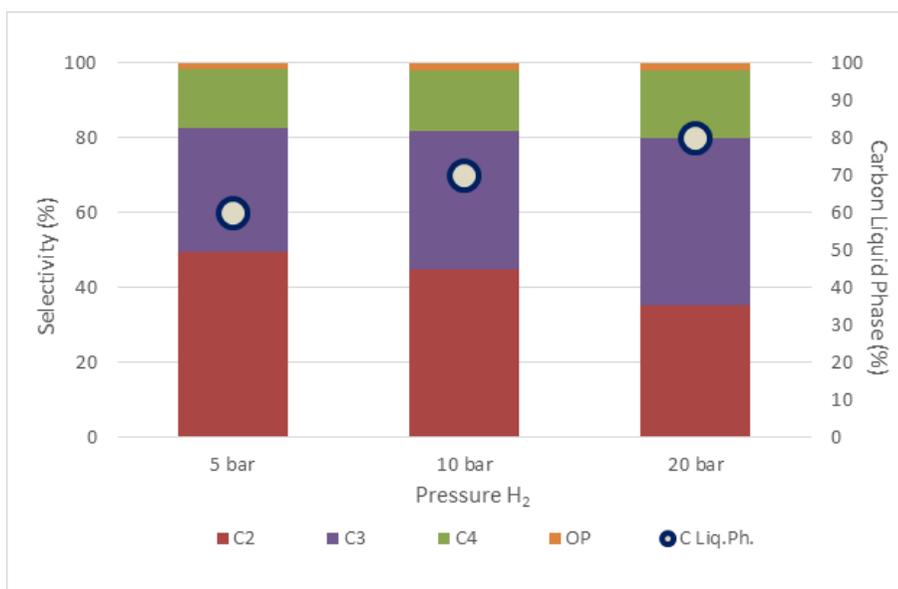
Figure 4.9 Effect of the initial H_2 pressure increase (5-20 bar) on the product distribution expressed in terms of selectivity (%) and carbon in liquid phase (%) obtained through hydrogenolysis of sorbitol carried out in presence of H_2 at 210°C, with Pd/Fe$_3$O$_4$ catalyst after 24 h of reaction.

4.2.2. *Hydrogenolysis of C5-C3 polyols*

In order to achieve a complete pattern of reactions, the hydrogenolysis of C5-C3 polyols, over the Pd/Fe3O4 catalyst, was also investigated under the same operative conditions. The results obtained at 240, 210 and 180°C are detailed in Tables 4.9-4.11, respectively.

The conversion of all C5-C3 polyols at 240°C is very high ranging from 78.7 to 100% except for 2,3-butanediol (2,3-BDO) that, as expected, is a stable molecule and does not give any appreciable reactivity [48]. From the distribution of products in liquid phase, it is quite clear that ethanol is mainly formed from xylitol, 1,4-butanediol, 1,2-propanediol and glycerol hydrogenolysis, demonstrating that, under the reaction conditions adopted, both C-O and C-C cleavages simultaneously occur.

Table 4.9 Conversion of C5-C3 polyols promoted by the Pd/Fe3O4 catalyst under hydrogen pressure. *Operating Conditions:* 40 ml of aqueous solution with 4% wt of polyol, 0.25g of Pd/Fe3O4 catalyst, initial pressure of H2: 5 bar, 240°C, 24 h of reaction, within an autoclave of 100mL.

| Entry | n°C | Conv. [%] | Liq Ph. [%] | Molar Selectivity [%] | | | | | | | | |
| | | | | C4 | | | C3 | | | C2 | | |
				1,2- BDO	1,4- BDO	2,3-BDO	1,2-PDO	1-PO	2-PO	EG	EtOH	OP
Xyl	C5	100.0	40.0	2.4	0.0	2.9	5.4	16.0	0.0	1.2	64.1	8.0
Eryth	C4	100.0	36.0	2.1	0.0	15.1	9.1	31.0	1.0	0.8	34.3	6.6
1,2-BDO		98.0	63.0	-	0.0	0.0	18.0	80.0	0.0	0.0	1.0	1.0
1,4-BDO		100.0	73.0	0.0	-	0.0	0.0	6.5	0.0	0.0	92.5	1.0
2,3-BDO		0.0	100.0	0.0	0.0	-	0.0	0.0	0.0	0.0	0.0	0.0
Gly	C3	100.0	57.2	-	-	-	9.3	8.0	2.0	0.5	70.5	9.7
1,2-PDO		78.7	67.7	-	-	-	-	7.6	1.0	0.0	90.0	1.4

Abbreviations: Xyl: Xylitol; Eryth: Erythritol; 1,2-BDO: 1,2-Butanediol; 1,4-BDO: 1,4-Butanediol; 2,3-BDO: 2,3-Butanediol; Gly: Glycerol; 1,2-PDO: 1,2-Propanediol; 1-PO: 1-Propanol; 2-PO: 2-Propanol; EG: Ethylene glycol; EtOH: Ethanol; OP: Other products.
*Note:* (-) means that such product is not considerable for the reaction considered, while (0.0) means that such product has not been detected.

Xylitol is mostly converted into C2 and C3 alcohols, respectively ethanol (64.1% mol-based selectivity, 25.6% carbon-based yield) and POs (16% mol-

based selectivity, 8.6% carbon-based yield) and, in a lesser amount, di-alcohols, such as butanediols and 1,2-propanediol.

Erythritol follows a similar pattern affording C_2 and C_3 alcohols in almost equal amount. However, di-alcohols are also obtained, being butanediols (BDOs) the most abundant products, confirming the efficiency of erythritol to produce butanediols [48]. The investigated butanediols show a different pattern in the hydrogenolysis reaction. 1,2-Butanediol produces preferentially 1-propanol (80% mol-based selectivity, 49.4% carbon-based yield) followed by a smaller amount of 1,2-propanediol (18% mol-based selectivity, 11.1% carbon-based yield). On the contrary, 1,4-butanediol breaks preferentially the C_2-C_3 bond leading to an ethanol mol-based selectivity, that slightly overcomes 90% (67,5% carbon-based yield). As previously mentioned, the 2,3-BDO does not give any reactivity.

The C_3 polyols reactivity, in analogy with our previous report [36], follows the order: glycerol (100%) > 1,2-PDO (78.7%) being both very selective in ethanol production.

Table 4.10 Liquid product selectivity (mol %) in the hydrogenolysis of C_5-C_3 Polyols promoted by the Pd/Fe$_3$O$_4$ catalyst. *Operating Conditions:* 40 ml of aqueous solution with 4% wt of polyol, 0.25g of Pd/Fe$_3$O$_4$ catalyst, initial pressure of H$_2$: 5 bar, 210°C, 24 h of reaction, within an autoclave of 100mL.

Entry	Conv. [%]	Liq Ph. [%]	**C4** Eryth	1,2 -BDO	1,4 -BDO	2,3 -BDO	**C3** 1,2-PDO	1-PO	2-PO	**C2** EG	EtOH	OP
Xyl	100	45.0	0.5	5.0	2.0	7.0	20.4	8.3	0.0	13.0	40.8	3.0
Eryth	100	50.0	-	1.2	0.0	31.2	11.3	21.4	1.4	0.8	22.8	9.9
1,2-BDO	66.5	76.0	-	-	0.0	0.0	7.0	67.0	0.0	0.0	0.0	26.0
1,4-BDO	64.0	80.0	-	0.0	-	0.0	0.0	8.0	0.0	0.0	91.0	1.0
2,3-BDO	0.0	0.0	-	0.0	0.0	-	0.0	0.0	0.0	0.0	0.0	0.0
Gly	100	67.6	-	-	-	-	57.7	1.7	0.0	9.7	27.2	3.7
1,2-PDO	61.5	72.2	-	-	-	-	-	5.5	0.6	0.0	93.9	0.0

Abbreviations: Xyl: Xylitol; Eryth: Erythritol; 1,2-BDO: 1,2-Butanediol; 1,4-BDO: 1,4-Butanediol; 2,3-BDO: 2,3-Butanediol; Gly: Glycerol; 1,2-PDO: 1,2-Propanediol; 1-PO: 1-Propanol; 2-PO: 2-Propanol; EG: Ethylene glycol; EtOH: Ethanol; OP: Other products.

Note: *(-) means that such product is not considerable for the reaction considered, while (0.0) means that such product has not been detected.*

Table 4.11 Liquid product selectivity (mol %) in the hydrogenolysis of C₅-C₃ Polyols promoted by the Pd/Fe₃O₄ catalyst. *Operating Conditions:* 40 ml of aqueous solution with 4% wt of polyol, 0.25g of Pd/Fe₃O₄ catalyst, initial pressure of H₂: 5 bar, 180°C, 24 h of reaction, within an autoclave of 100mL.

Entry	Conv [%]	Liq.Ph. [%]	C4				C3				C2		
			Eryth	1,2-BDO	1,4-BDO	2,3-BDO	Gly	1,2-PDO	1-PO	2-PO	EG	EtOH	OP
Xyl	68.0	70.0	4.0	3.9	0.0	2.6	9.5	20.0	0.5	0.0	20.0	12.5	27.0
Eryth	94.0	76.0	-	14.0	1.0	16.0	9.5	16.0	1.4	0.0	9.8	3.1	29.2
1,2-BDO	23.5	93.0	-	-	0.0	0.0	0.0	5.4	65.2	0.0	0.0	0.0	29.4
1,4-BDO	30.0	100	-	0.0	-	0.0	0.0	0.0	4.0	0.0	0.0	91.0	5.0
2,3-BDO	0.0	0.0	-	0.0	0.0	-	0.0	0.0	0.0	0.0	0.0	0.0	0.0
Gly	92.4	78.6	-	-	-	-	-	77.1	0.2	0.0	15.0	7.7	0.0
1,2-PDO	14.2	98.6	-	-	-	-	0.0	-	5.0	0.3	0.0	94.7	0.0

Abbreviations: Xyl: xylitol; Eryth: erythritol; 1,2-BDO: 1,2-butanediol; 1,4-BDO: 1,4-butanediol; 2,3-BDO: 2,3-butanediol; Gly: glycerol; 1,2-PDO: 1,2-propanediol; 1-PO: 1-propanol; 2-PO: 2-propanol; EG: ethylene glycol; EtOH: ethanol; OP: other product.

Note: (-) means that such product is not considerable for the reaction considered, while (0.0) means that such product has not been detected.

4.2.3. *Understanding the reaction mechanism: C-O and C-C bond cleavages*

Consistent with the catalytic results obtained from the hydrogenolysis of sorbitol and C₅-C₃ polyols, a global reaction pathway, promoted by the bimetallic co-precipitated Pd/Fe₃O₄ catalyst, is proposed in Figure 4.10.

It is well accepted that the initial reaction step, in the hydrogenolysis of polyols, is the dehydrogenation of primary or secondary alcoholic group, leading to an aldehyde or a ketone [49–51]. In the light of observed reaction products, the hydrogenolysis of sorbitol follows, at the beginning, two main alternative ways: (i) the dehydrogenation/decarbonylation of terminal C—OH groups and (ii) the cleavage of internal C—C bonds via the dehydration/retro-aldol reaction.

The first steps, in sorbitol hydrogenolysis, are sketched in Figure 4.11. Three possible reaction routes have to be considered. In the case of an adsorption of a primary hydroxyl group on the catalyst surface, the dehydrogenation process allows an initial formation of glucose (open chain).

The following reaction pathway leads to shorten the polyol chain and the terminal C-CO breaking enables the production of xylitol (Route A).
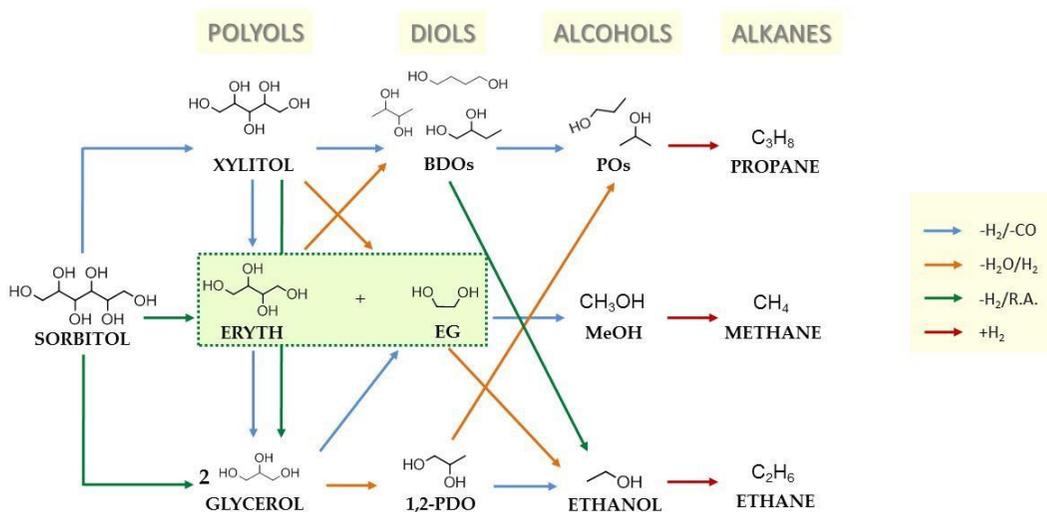
Figure 4.10 Schematic representation of cascade reactions involved in the sorbitol hydrogenolysis carried out over Pd/Fe₃O₄ catalyst.

On the other hand, if the internal C—C bond of glucose is cleaved by a retro-aldol mechanism, erythritol and ethylene glycol are formed as reaction products (Route B). Conversely, if a secondary hydroxyl group is dehydrogenated, the retro-aldol cleavage of C_3-C_4 bond affords two molecules of glycerol (Route C). Subsequently, consecutive reactions such as dehydrogenation/decarbonylation and dehydration/hydrogenation occur, leading, to final products including butanediols and C_2-C_3 alcohols, particularly ethanol (Figure 4.10). The contribution of other reaction mechanisms, such as the dehydration of sorbitol into cyclic compounds (e.g. isosorbide and 1,4-sorbitan) was not found to be operating in the reaction network over the Pd/Fe₃O₄ catalyst. Therefore, sorbitol appears to be simultaneously and consecutively subjected to two alternative patterns, as data at 150°C, where the conversion degree is low but useful to appreciate the initial steps, demonstrate (Table 4.5). The dehydrogenation/ decarbonylation of terminal C —OH groups produces xylitol (33% mol-based selectivity), while the retro-aldol condensation operates on the internal chain either breaking the C_3-C_4 bond, that forms two molecules of glycerol (35% mol-based

101

selectivity at 150°C) or, to a lesser extent, breaks the C_2-C_3 bond producing erythritol (7% mol-based selectivity) and ethylene glycol (8% mol-based selectivity).
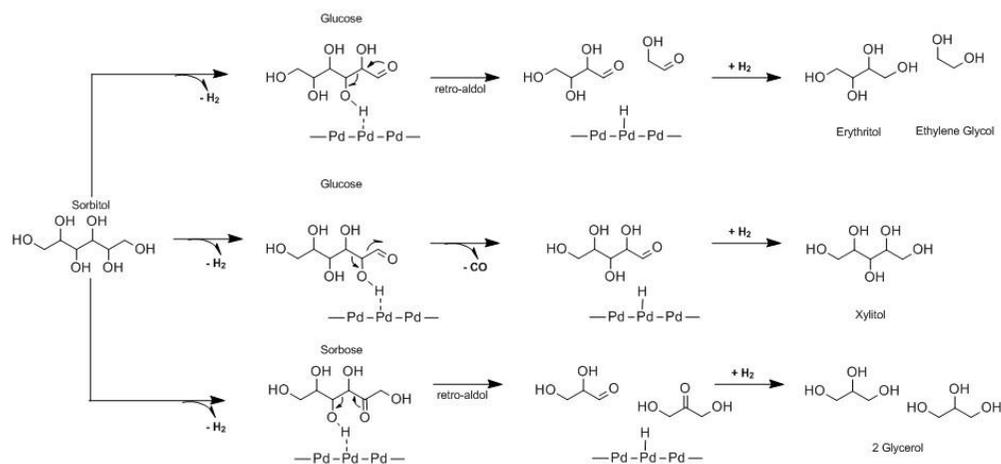
Figure 4.11 First steps in sorbitol conversion: the initial dehydrogenation is followed by retro-aldol condensation or decarbonylation reactions.

Xylitol is, in turn, converted into erythritol through dehydrogenation/decarbonylation, or through retro-aldol condensation, affording glycerol and ethylene glycol. Production of butanediols probably stems from erythritol rather than directly from xylitol.

Indeed, erythritol, through the dehydration/hydrogenation, leads to butanediols (BDOs) in a considerable amount, while, through retro-aldol condensation, ethylene glycol is obtained. Glycerol undergoes successive hydrogenolysis reactions leading, in liquid phase, prevalently to propanols and ethanol.

Butanediols react through different hydrogenolysis patterns depending on the isomer considered. The 2,3-butanediol does not give any appreciable conversion in the operating conditions investigated. The 1,2-butanediol, probably through dehydrogenation/decarbonylation, affords mainly 1-propanol whereas the 1,4-butanediol through retro-aldol condensation breaks the C_2-C_3 bond producing ethanol, and leads, marginally, to propanols through dehydrogenation/ decarbonylation.

The glycerol detected during the hydrogenolysis of sorbitol, almost entirely, derives from the initial retro-aldol condensation of sorbitol and only

in slight percentages, from xylitol and erythritol hydrogenolysis. Furthermore, glycerol dehydration/hydrogenation or dehydrogenation /decarbonylation affords 1,2-propanediol and ethylene glycol, respectively. 1,2-propanediol then leads to propanols or ethanol, after dehydration/ hydrogenation or dehydration/decarbonylation, respectively.

Finally, the hydrogenolysis of ethylene glycol could lead to ethanol or methanol. It is worth noting that, at the beginning of the reaction, having 5 bar of H_2 pressure, the initial molar ratio of H_2/sorbitol is about 2,5. However, in order to perform the complex pattern of reactions observed (Figure 4.10) the amount of H_2 should be higher than that available on the vessel volume.

Nevertheless, it is useful to remember that H_2 can be also formed by APR of sorbitol itself (as well as from other polyols formed through the hydrogenolysis process):

$$C_xO_xH_{2(x+1)} + xH_2O \rightarrow xCO_2 + (2x+1) H_2$$
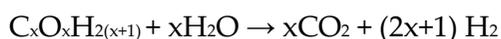
where the stoichiometry involves the sum of the two reactions:

(1) Reforming of polyol into hydrogen and carbon monoxide $(C_xO_xH_{(2x+1)} \rightarrow x\ CO + (x + 1)\ H_2)$

(2) Water Gas Shift (WGS) reaction of carbon monoxide into carbon dioxide and hydrogen $(xCO + x\ H_2O \rightarrow x\ CO_2 + x\ H_2)$

As mentioned above, in §4.2.1, the gas phase is composed, together with molecular H_2, by carbon dioxide and only traces of alkanes are detected (Table 4.6). Therefore, hydrogenation, leading to gaseous hydrocarbons is negligible with our catalyst. Moreover, the complete absence of carbon monoxide indicates that all the CO deriving from decarbonylation is converted into carbon dioxide through the water-gas-shift reaction promoted by the Pd/Fe_3O_4 catalyst.

Hydrogenolysis of sorbitol over Pd/C occurs with a similar reaction pathway as that observed on using the Pd/Fe_3O_4 catalyst.

However, both sorbitol conversion and products distribution point to a slower reactivity. Indeed, at a lower temperature (150°C) a very small amount of sorbitol seems to be converted entirely into glycerol, through retro-aldol condensation. This is then partially hydrogenolized into 1,2-propanediol and ethylene glycol. Conversely, upon increasing the temperature, starting from 180°C formation of erythritol, partially converted to butanediols, also occurs.

The lateral C—C cleavage of sorbitol into xylitol, seems to be absent. At temperatures above 200°C, the cascade hydrogenolysis processes are more shifted towards C_3-C_2 diols and alcohols and, at 240°C, ethanol is the prevalent product in liquid phase, although the amount is significantly lower than that obtained over the Pd/Fe_3O_4 catalyst.

The lower activity of the Pd/C catalyst, if compared with that of Pd/Fe_3O_4, can be correlated to its lower ability to dehydrogenate sorbitol in analogy with a recent report on the use of simple primary and secondary alcohols as H-donor molecules for the transfer hydrogenolysis of benzyl phenyl ether [39].

4.3. Conclusions

The main conclusions, emphasized by the investigation regarding the hydrogenolysis of polyols promoted by the Pd/Fe_3O_4 catalyst, are summarized here below.

The catalytic conversion of biomass-derived glycerol was investigated under both hydrogenolysis and aqueous phase reforming conditions over the bimetallic Pd/Fe_3O_4 catalyst. The starting alternative processes were found to be the dehydration/hydrogenation and the dehydrogenation /decarbonylation with the latter controlled by the initial O–H breaking followed by the β C–H elimination rather than the direct C–C bond cleavage. At 180°C, the C–O bond is preferentially cleaved allowing the production of 1,2-propanediol, while the C–C bond breaking becomes favorable at higher reaction temperatures leading to the formation of H_2 in a good yield.

In analogy, by using ethylene glycol (C_2 polyol) as the starting substrate, both C–O and C–C bonds are equally cleaved at 180 and 210°C, whereas a significant increase in dehydrogenation products is observed at higher temperatures.

Therefore, a change in selectivity in the C–O and C–C bond cleavage of biomass derived C_2–C_3 polyols, on using the Pd/Fe_3O_4 catalyst, is observed by varying the reaction temperature.

In all experiments, CO was never detected in the gas phase products thus revealing an excellent performance of the Pd/Fe_3O_4 catalyst in promoting the water gas shift reaction.

The catalytic conversion of the biomass-deriving sorbitol (C_6 polyol) and C_5-C_3 polyols was investigated under mild hydrogenolysis conditions over the bimetallic Pd/Fe_3O_4 catalyst, exhibiting a higher performance compared to that of the Pd/C catalyst. The hydrogenolysis reactions of C_5-C_3 polyols with the Pd/Fe_3O_4 catalyst were also carried out in order to completely understand the main pathways occurring in the reaction.

The starting reactions were found to be the dehydrogenation/ decarbonylation of the terminal C—COH group and the dehydrogenation followed by the retro-aldol reaction (internal C—C bond cleavage). At the beginning, the sorbitol carbon chain is preferentially shortened leading to xylitol and C_3 or C_4 & C_2 polyols. After the initial cleavage of sorbitol, a series

of cascade reactions (such as H_2/-CO, H_2O/H_2, retro-aldol condensation and hydrogenation) occur, leading to production of shorter diols, alcohols and gaseous products. A similar cascade pattern of reactions leads to the preferential formation of ethanol, at the highest temperature investigated (240°C). With the unique exception of 2,3-butanediol, C_2-C_3 alcohols are the main reaction products obtained by the hydrogenolysis of the investigated substrates suggesting that the co-precipitated Pd/Fe_3O_4 catalyst can be a suitable catalyst for the production of ethanol from bio-derived C_6-C_3 polyols.

Finally, the gas phase analysis, in all experiments, shows the total absence of CO revealing the excellent performance of the Pd/Fe_3O_4 catalyst in promoting the water-gas-shift reaction.

REFERENCES

[1] M. Pagliaro, R. Ciriminna, H. Kimura, M. Rossi, C. Della Pina 'From glycerol to value-added products' *Angew. Chem. Int. Ed.* **2007**, *46*, 4434 – 4440.

[2] J.J. Bozell, G.R. Petersen 'Technology development for the production of biobased products from biorefinery carbohydrates–the US Department of Energy's Top 10 revisited' *Green Chem.* **2010**, *12*, 539–554.

[3] H. Kobayashi, A. Fukuoka 'Synthesis and utilization of sugar compounds derived from lignocellulosic biomass' *Green Chem.* **2013**, 15, 1740–1763.

[4] J.H. Bernas, A. Taskinen, J. Wärnå, D.Y. Murzin 'Describing the inverse dependence of hydrogen pressure by multi-site adsorption of the reactant: Hydrogenolysis of hydroxymatairesinol on a Pd/C catalyst' *J. Mol. Catal. A: Chem.* **2009**, *306*, 33-39.

[5] M.G. Musolino, L.A. Scarpino, F. Mauriello, R. Pietropaolo 'Glycerol hydrogenolysis promoted by supported palladium catalysts' *ChemSusChem* **2011**, *4*, 1143-1150.

[6] R. D. Cortright, R. R. Davda, J. A. Dumesic 'Hydrogen from catalytic reforming of biomass-derived hydrocarbons in liquid water' *Nature* **2002**, *418*, 964-967.

[7] G. W. Huber and J. A. Dumesic 'An overview of aqueous-phase catalytic processes for production of hydrogen and alkanes in a biorefinery' *Catal. Today* **2006**, *111*, 119-132.

[8] N. H. Tran and G. S. K. Kannangara 'Conversion of glycerol to hydrogen rich gas' *Chem. Soc. Rev.* **2013**, *42*, 9454-9479.

[9] F. Mauriello, H. Ariga, M.G. Musolino, R. Pietropaolo, S. Takakusagi, K. Asakura 'Exploring the catalytic properties of supported palladium catalysts in the transfer hydrogenolysis of glycerol' *Appl. Catal. B: Environ.* **2015**, *166–167*, 121–131.

[10] F. Liao, T. W. B. Lo, D. Sexton, J. Qu, C. T. Wu and S. C. E. Tsang 'PdFe nanoparticles as selective catalysts for C–C cleavage in hydrogenolysis of vicinal diol units in biomass-derived chemicals' *Catal. Sci. Technol.* **2015**, *5*, 887-896.

[11] Y. Amada, S. Koso, Y. Nakagawa, K. Tomishige 'Hydrogenolysis of 1,2-propanediol for the production of biopropanols from glycerol' *ChemSusChem* **2010**, *3*, 728-736.

[12] Y.R. Luo *Comprehensive Handbook of Chemical Bond Energies*, CRC Press, Boca Raton, USA, **2007**.

[13] M.K. Weldon, C.M. Friend 'Probing surface reaction mechanisms using chemical and vibrational methods: Alkyl oxidation and reactivity of alcohols on transitions metal surfaces' *Chem. Rev.* **1996**, *96*, 1391-1412.

[14] R.M. Rioux, M.A. Vannice 'Hydrogenation/dehydrogenation reactions: isopropanol dehydrogenation over copper catalysts' *J. Catal.* **2003**, *216*, 362-376.

[15] A. Wawrzetz, B. Peng, A. Hrabar, A. Jentys, A.A. Lemonidou, J.A. Lercher 'Towards understanding the bifunctional hydrodeoxygenation and aqueous phase reforming of glycerol' *J. Catal.* **2010**, *269*, 411-420.

[16] B. Peng, C. Zhao, I. Mejía-Centeno, G.A. Fuentes, A. Jentys, J.A. Lercher 'Comparison of kinetics and reaction pathways for hydrodeoxygenation of C_3 alcohols on Pt/Al$_2$O$_3$' *Catal. Today* **2012**, *183*, 3-9.

[17] Y. Chen, M. Salciccioli, D.G. Vlachos 'An efficient reaction pathway search method applied to the decomposition of glycerol on platinum' *J. Phys. Chem. C* **2011**, *115*, 18707-18720.

[18] M. Salciccioli, W. Yu, M.A. Barteau, J.G. Chen, D.G. Vlachos 'Differentiation of O–H and C–H bond scission mechanisms of ethylene glycol on Pt and Ni/Pt using theory and isotopic labeling experiments' *J. Am. Chem. Soc.* **2011**, *133*, 7996-8004.

[19] G.W. Huber, J.W. Shabaker, S.T. Evans, J.A. Dumesic 'Aqueous-phase reforming of ethylene glycol over supported Pt and Pd bimetallic catalysts' *Appl. Catal. B: Environ* **2006**, *62*, 226-235.

[20] T. Werpy, G. Petersen 'Top value added chemicals from biomass' *1*, **2004**.

[21] M. Besson, P. Gallezot, C. Pinel 'Conversion of biomass into chemicals overmetal catalysts' *Chem. Rev.* **2014**, *114*, 1827–1870.

[22] J. Zhang, J.B. Li, S.B. Wu, Y. Liu 'Advances in the catalytic production and utilization of sorbitol' *Ind. Eng. Chem. Res.* **2013**, *52*, 11799–11815.

[23] Grand View Research–Global Sorbitol Market, **2017**, http://www.grandviewresearch.com/press-release/global-sorbitol-market 2017.

[24] M. Grembecka 'Sugar alcohols–their role in the modern world of sweeteners: a review' *Eur. Food Res. Technol.* **2015**, *241*, 1–14.

[25] J. Lee, Y.T. Kim, G.W. Huber 'Aqueous-phase hydrogenation and hydrodeoxygenation of biomass–derived oxygenates with bimetallic catalysts' *Green Chem.* **2014**, *16*, 708–718.

[26] S. Liu, Y. Okuyama, M. Tamura, Y. Nakagawa, A. Imai, K. Tomishige 'Catalytic conversion of sorbitol to gasoline-ranged products without externalhydrogen over Pt-modified Ir-ReO$_x$/SiO$_2$' *Catal. Today* **2015**, *269*, 122–131.

[27] L. Vilcocq, A. Cabiac, C. Especel, E. Guillon, D. Duprez 'Transformation of sorbitol to biofuels by heterogeneous catalysis: chemical and industrial considerations' *Oil gas sci, Technol. –Rev. d'IFP Energies Nouv.* **2013**, *68*, 841–860.

[28] G.W. Huber, R.D. Cortright, J.A. Dumesic 'Renewable alkanes by aqueous-phase reforming of biomass-derived oxygenates' *Angew. ChemieInt. Ed.* **2004**, *43*, 1549–1551.

[29] A.V. Kirilin, A.V. Tokarev, E.V. Murzina, L.M. Kustov, J.P. Mikkola, D.Y. Murzin 'Reaction products and transformations of intermediates in theaqueous-phase reforming of sorbitol' *ChemSusChem* **2010**, *3*, 708–718.

[30] N. Li, G.W. Huber 'Aqueous-phase hydrodeoxygenation of sorbitol with Pt/SiO$_2$-Al$_2$O$_3$: Identification of reaction intermediates' *J. Catal.* **2010**, *270*, 48–59.

[31] Y.T. Kim, J.A. Dumesic, G.W. Huber 'Aqueous-phase hydrodeoxygenation of sorbitol: a comparative study of Pt/Zr phosphate and PtReO$_x$/C' *J. Catal.* **2013**, *304*, 72–85.

[32] B.M. Moreno, N. Li, J. Lee, G.W. Huber, M.T. Klein 'Modeling aqueous-phase hydrodeoxygenation of sorbitol over Pt/SiO$_2$–Al$_2$O$_3$' *RSC Adv.* **2013**, *3*, 23769–23784.

[33] H. Schiweck, A. Bär, R. Vogel, E. Schwarz, M. Kunz, B. Lüssem, M. Moser, S. Peters *Sugar alcohols* Ullmann's Encyclopedia of Industrial Chemistry, Wiley-VCH Verlag GmbH & Co, Weinheim, **2012**.

[34] C. Espro, B. Gumina, E. Paone, F. Mauriello 'Upgrading lignocellulosic biomasses: Hydrogenolysis of platform derived molecules promoted by heterogeneous Pd-Fe catalysts' *Catalysts* **2017**, *7*, 78.

[35] F. Liao, T.W.B. Lo, S.C.E. Tsang 'Recent developments in palladium-based bimetallic catalysts' *ChemCatChem* **2015**, *7*, 1998–2014.

[36] F. Mauriello, A. Vinci, C. Espro, B. Gumina, M.G. Musolino, R. Pietropaolo 'Hydrogenolysis vs. aqueous phase reforming (APR) of glycerol promoted by a heterogeneous Pd/Fe catalyst' *Catal. Sci. Technol.* **2015**, *5*, 4466-4473.

[37] M.G. Musolino, L.A. Scarpino, F. Mauriello, R. Pietropaolo 'Selective transfer hydrogenolysis of glycerol promoted by palladium catalysts in absence of hydrogen' *Green Chem.* **2009**, *11*, 1511–1513.

[38] J. Liu, B. Sun, J. Hu, Y. Pei, H. Li, M. Qiao 'Aqueous-phase reforming of ethylene glycol to hydrogen on Pd/Fe_3O_4 catalyst prepared by co-precipitation: metal-support interaction and excellent intrinsic activity' *J. Catal.* **2010**, *274*, 287–295.

[39] E. Paone, C. Espro, R. Pietropaolo, F. Mauriello 'Selective arene production from transfer hydrogenolysis of benzyl phenyl ether promoted' *Catal. Sci. Technol.* **2016**, *6*, 7937–7941.

[40] D. Cozzula, A. Vinci, F. Mauriello, R. Pietropaolo, T.E. Müller 'Directing the cleavage of ester CO bonds by controlling the hydrogen availability on the surface of co-precipitated Pd/Fe_3O_4' *ChemCatChem* **2016**, *8*, 1515–1522.

[41] M.G. Musolino, C. Busacca, F. Mauriello, R. Pietropaolo 'Aliphatic carbonyl reduction promoted by palladium catalysts under mild conditions' *Appl. Catal. A Gen.* **2010**, *379*, 77–86.

[42] D. Scholz, C. Aellig, I. Hermans 'Catalytic transfer hydrogenation / hydrogenolysis for reductive upgrading of furfural and 5-(hydroxymethyl) furfural' *ChemSusChem* **2014**, *7*, 268–275.

[43] Y. Hong, H. Zhang, J. Sun, K.M. Ayman, A.J.R. Hensley, M. Gu, M.H. Engelhard, J.S. McEwen, Y. Wang 'Synergistic catalysis between Pd and Fe in gas phase hydrodeoxygenation of m-cresol' *ACS Catal.* **2014**, *4*, 3335–3345.

[44] J. Sun, A.M. Karim, H. Zhang, L. Kovarik, X.S. Li, A.J. Hensley, J.S. McEwen, Y. Wang 'Carbon-supported bimetallic Pd-Fe catalysts for vapor-phase hydrodeoxygenation of guaiacol' *J. Catal.* **2013**, *306*, 47–57.

[45] M.S. Yalfani, S. Contreras, J. Llorca, M. Dominguez, J.E. Sueiras, F. Medina 'Simultaneous in situ generation of hydrogen peroxide and Fenton reactionover PdFe catalysts' *Phys. Chem. Chem. Phys.* **2010**, *12*, 14673–14676.

[46] S. Marx, A. Baiker 'Beneficial interaction of gold and palladium in bimetallic catalysts for the selective oxidation of benzyl alcohol' *J. Phys. Chem. C* **2009**, *113*, 6191–6201.

[47] H. Bernas, A. Taskinen, J. Wärnå, D.Y. Murzin 'Describing the inverse dependence of hydrogen pressure by multi-site adsorption of the reactant: hydrogenolysis of hydroxymatairesinol on a Pd/C catalyst' *J. Mol. Catal. A Chem.* **2009**, *306*, 33–39.

[48] Y. Amada, H. Watanabe, Y. Hirai, Y. Kajikawa, Y. Nakagawa, K. Tomishige 'Production of biobutanediols by the hydrogenolysis of erythritol' *ChemSusChem* **2012**, *5*, 1991–1999.

[49] D.G. Lahr, B.H. Shanks 'Kinetic analysis of the hydrogenolysis of lower polyhydric alcohols: glycerol to glycols' *Ind. Eng. Chem. Res.* **2003**, *42*, 5467–5472.

[50]D.G. Lahr, B.H. Shanks 'Effect of sulphur and temperature on ruthenium-catalyzed glycerol hydrogenolysis to glycols' *J. Catal.* **2005**, *232*, 386–394.

[51] K.L. Deutsch, D.G. Lahr, B.H. Shanks 'Probing the ruthenium-catalyzed higher polyol hydrogenolysis reaction through the use of stereoisomers' *GreenChem.* **2012**, *14*, 1635–1642.

Chapter 5

CONVERSION OF CELLULOSE

5.1. Microcrystalline cellulose and pretreated cellulose

The cellulose used in this work is the microcrystalline cellulose (MCC) having a mean particle size of 51 μm, purchased from Sigma Aldrich, whose x-ray diffraction pattern is reported in Figure 5.1 (black profile).

All the typical reflection peaks for cellulose containing high crystalline degree were observed (Figure 5.1) [1,2].

The opinion concerning the fundamental importance to pretreat the cellulose, in order to reduce the crystallinity degree, making the cellulose more suitable towards the conversion in milder processes, rather than the *un-pretreated* one, is commonly accepted by the scientific community [3-7]. Following this scientific evidence, some aliquots of the microcrystalline cellulose have been mechanically treated within a planetary ball milling, for 3 h at a speed rate of 400 rpm. The XRD pattern of the ball milled cellulose (BMC) is shown in Figure 5.1 (blue profile). At a glance, it is possible to observe the significant structural change occurred after the mechanical pretreatment that consistently increases the amount of amorphous regions in BMC samples.

In particular, the crystallinity index of the MCC and BMC has been calculated through the Segal method, based on the XRD patterns, as described in the section 2.3.1. The microcrystalline cellulose has a crystallinity index of 92%. However, the ball milled cellulose shows a significantly lower crystallinity index of 12%.
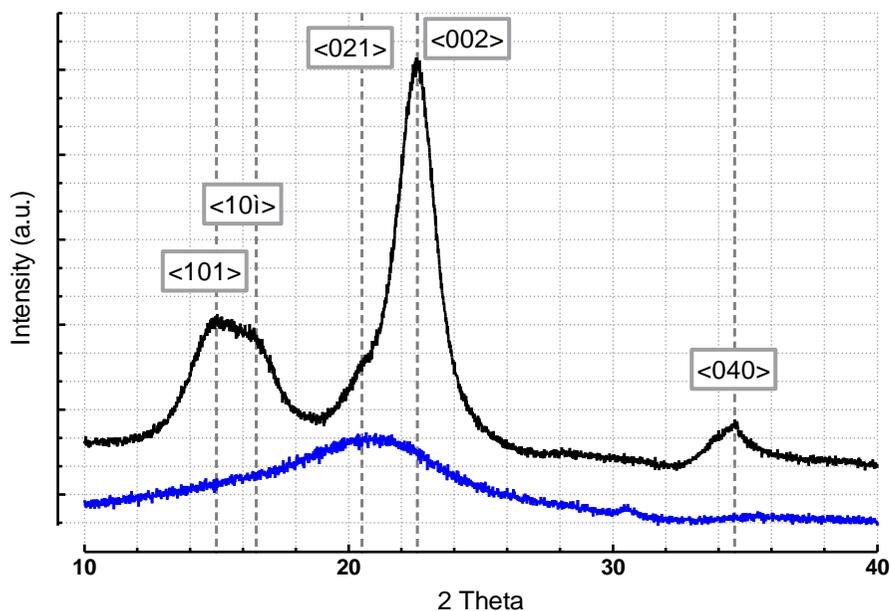
Figure 5.1. Diffraction patterns of microcrystalline cellulose (black profile) and ball milled cellulose (blue profile).

5.2. Hydrogenolysis of Cellulose

The hydrogenolysis of the ball milled cellulose (BMC), pretreated as previously described, was studied in the temperature range of 180-240°C, using a very low initial pressure of H_2 (5 bar), within 24 h of reaction, in presence of the pre-reduced bimetallic Pd/Fe_3O_4 catalyst (Table 5.1, entries 1-3). The hydrogenolysis of BMC reaches a considerable value also at the lowest temperature investigated (i.e. 58.8% at 180°C), and becomes complete when approaches 210°C. As the temperature increases, the product distribution is directed towards the ethanol formation. In particular, ethanol is the main product at 240°C, reaching a molar selectivity of 64.5%. In general, the distribution of products, in liquid phase, is in agreement with the performance observed in the hydrogenolysis of sorbitol and shorter polyols [8, 9], in presence of the same Pd/Fe_3O_4 catalyst. The reaction pattern involves a preliminary dehydrogenation, followed by decarbonylation and retro-aldol reactions, subsequently followed by a series of hydrogenolitic cascade reactions, leading to a high selectivity to ethanol.

Table 5.1. Conversion of ball milled cellulose (BMC) and microcrystalline cellulose (MCC), both in presence and in absence of molecular H_2, promoted by the pre-reduced Pd/Fe$_3$O$_4$ catalyst. *Operating conditions*: 40 mL of water with 4% wt of BMC or MCC, 0.25g of Pd/Fe$_3$O$_4$ catalyst, initial pressure of H_2 or N_2: 5 bar, 180-240°C, 24 h of reaction, within an autoclave of 100mL.

							C6	C5	C4		C3		C2			
Entry	Substr.	Gas	Temp.	Conv.	Liq. Ph	Gas Ph	Sorb	Xyl	1,2-BDO	2,3-BDO	Gly	1,2-PDO	1-PO	EG	EtOH	OP [a]
			[°C]	[%]	[%]	[%]										
1	**BMC**	H_2	180	**58.8**	58.8	0.0	2.6	3.9	14.7	12.1	23.7	21.5	0.0	10.0	10.5	1.0
2	**BMC**	H_2	210	**100.0**	63.0	37.0	0.0	0.5	10.2	7.4	0.4	26.5	0.0	4.5	43.9	6.6
3	**BMC**	H_2	240	**100.0**	50.0	50.0	0.0	0.3	8.0	8.1	0.0	11.6	0.0	1.8	64.5	5.7
4	**MCC**	H_2	180	**23.0**	23.0	0.0	1.0	2.9	12.1	15.8	24.7	23.2	0.0	7.2	10.1	3.0
5	**MCC**	H_2	210	**92.5**	67.6	24.9	0.3	0.8	16.9	10.0	3.2	26.8	0.0	7.0	30.4	4.6
6	**MCC**	H_2	240	**100.0**	50.0	50.0	0.0	0.3	3.9	5.0	0.0	10.1	0.0	6.0	68.7	6.0
7	**MCC**	N_2	180	**21.0**	21.0	0.0	0.5	4.5	12.9	7.2	3.7	36.5	2.2	0.0	27.3	5.2
8	**MCC**	N_2	210	**85.9**	59.6	26.3	0.2	2.2	9.7	4.9	0.5	24.0	17.5	0.9	32.9	7.2
9	**MCC**	N_2	240	**100.0**	41.7	58.3	0.0	0.7	3.8	3.7	0.1	9.6	11.9	0.2	58.4	11.6

Abbreviations: Sorb: sorbitol; Xyl: xylitol; 1,2-BDO: 1,2-butanediol; 2,3-BDO: 2,3-butanediol; Gly: glycerol; 1,2-PDO: 1,2-propanediol; 1-PO: 1-propanol; EG: ethylene glycol; EtOH: ethanol; OP: other products.
[a] Other products, such as: erythritol, oxalic acid, acetic acid and others.

As expected, using the unpretreated microcrystalline cellulose (MCC) as starting material, lower conversions were registered at all investigated temperatures (Table 5.1, entries 4-6).

Therefore, at first instance, it is possible to affirm that through a one-pot process, carried out under neutral conditions, without any further addition of acid or basic reagents, the production of ethanol with a high selectivity, starting from cellulose, is feasible thanks to the reaction pattern activated by the bimetallic Pd/Fe$_3$O$_4$ catalyst.

It is commonly ascertained that one of the main drawbacks of hydrogenolysis processes is closely related to the use of molecular hydrogen, which makes difficult the application of such process, due to economical and safety reasons. In order to overcome the limit linked to the use of molecular H_2, the *un*-pretreated microcrystalline cellulose (MCC), under inert and neutral conditions, was directly processed in presence of the Pd/Fe$_3$O$_4$ catalyst (Table 5.1, entries 7-9). Surprisingly, the results obtained highlight that it is

not necessary to pretreat the cellulose. Indeed, it was reported that water, under the operating conditions, is in a *quasi*-subcritical state (Figure 5.2) [10], favoring the initial hydrolytic step of the cellulose, through the breaking of the glucosidic bonds. In the operating conditions of reaction, water enhances the *auto*-hydrolysis reaction, allowing to obtaining a higher concentration of protonic species that act themselves as pretreatment step, favoring the hydrolysis of cellulose [11-12].
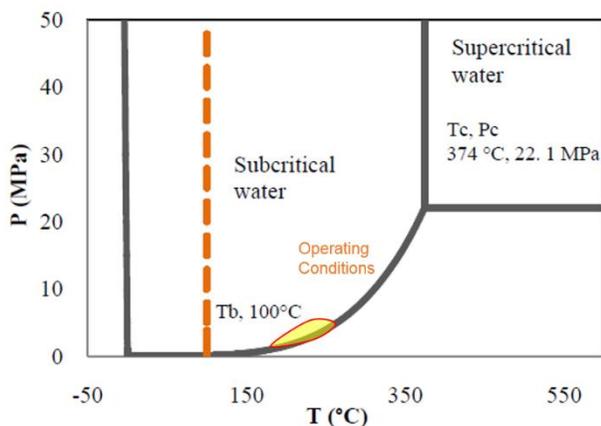
Figure 5.2. Indicative representation of the quasi-subcritical state of water, within the operating conditions adopted during the reaction: T=180 – 240°C; P<50bar.

At temperatures >200°C the effect of the *quasi*-subcritical water becomes higher, therefore considerable conversions are obtained at 210 and 240°C (Table 5.1, entries 8-9). The time effect on the conversion of MCC, at 210 and 240°C, under inert atmosphere, is reported in Tables 5.2 – 5.3.

In agreement with these results, the hydrogen produced from dehydrogenation and/or APR reactions involved in the process, is enough to allow the *self*-sustainability without the addition of any external hydrogen source.

In Figure 5.3 the HPLC chromatograms relative to the conversion of MCC in the same operating conditions (240°C, 5bar N_2, 24h) are compared: in the first case in absence of catalyst and in the second case in presence of the Pd/Fe_3O_4 catalyst. In absence of catalyst the conversion of MCC is 66% and with the Pd/Fe_3O_4 catalyst is 100%. Therefore the role, played by water, in the *quasi*-subcritical state, where the favored *auto*-hydrolysis of water enables the

hydrolysis of MCC, obtaining only glucose, fructose and C_6 polyols, in agreement with the literature [13-15] is certainly highlighted. When the reaction is performed in presence of the Pd/Fe_3O_4 catalyst, besides the full conversion of cellulose, the distribution of products in liquid phase goes towards the formation of C_3-C_4 polyols and C_2-C_3 alcohols, mainly ethanol (Table 5.1, entry 9).
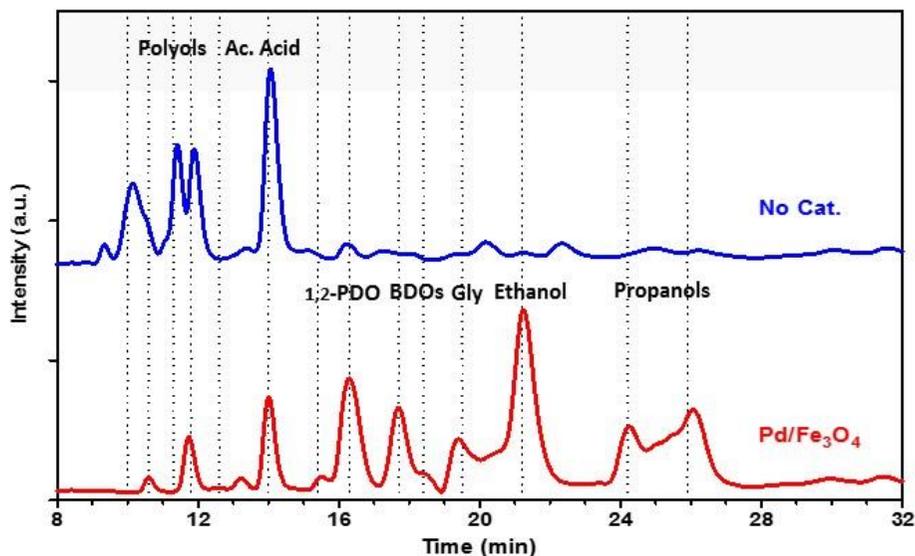
Figure 5.3. Comparison of HPLC chromatograms of MCC conversion at 240°C, initial pressure of N_2: 5bar, 24h of reaction performed in presence of the Pd/Fe_3O_4 catalyst (red profile) or in absence of catalyst (blue profile).

Finally, the reactivity of the bimetallic Pd/Fe_3O_4 catalyst was compared at 240°C, when the selectivity to ethanol is maximized, with benchmark catalysts of monometallic species: Pd/C and Fe_3O_4. As it can be seen from Table 5.4, complete conversion and high selectivity to ethanol is obtained only in presence of the bimetallic catalyst Pd/Fe_3O_4, whereas Pd/C reaches a conversion lower than 80% and a different distribution of products in liquid phase is observed (e.g. acids). Also the Fe_3O_4 shows a scarce reactivity. Therefore, the peculiar reactivity of Pd/Fe_3O_4 catalyst is ascribable to the presence of bimetallic ensembles that act as active phase and are responsible of the pattern of products observed [8].

Table 5.2 Reaction time effect (6-24 h) at 210°C. Conversion of microcrystalline cellulose (MCC) under inert atmosphere, promoted by the pre-reduced Pd/Fe$_3$O$_4$ catalyst. *Operating conditions*: 40 mL of water with 4% wt of MCC, 0.25g of Pd/Fe$_3$O$_4$ catalyst, initial pressure of N$_2$: 5 bar, 210°C, 6-24 h of reaction, within an autoclave of 100mL.

| | | | | Molar Selectivity [%] | | | | | | | | |
| | | | | C5 | C4 | | C3 | | | C2 | | |
Time [h]	Conv. [%]	LiqPh [%]	GasPh [%]	Xyl	1,2-BDO	2,3-BDO	Gly	1,2-PDO	1-PO	EG	EtOH	OP
6	29.4	21.2	8.2	2.3	15.0	0.0	6.3	26.5	5.1	18.2	25.3	1.3
12	52.9	40.4	12.5	2.4	14.2	1.8	2.7	33.1	7.4	0.0	32.8	5.6
24	85.9	59.6	26.3	2.2	9.7	4.9	0.5	24.0	17.5	0.9	32.9	7.4

Abbreviations: Xyl: xylitol; 1,2-BDO: 1,2-butanediol; 2,3-BDO: 2,3-butanediol; Gly: glycerol; 1,2-PDO: 1,2-propanediol; 1-PO: 1-propanol; EG: ethylene glycol; EtOH: ethanol; OP: other products.

Table 5.3. Reaction time effect (1-48 h) at 240°C. Conversion of microcrystalline cellulose (MCC) under inert atmosphere, promoted by the pre-reduced Pd/Fe$_3$O$_4$ catalyst. *Operating conditions*: 40 mL of water with 4% wt of MCC, 0.25g of Pd/Fe$_3$O$_4$ catalyst, initial pressure of N$_2$: 5 bar, 240°C, 1-48 h of reaction, within an autoclave of 100mL.

| | | | | Molar Selectivity [%] | | | | | | | | |
| | | | | C5 | C4 | | C3 | | | C2 | | |
Time [h]	Conv. [%]	LiqPh [%]	GasPh [%]	Xyl	1,2-BDO	2,3-BDO	Gly	1,2-PDO	1-PO	EG	EtOH	OP
1	70.9	70.9	0.0	3.2	7.7	5.1	2.5	20.7	9.6	32.0	9.7	9.5
3	73.4	72.1	1.3	1.5	9.7	5.0	0.2	21.4	14.1	4.5	37.3	6.3
6	93.5	63.0	30.5	1.2	7.5	4.6	0.3	17.7	19.2	2.7	39.4	7.4
12	98.3	53.0	45.3	1.1	4.8	4.3	0.2	10.5	19.7	1.0	50.5	7.9
24	100.0	41.7	58.3	0.7	3.8	3.7	0.1	9.6	11.9	0.2	58.4	11.6
48	100.0	40.0	60.0	1.4	2.0	2.7	0.4	8.3	9.1	0.0	44.3	31.8

Abbreviations: Xyl: xylitol; 1,2-BDO: 1,2-butanediol; 2,3-BDO: 2,3-butanediol; Gly: glycerol; 1,2-PDO: 1,2-propanediol; 1-PO: 1-propanol; EG: ethylene glycol; EtOH: ethanol; OP: other products.

Table 5.4 Comparison of catalysts in the conversion of microcrystalline cellulose (MCC) at 240°C, in absence of molecular H₂. *Operating conditions*: 40 mL of water with 4% wt of MCC, 0.25g of catalyst, initial pressure of N₂: 5 bar, 240°C, 24 h of reaction, within an autoclave of 100mL.

				Molar Selectivity [%]										
				Polyols			C4		C3			C2		
Cat.	Conv.	LiqPh	GasPh	C6 [a]	C5 [b]	C4 [c]	1,2-BDO	2,3-BDO	Gly	1,2-PDO	1-PO	EG	EtOH	OP [d]
	[%]	[%]	[%]											
Pd/C	**78.8**	39.8	39.0	0.5	7.1	7.5	2.7	1.4	1.5	12.3	8.4	3.0	6.5	49.1
Fe₃O₄	**66.5**	27.7	38.8	1.6	11.0	12.6	0.0	3.9	0.0	3.0	0.0	2.5	0.0	65.4
Pd/Fe₃O₄	**100.0**	41.7	58.3	0.0	0.7	0.0	3.8	3.7	0.1	9.6	11.9	0.2	58.4	11.6

Abbreviations. **1,2-BDO**: 1,2-butanediol; **2,3-BDO**: 2,3-butanediol; **Gly**: glycerol; **1,2-PDO**: 1,2-propanediol; **1-PO**: 1-propanol; **EG**: ethylene glycol; **EtOH**: ethanol; **OP**: other products

[a] C6 Sugars: Fructose, Glucose;
[b] C5 Polyols: Xylitol, Adonitol;
[c] C4 Polyols: Erythritol, Erythrose;
[d] Other products, such as acetic acid, aceton and others.

5.3. Conclusions

The reactivity of the co-precipitated bimetallic Pd/Fe_3O_4 catalyst, applied to the conversion of cellulose into short polyols and C_2-C_3 alcohols has been investigated and has demonstrated the possibility to perform the hydrogenolysis of both pretreated (BMC) and unpretreated (MCC) cellulose, also without any external addition of molecular hydrogen.

Indeed, a synergistic effect is played by water (that favors its *auto*-hydrolysis, at the operating conditions, acting as pretreatment and favoring the hydrolytic step) and the Pd/Fe_3O_4 catalyst (that activates the hydrogenolysis and rules the pattern of products obtained). Therefore, the consequent main result is a *self*-sustainable, one-pot hydrogenolysis, leading to a liquid phase mainly constituted by ethanol (58.4-68.7%).

The process is performed under neutral conditions, without any further addition of acids or bases for enhancing the cellulose conversion. Finally, through the comparison of the bimetallic catalyst Pd/Fe_3O_4 with two benchmark catalysts (Pd/C and Fe_3O_4), was revealed the role of the bimetallic ensemble: the main responsible for the peculiar reactivity observed.

REFERENCES

[1] S. Park, J.O. Baker, M.E. Himmel, P.A. Parilla, D.K. Johnson 'Cellulose crystallinity index: measurement techniques and their impact on interpreting cellulase performance' *Biotechnol. Biofuels* **2010**, *3*, 10-20.

[2] N.V. Gromov, O.P. Tarana, I.V. Delidovich, A.V. Pestunov, Y.A. Rodikova, D.A. Yatsenko, E.G. Zhizhina, V.N. Parmon 'Hydrolytic oxidation of cellulose to formic acid in the presence of Mo-V-P heteropoly acid catalysts' *Catal. Tod.* **2016**, *278*, 74-81.

[3] L.S. Ribeiro, J.J.M. Órfão, M.F.R. Pereira 'Enhanced direct production of sorbitol by cellulose ball-milling' *Green Chem.* **2015**, *17*, 2973–2980.

[4] A. Shrotri, H. Kobayashi, A. Fukuoka 'Cellulose depolymerization over heterogeneous catalysts' *Acc. Chem. Res*. **2018**, *51*, 761–768.

[5] M. Yabushita, H. Kobayashi, A. Fukuoka 'Catalytic transformation of cellulose into platform chemicals' *Appl. Catal. B Environ* **2014**, *145*, 1-9.

[6] M.H.L. Silveira, A.R.C. Morais, A.M. da Costa Lopes, D.N. Olekszyszen, R. Bogel-Łukasik, J. Andreaus, L. Pereira Ramos 'Current pretreatment technologies for the development of cellulosic ethanol and biorefineries' *ChemSusChem* **2015**, *8*, 3366 – 3390.

[7] A.K. Kumar, S. Sharma 'Recent updates on different methods of pretreatment of lignocellulosic feedstocks: a review' *Bioresour. Bioprocess.* **2017**, *4*, 7.

[8] B. Gumina, F. Mauriello, R. Pietropaolo, S. Galvagno, C. Espro 'Hydrogenolysis of sorbitol into valuable C_3-C_2 alcohols at low H_2 pressure promoted by the heterogeneous Pd/Fe_3O_4 catalyst' *Mol. Catal.* **2018**, *446*, 152-160.

[9] F. Mauriello, A. Vinci, C. Espro, B. Gumina, M.G. Musolino, R. Pietropaolo 'Hydrogenolysis vs. aqueous phase reforming (APR) of glycerol promoted by a heterogeneous Pd/Fe catalyst' *Catal. Sci. Technol.* **2015**, *5*, 4466-4473.

[10] F.P. Cardenas-Toro, S.C. Alcazar-Alay, T. Forster-Carneiro, M.A.A. Meireles 'Obtaining oligo- and monosaccharides from agro-industrial and agricultural residues using hydrothermal treatments' *Food and Public Health* **2014**, *4*, 123-139.

[11] F. Carvalheiro, L.C. Duarte, F.M. Gìrio 'Hemicellulose biorefineries: a review on biomass pretreatment' *J. Sci. Ind. Res.* **2008**, *67*, 849-864.

[12] A. Romero, D.A. Cantero, A. Nieto-Márquez, C. Martínez, E. Alonso, M.J. Cocero 'Supercritical water hydrolysis of cellulosic biomass as effective pretreatment to catalytic production of hexitols and ethylene glycol over Ru/MCM-48' *Green Chem.* **2016**, *18*, 4051–4062.

[13] M. Sasaki, Z. Fang, Y. Fukushima, T. Adschiri, K. Arai 'Dissolution and hydrolysis of cellulose in subcritical and supercritical water' *Ind. Eng. Chem. Res.* **2000**, *39*, 2883-2890

[14] M. Sasaki, B. Kabyemela, R. Malaluan, S. Hirose, N. Takeda, T. Adschiri, K. Arai 'Cellulose hydrolysis in subcritical and supercritical water' *J. Supercrit. Fluids* **1998**, *13*, 261–268.

[15] T. Sakaki, M. Shibata, T. Miki, H. Hirosue, N. Hayashi 'Reaction model of cellulose decomposition in near-critical water and fermentation of products' *Biores. Technol.* **1996**, *58*, 197-202.

Chapter 6

CONVERSION OF CELLULOSE USING *H*-DONOR MOLECULES

6.1. Introduction to the approach

With the aim to convert directly the cellulose into C_3-C_2 alcohols, through a one pot process, the hydrogenolysis promoted by the Pd/Fe_3O_4 catalyst was investigated. The hydrogenolysis traditionally uses water as solvent and high pressure molecular hydrogen to break C-C, C-O, O-H bonds presents several drawbacks. Therefore, it is worth to investigate the possibility to use less conventional sources of hydrogen, like some molecules which furnish hydrogen through a dehydrogenation process, commonly called hydrogen donor (H-donor) molecules.

In particular, the present investigation is focused on the study of performance of limonene and 2-propanol used as H-donor for the direct conversion of cellulose into short chain alcohols.

Limonene is an interesting bio-derivable molecule, from waste orange peels, and is gaining increasing attention for its valuable products and possible applications [1]. Furthermore, limonene is a molecule with a consistent ability to give, through dehydrogenation, p-cymene and hydrogen (two products with added value) [2, 3]. Therefore, the aim is to investigate a process based on the reaction of two bio-derivable reagents, cellulose and limonene, in order to obtain high value added products from their respective sustainable conversion.
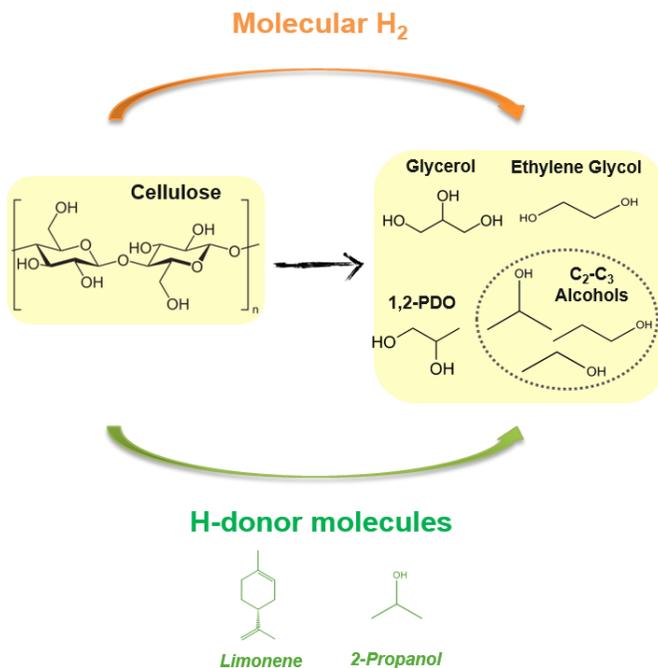
Figure 6.1 Schematic representation of the approach pursued to perform the cellulose conversion through a less conventional route, using H-donor molecules: limonene and 2-propanol.

2-Propanol is a C_3 alcohol that, through dehydrogenation, produces acetone, and it is well known in organic chemistry as H-donor molecule. Recently, Fukuoka and co-workers, for the first time, applied 2-propanol as source of hydrogen for the conversion of cellulose into C_6 sugars (i.e. sorbitol and mannitol), using Ru-based catalysts [4].

6.2. Conversion of cellulose in presence of limonene

The whole reaction pattern that can start from limonene, including all obtainable products, is depicted in Figure 6.2 [2, 5-7]. In principle, limonene can undergo four types of reactions, such as (i) *isomerization* into terpinenes (α-terpinene and γ-terpinene) and α-terpinolene, where products maintain two insaturation sites, like limonene; (ii) *hydrogenation* into menthenes (p-menth-1-ene and p-menth-3-ene) and through further hydrogenation menthanes (*trans*-p-menthane and *cis*-p-menthane); (iii) *dehydrogenation* into

the aromatic p-cymene; (iv) *disproportionation* into menthanes and p-cymene.
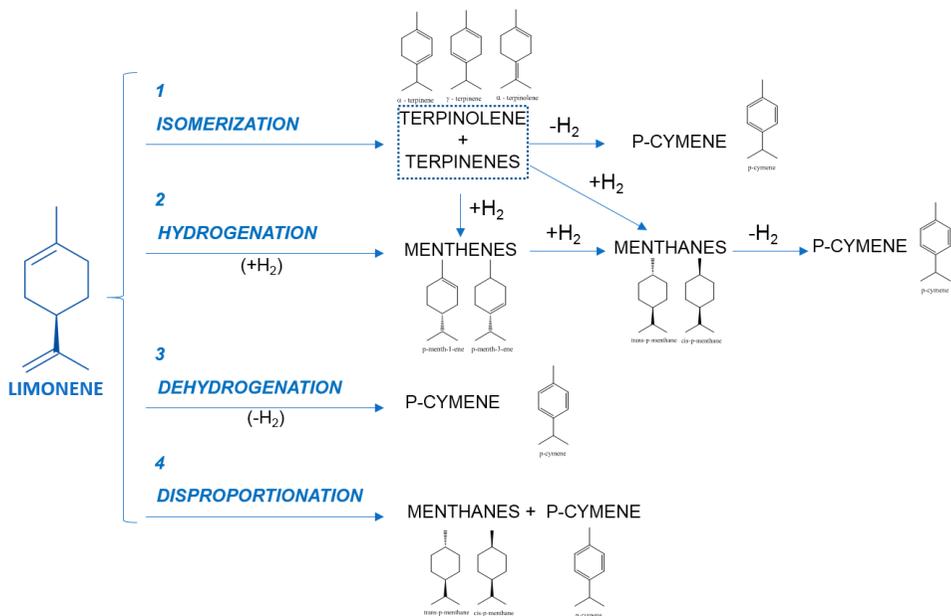
Figure 6.2 Summary of reactions and products obtainable from limonene.

At the beginning of the work, the co-precipitated bimetallic Pd/Fe_3O_4 and commercial Pd/C and Ru/C systems were used for an initial screening of limonene reactivity under inert atmosphere and results referring to *every* catalyst used are summarized in Table 6.1.

Both Pd-based catalysts, Pd/Fe_3O_4 and Pd/C, showed full conversion and the disproportionation reaction (Figure 6.3) rules the reaction pattern, with a selectivity of ca. 70% into p-cymene, within the temperature range investigated (180-240°C). Whilst Ru/C showed a different product distribution, which gives dehydrogenation (48.5% p-cymene) and isomerization (18.9% terpinolene and 32.6% phellandrene), and a significantly inferior reactivity, because at the highest temperature investigated (240°C) the conversion reached only 26.7%, assessing that Ru/C has not a great fitting toward the conversion of limonene.

The first significant evidence is the possibility to convert a bulk liquid solution of limonene into an organic solution containing the 70% of the valuable product p-cymene.

Table 6.1 Conversion of limonene promoted by Pd/Fe₃O₄, Pd/C and Ru/C catalysts. *Operating conditions*: 30 mL of limonene, 0.19g of catalyst, initial pressure of N₂: 5 bar, 180-240°C, 24 h of reaction, within an autoclave of 75mL.

Catalyst	Temp [°C]	Conv. [%]	Molar Selectivity of Products from limonene [%]			
			P-Cymene (3)[a]	Terpinolene (2)	Phellandrene (2)	P-Menthane (0)
Pd/Fe₃O₄	180	100.0	67.5	0.0	0.0	32.5
	240	100.0	69.6	0.0	0.0	30.4
Pd/C	180	98.9	70.0	0.0	5.2	24.8
	240	100.0	68.3	0.0	0.0	31.7
Ru/C	240	26.7	48.5	18.9	32.6	0.0

[a] The number reported in brackets indicates the amount of insaturations present within the referring molecule.

Subsequently, the effect of the reaction time on the conversion of limonene at 180 and 240°C, again under inert atmosphere, has been investigated in order to understand the reaction pattern change within 24 h, in presence of both Pd/Fe₃O₄ (Table 6.2) and Pd/C (Table 6.3) catalysts. The Pd/Fe₃O₄ system is certainly more active than Pd/C, since its conversion is complete also at the lowest temperature investigated and at the shorter reaction time (3 h). Also the pattern of reactions does not change significantly, showing a systematic selectivity of ca. 70% into p-cymene. Analogously, Pd/C doesn't show any appreciable variation in its product distribution. Only slightly lower conversion values are detected at 180°C, revealing a scarcer reactivity in comparison with the bimetallic catalyst.
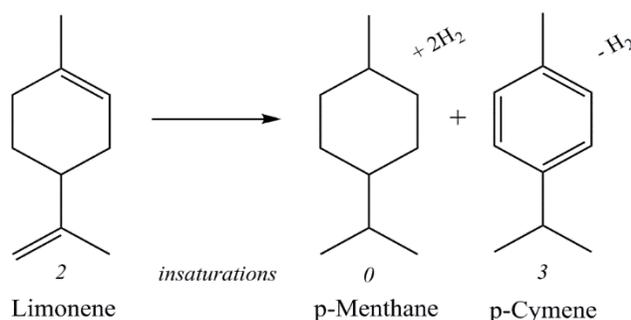

Figure 6.3 Disproportionation reaction of limonene leads the formation of p-cymene and p-menthane.

Table 6.2 Time effect relative to the conversion of limonene promoted by Pd/Fe$_3$O$_4$ catalyst. *Operating conditions*: 30 mL of limonene, 0.19g of Pd/Fe$_3$O$_4$ catalyst, initial pressure of N$_2$: 5 bar, 180-240°C, 3-24 h of reaction, within an autoclave of 75mL.

Temp. [°C]	Time [h]	Conv. [%]	Molar Selectivity of Products from limonene [%]			
			P-Cymene (3)	Terpinolene (2)	Phellandrene (2)	P-Menthane (0)
180	3	100	68.7	0.0	2.4	28.9
180	6	100	68.6	0.0	2.0	29.4
180	24	100	67.5	0.0	0.0	32.5
240	3	100	70.2	0.0	9.4	20.4
240	6	100	70.2	0.0	9.4	20.4
240	24	100	69.6	0.0	0.0	30.4

Table 6.3 Time effect relative to the conversion of limonene promoted by Pd/C catalysts. *Operating conditions*: 30 mL of limonene, 0.19g of Pd/C catalyst, initial pressure of N$_2$: 5 bar, 180-240°C, 3-24 h of reaction, within an autoclave of 75mL.

Temp [°C]	Time [h]	Conv. [%]	Molar Selectivity of Products from limonene [%]			
			P-Cymene (3)	Terpinolene (2)	Phellandrene (2)	P-Menthane (0)
180	3	97.7	72.5	0.0	15.0	12.5
180	24	98.9	70.0	0.0	5.2	24.8
240	3	100	89.4	0.0	0.0	10.6
240	6	100	67.3	0.0	0.0	32.7
240	24	100	68.3	0.0	0.0	31.7

When 4% wt of the unpretreated cellulose (microcrystalline cellulose, MCC) is added to a bulk solution of limonene, under inert atmosphere at 240°C, within 24 h of reaction, in presence of the bimetallic Pd/Fe$_3$O$_4$ catalyst,

a conversion value of 67% of cellulose can be observed. On the other hand, when the reaction is performed in presence of Pd/C catalyst only a conversion of 35.4% is registered (Table 6.4). At the same time, the limonene pathway and product distribution remains unchanged.

It is worth to underline that the conversion of cellulose implies the disappearance of the solid amount of the polymer (and through the gravimetric method the conversion degree is calculated, as explained in § 2.6) but it was not possible to identify the products in which cellulose should be converted. Indeed, in Figure 6.4 is schematized the procedure followed to analyze both solid and liquid phases, obtained after the reaction. In particular, the treatment of the organic liquid phase, containing both products derived from limonene and those obtained from cellulose (unknown), in order to be safely analyzed through the gas chromatographic technique, was consistently diluted. Therefore, products derived from limonene have been determined without any problem, but products formed from cellulose, whose concentration is significantly lower than those deriving from limonene, are impossible to be individuated. Extraction with an aqueous phase of the bulk organic liquid solution does not give any result by using the HPLC technique, probably due to the low concentration. Alternatively, it could be possible that cellulose, being in an apolar medium like limonene may be degraded, probably thanks to the high temperature of reaction, into oligomer products, that are not detectable through HPLC measurements.

However, the conversion of cellulose in such conditions shouldn't be only a thermal effect of degradation, because the catalyst surely plays some role since the conversion values, at the same temperature, are significantly different when the catalytic system is changed: 67% (Pd/Fe$_3$O$_4$), 45.4% (Ru/C), 35.4% (Pd/C) and 30% (in absence of catalyst). Again, the role of the bimetallic Pd/Fe$_3$O$_4$ catalyst has to be highlighted.

Table 6.4 Conversion of MCC in presence of an organic solution of limonene, promoted by Pd/Fe₃O₄, Pd/C and Ru/C catalysts. *Operating conditions*: 30 mL of limonene with 4% wt of MCC, 0.19g of catalyst, initial pressure of N₂: 5 bar, 180-240°C, 24 h of reaction, within an autoclave of 75mL.

| Catalyst	Temp [°C]	$X_{Cellulose}$ [%]	$X_{Limonene}$ [%]	Molar Selectivity of Products from limonene [%]			
				P-Cymene (3)	Terpinolene (2)	Phellandrene (2)	P-Menthane (0)
Pd/Fe₃O₄	180	3.5	100.0	68.1	0.0	0.5	31.4
	240	67.0	100.0	71.0	0.0	1.0	28.0
Pd/C	180	0.0	100.0	68.0	0.0	0.0	32.0
	240	35.4	100.0	74.1	0.0	12.2	13.7
Ru/C	180	0.0	6.1	57.1	42.9	0.0	0.0
	240	45.4	28.1	51.0	26.2	22.8	0.0
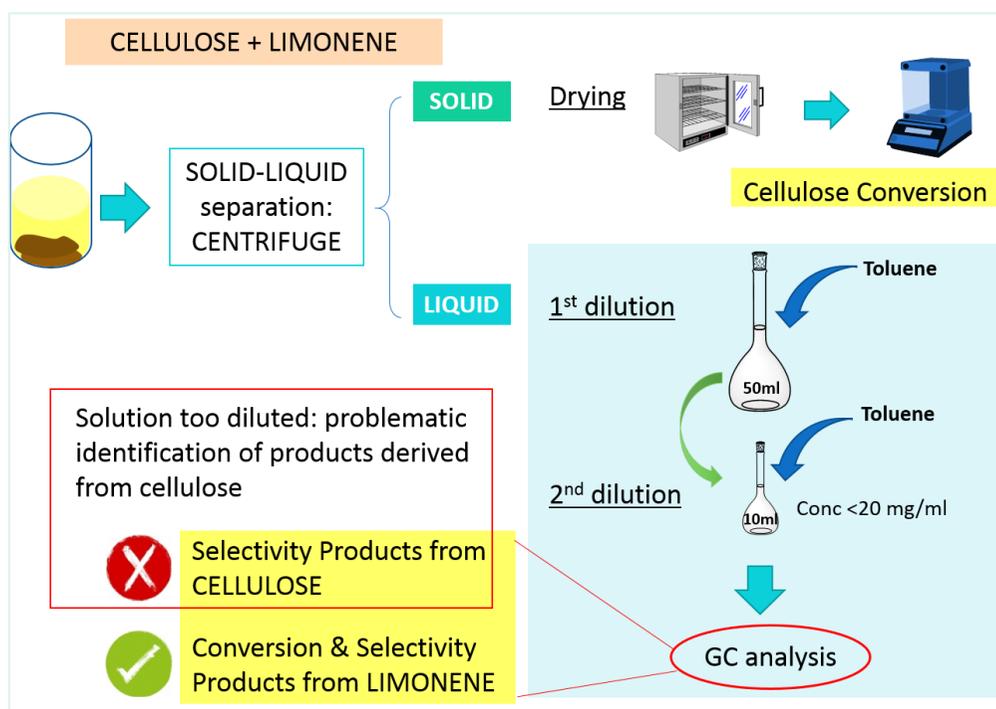
Figure 6.4 Schematic description of the post reaction treatment of solid and liquid phases obtained from reactions performed by using a mixture of bulk limonene and 4% wt of MCC, promoted by catalysts.

Furthermore, when the conversion of cellulose is carried out in a biphasic mixture of limonene and water, an interfacial contact occurs during the reaction, enabling to vehicle the aqueous phase water-soluble products deriving from cellulose reactions. The post reaction treatment of solid and liquid (both organic and aqueous phases) are illustrated in Figure 6.5. Here it is indicated that the analytical identification of products obtained both from the organic phase of limonene and the aqueous phase deriving from cellulose have been identified through GC and HPLC measurements, respectively.
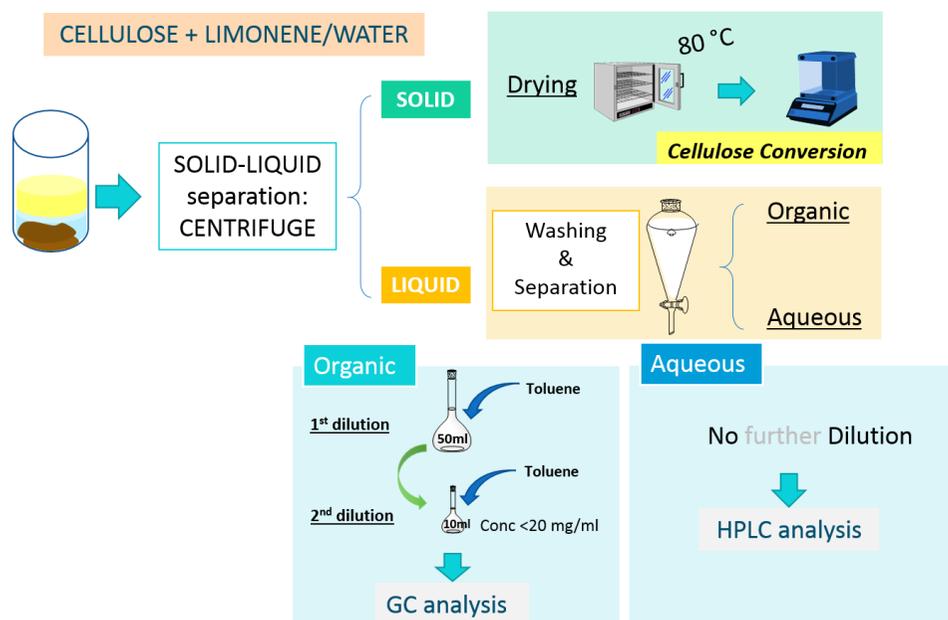

Figure 6.5 Schematic description of the post reaction treatment of solid and liquid phases obtained from reactions performed by using biphasic 50% vol limonene/water mixture and 4% wt of MCC, promoted by catalysts.

Results obtained performing the conversion of MCC in presence of the biphasic mixture of limonene and water at 50% vol, are summarized in Table 6.5. Conversion and selectivity related to limonene and its derived products, have not been reported because their values remain identical to those previously reported (Tables 6.1 and 6.4). For what the catalytic conversion of cellulose is concerned, the highest conversion value (85%) was obtained at 240°C when the reaction was promoted by the bimetallic Pd/Fe_3O_4 catalyst and the products distribution shows a consistent selectivity to ethanol (56%), analogously to that observed when the reaction was performed entirely in water (see § 5.2).

It is worth to underline the possibility to obtain, from this biphasic process, two products with high added value, such as p-cymene from limonene and ethanol from cellulose, considering that both starting materials can be wastes from agricultural and food industries. Furthermore, two valuable products can be directly obtained, at the same time, within the two different liquid phases, easily separable: p-cymene (ca. 70%) in the organic phase and ethanol (ca. 60%) in the aqueous one.

When the process is promoted by the Pd/C catalyst lower conversion values are observed (17,4% at 180°C and 72% at 240°C) and a different product distribution leads, at higher temperature to organic acids with short carbon chain, generally reported as other products. A lower temperature 24.5% of 1,2-propanediol, followed by 16% of xylitol can be obtained.

Conversion and product distribution promoted by the Ru/C catalyst are not particularly interesting (Table 6.5).

Table 6.5 Conversion of MCC in presence of biphasic mixture of 50% vol limonene/water, promoted by Pd/Fe$_3$O$_4$, Pd/C and Ru/C catalysts. *Operating conditions*: 30 mL of limonene/water (50% vol) with 4% wt of MCC, 0.19g of catalyst, initial pressure of N$_2$: 5 bar, 180-240°C, 24 h of reaction, within an autoclave of 75mL.

Cat	Temp	X$_{Cellulose}$	Molar Selectivity of Products from Cellulose [%]								
			C6	C5	C4		C3			C2		
	[°C]	[%]		Xyl	Eryth	BDOs	Gly	1,2-PDO	EG	EtOH	OP
Pd/Fe	180	**31.5**	1.0	1.4	1.3	25.2	11.5	19.6	9.3	20.8	9.9
	240	**84.9**	0.7	1.3	1.1	12.9	2.2	1.0	5.3	56.1	19.4
Pd/C	180	**17.4**	4.3	16.1	0.0	13.3	1.3	24.6	1.9	11.0	27.5
	240	**72.2**	1.6	1.8	4.6	10.1	0.3	2.6	15.2	5.8	58.0
Ru/C	180	**24.9**	12.8	11.1	4.0	8.1	1.1	18.9	2.6	2.2	39.2
	240	**77.9**	5.3	3.4	2.9	7.3	0.0	3.0	0.0	25.6	52.5

6.3. Conversion of cellulose using 2-propanol

In this paragraph the investigation regarding the behavior of 2-propanol, as hydrogen source, is summarized.

The Pd/Fe_3O_4 catalyst has been chosen as reference catalyst because it showed the best performance in all reactions previously investigated. In this case the investigation starts from sorbitol (C_6 polyol), in order to have a preliminary idea about the role of 2-propanol in presence of water played in the conversion of cellulosic bio-derivable molecules.

When a bulk solution of 2-propanol is used as H-source in presence of 4% wt of sorbitol and Pd/Fe_3O_4 as catalyst (Table 6.6), the conversion of sorbitol is complete at every temperature investigated (210 and 240°C), whereas the selectivity is mainly oriented towards 1,2-propanediol (31.7 and 30.2%) and ethanol (35.9 and 37%), respectively C_3 diol and C_2 alcohol. No significant changes have been found upon increasing the temperature, except for the conversion of the bulk 2-propanol that increases from 14% (210°C) to ca. 28% (240°C).

However, when water is added at the liquid mixture of 2-propanol (50% vol), a significant variation in the distribution of products is observed, obtaining a selectivity of ca. 50% into ethanol, in analogy to the result previously obtained on using 100% water as reaction medium (Table 6.7).

Table 6.6 Conversion of sorbitol in presence of a 2-propanol bulk liquid phase, promoted by Pd/Fe_3O_4 catalysts. *Operating conditions*: 30 mL of 2-propanol with 4% wt of sorbitol, 0.19g of Pd/Fe_3O_4 catalyst, initial pressure of N_2 5 bar, 210-240°C, 24 h of reaction, within an autoclave of 75mL.

	Temp [°C]	$X_{2\text{-}PO}$ [%]	$X_{Sorbitol}$ [%]	C4 2,3-BDO	C3 1,2-BDO	Gly	1,2-PDO	1-PO	C2 EG	EtOH	OP
2-PO	210	14.1	100	6.8	2.3	3.4	31.7	0.0	11.0	35.8	9.0
100%	240	27.9	100	4.4	7.5	1.0	30.2	13.5	5.8	37.0	0.6

Table 6.7 Conversion of sorbitol promoted by Pd/Fe₃O₄ catalysts, varying the composition of the liquid mixture: 2-propanol 100%, 50% and 0% (remaining is water). *Operating conditions*: 30 mL of 2-propanol (100%) or a mixture of 2-propanol/water (50% vol) with 4% wt of sorbitol, 0.19g of Pd/Fe₃O₄ catalyst, initial pressure of N_2: 5 bar, 240°C, 24 h of reaction, within an autoclave of 75mL.

| | | | | Molar Selectivity of Products from Cellulose [%] | | | | | | | |
| | Temp | $X_{2\text{-}PO}$ | $X_{Sorbitol}$ | C4 | | C3 | | | C2 | | |
2-PO	[°C]	[%]	[%]	2,3-BDO	1,2-BDO	Gly	1,2-PDO	1-PO	EG	EtOH	OP
100%	240	27.9	100	4.4	7.5	1.0	30.2	13.5	5.8	37.0	0.6
50%	240	26.8	100	3.0	5.7	1.0	23.0	5.1	6.1	49.8	6.3
0% [*]	240	-	100	2.8	0.0	0.0	5.9	13.0	0.0	63.5	14.8

[*] Data obtained in water, already reported in Table 4.5.

A variation is observed when the process is carried out using the microcrystalline cellulose as reagent substrate. As reported in Table 6.8, a conversion of cellulose (ca. 4% at 210°C and ca. 36% at 240°C) was found, but no products were detected through HPLC measurements. The lack of detection of products, may be ascribable to the lack of polarity necessary to break the cellulose into short chain products (from C₆ hexitols to shorter products) detectable on HPLC instrument. Again, it is plausible to assume that cellulose is degraded into oligomers. In order to corroborate the theory that the lack of sufficient polarity of reaction solvent does not allow the cleavage of C-C and C-O bonds, water was added to 2-propanol in the reaction medium (Table 6.9). When only 25% vol of water was added to 2-propanol, a significant conversion of cellulose (93% at 240°C, either in presence of 25%vol or 50%vol of water) carries out to short diols and alcohols. A higher amount of 2-propanol (75%vol) favors the formation of 1-propanol (C₃ alcohol) and ethanol (C₂ alcohol) in comparable amounts. When there is an equivalent amount in volume of 2-propanol and water, the main products become 1,2-propanediol (C₃ diol) and ethanol. Finally, when the process is performed entirely in water, the main product become only ethanol. The composition of the reacting liquid mixture seems to play a clear role to

determine the reaction pathway and therefore the nature of obtained products.

Table 6.8 Conversion of MCC in presence of a 2-propanol bulk liquid phase, promoted by Pd/Fe_3O_4 catalysts. *Operating conditions*: 30 mL of 2-propanol with 4% wt of MCC, 0.19g of Pd/Fe_3O_4 catalyst, initial pressure of N_2: 5 bar, 210-240°C, 24 h of reaction, within an autoclave of 75mL.

| | Temp | X_{2-PO} | $X_{Cellulose}$ | Molar Selectivity of Products from Cellulose [%] | | | | | | | |
| | | | | C4 | | C3 | | | C2 | | |
	[°C]	[%]	[%]	2,3-BDO	1,2-BDO	Gly	1,2-PDO	1-PO	EG	EtOH	OP
2-PO 100%	210	10.8	3.9	-	-	-	-	-	-	-	-
	240	27.9	35.9	-	-	-	-	-	-	-	-

Table 6.9 Conversion of MCC promoted by Pd/Fe_3O_4 catalysts, varying the composition of the liquid mixture: 2-propanol 100%, 75%, 50% and 0% (remaining is water). *Operating conditions*: 30 mL of liquid mixture with 4%wt of MCC, 0.19g of Pd/Fe_3O_4 catalyst, initial pressure of N_2: 5 bar, 240°C, 24 h of reaction, within an autoclave of 75mL.

| | Temp | X_{2-PO} | $X_{Cellulose}$ | Molar Selectivity of Products from Cellulose [%] | | | | | | | |
| 2-PO | | | | C4 | | C3 | | | C2 | | |
	[°C]	[%]	[%]	2,3-BDO	1,2-BDO	Gly	1,2-PDO	1-PO	EG	EtOH	OP
100%	240	27.9	35.9	-	-	-	-	-	-	-	-
75%	240	23.7	93.2	0.0	0.0	1.8	13.5	31.9	7.3	33.0	12.5
50%	240	20.0	93.0	0.0	0.0	1.0	31.8	19.6	6.4	27.3	13.9
0% [*]	240	-	100	3.7	3.8	0.1	9.6	11.9	0.2	58.4	11.6

[*] Data obtained in water, already reported in Table 5.1, entry 9.

6.4. Conclusions

This chapter, dedicated to the evaluation of the possibility to use hydrogen donor (H-donor) molecules (such as limonene and 2-propanol), as source of hydrogen to convert cellulose, permits to summarize the conclusions reported here below.

Dehydrogenation of limonene into p-cymene, which is a valuable product required in several industrial fields, is efficiently promoted through both Pd-based catalysts (Pd/Fe$_3$O$_4$ and Pd/C) obtaining full conversion of a bulk solution of limonene, with a ca. 70% selectivity into p-cymene.

When a biphasic mixture of limonene and water (50% vol) is used to convert microcrystalline cellulose, at 240°C it is possible to obtain from each phase a high added value product: (i) p-cymene (ca. 70%) from the organic phase and (ii) ethanol (ca. 56%) from the aqueous phase.

In the case in which a 4% wt of microcrystalline cellulose is put into a bulk limonene organic phase, in presence of the bimetallic Pd/Fe$_3$O$_4$ catalyst, was reached the highest conversion of cellulose (67%) occurs. However, it was not possible to detect cellulose deriving products.

Several evidences have been highlighted from the use of 2-Propanol.

First of all, 2-propanol enables to perform the full conversion of sorbitol and mainly 1,2-propanediol and ethanol are obtained. Therefore, 2-propanol - in the transfer hydrogenolysis of sorbitol - acts as H-donor molecule driving the selectivity into C$_3$ products, while the presence of water favors the C$_2$ alcohol formation.

The presence of water plays a crucial role to enable the hydrogenolysis and to obtain products with a short carbon chain. Therefore, 2-propanol may be a hydrogen source for the cellulose, only in presence of water. Besides, using cellulose as starting molecule, the prevailing formation of C$_3$ products in presence of high amounts of 2-propanol was observed.

REFERENCES

[1] R. Ciriminna, M. Lomeli-Rodriguez, P. Demma Carà, J.A. Lopez-Sanchez, M. Pagliaro 'Limonene: a versatile chemical of the bioeconomy' *Chem. Commun.* **2014**, *50*, 15288-15296.

[2] A.F. Thomas, Y. Bessière 'Limonene' *Natural Products Reports* **1989**, *6*, 291-309.

[3] J. Zhang, C. Zhao 'Development of a bimetallic Pd-Ni/HZSM-5 catalyst for the tandem limonene dehydrogenation and fatty acid deoxygenation to alkanes and arenes for use as biojet fuel' *ACS Catal.* **2016**, *6*, 4512–4525.

[4] H. Kobayashi, H. Matsuhashi, T. Komanoya, K. Hara, A. Fukuoka 'Transfer hydrogenation of cellulose to sugar alcohols over supported ruthenium catalysts' *Chem. Commun.* **2011**, *47*, 2366–2368.

[5] H. Cui, J. Zhang, Z. Luo, C. Zhao 'Mechanisms into dehydroaromatization of bioderived limonene to p-cymene over Pd/HZSM-5 in the presence and absence of H_2' *RSC Adv.* **2016**, *6*, 66695–66704.

[6] G. Rubulotta, K.L. Luska, C.A. Urbina-Blanco, T. Eifert, R. Palkovits, E. A. Quadrelli, C. Thieuleux, W. Leitner 'Highly selective hydrogenation of R-(+)-limonene to (+)-p-1-menthene in batch and continuous flow reactors' *ACS Sustainable Chem. Eng.* **2017**, *5*, 3762–3767.

[7] E. Bogel-Łukasik, R. Bogel-Łukasik, M. Nunes da Ponte 'Pt- and Pd-catalysed limonene hydrogenation in high-density carbon dioxide' *Monatsh Chem* **2009**, *140*, 1361–1369.

Chapter 7

FINAL CONCLUSIONS

In this doctoral work, the performance of the co-precipitated bimetallic Pd/Fe$_3$O$_4$ catalyst has been investigated for the conversion of biomass-derivable molecules, starting from model molecules, such as C$_6$-C$_2$ polyols and, finally, cellulose. Mild operating conditions, the presence and the absence of molecular hydrogen, and the feasibility to use other molecules, as hydrogen donors, have been investigated.

The physico-chemical and the structural properties of the co-precipitated Pd/Fe$_3$O$_4$ catalyst have been characterized through XRD, TEM, H$_2$-TPR, XPS and EXAFS measurements. These techniques highlight the presence of highly dispersed palladium nanoparticles on the support, revealing a majority of particles having an average diameter of 1.2 nm. The existence of a strong metal-support interaction (SMSI) that enables the promoting effect played by palladium in the reduction of hematite to magnetite has been ascertained. Intimate interactions between palladium nanoparticles and the iron oxide support are present and the existence of Pd-Fe bimetallic ensembles on the surface of the reduced Pd/Fe$_3$O$_4$ catalyst has been confirmed.

The catalytic conversion of biomass-derived glycerol (C$_3$ polyol) both under hydrogenolysis and aqueous phase reforming conditions, over the bimetallic Pd/Fe$_3$O$_4$ catalyst, has been investigated. The starting processes were found to be the dehydration/hydrogenation and the dehydrogenation /decarbonylation with the latter controlled by the initial O–H breaking followed by β C–H elimination rather than direct C–C bond cleavage. At

180°C, the C–O bond breaking is preferentially cleaved allowing the production of 1,2-propanediol, while C–C bond breaking becomes favorable at higher reaction temperatures leading to formation of H_2 in a good yield.

Similarly, when ethylene glycol (C_2 polyol) is the starting substrate, the C–O and C–C bonds are equally cleaved at 180 and 210°C, whereas at higher temperatures a significant increase in dehydrogenation products has been observed.

Starting from C_2-C_3 polyols, the change in selectivity from the C–O to the C–C bond cleavage is better appreciable upon the variation of the reaction temperature.

The hydrogenolysis of sorbitol (C_6 polyol) and C_5-C_3 polyols has been investigated under mild operating conditions (using only 5 bar of initial H_2) promoted by the bimetallic Pd/Fe_3O_4 catalyst, exhibiting a higher performance compared to that of the commercial Pd/C catalyst. With the aim to gain a complete understanding of the main pathways involved in the process catalyzed by Pd/Fe_3O_4, the screening regarding the hydrogenolysis of C_5-C_3 polyols have also been performed.

The starting reactions were found to be the dehydrogenation/ decarbonylation of the terminal C–COH group and the dehydrogenation followed by the retro-aldol reaction (internal C–C bond cleavage). At the beginning, the sorbitol carbon chain is preferentially shortened leading to xylitol and C_3 or C_4-C_2 polyols. After the initial cleavage, a series of cascade reactions occurs (such as H_2/-CO, H_2O/H_2, retro-aldol condensation and hydrogenation), leading to the production of shorter diols, alcohols and gaseous products. A similar cascade pattern of reactions leads to the preferential formation of ethanol, at the highest temperature investigated (240°C). C_2-C_3 alcohols, in particular ethanol, are the main reaction products obtained by the hydrogenolysis of the investigated substrates, suggesting that the co-precipitated Pd/Fe_3O_4 catalyst can be suitable for the production of ethanol from bio-derived C_6-C_3 polyols.

Furthermore, the gaseous phase analysis, in all experiments concerning polyols, shows the total absence of CO, revealing the excellent performance of the Pd/Fe_3O_4 catalyst in promoting the water gas shift (WGS) reaction.

The subsequent investigation of cellulose to be transformed directly into short polyols and C_2-C_3 alcohols, in a one-pot process, through the use of Pd/Fe$_3$O$_4$ catalyst has been carried out.

Within this investigation it was demonstrated the possibility to perform the hydrogenolysis of unpretreated (MCC) cellulose and not only the pretreated one. Moreover, the hydrogenolysis process was found *self*-sustainable, being performable also without any external addition of molecular hydrogen.

A synergistic effect played by water, used as solvent, and the Pd/Fe$_3$O$_4$ catalyst was found. Water, through its *auto*-hydrolysis, acts as a pretreatment favouring the initial hydrolytic step of cellulose; whereas the Pd/Fe$_3$O$_4$ catalyst activates the hydrogenolysis reaction and rules the pattern of products obtained as ascertained by the reactivity already reported on using C_6-C_3 polyols. Blank tests of C_6-C_3 polyols in absence of catalyst show no reactivity, whilst the same blank test starting from cellulose have shown the role of water as promoter of hydrolysis into glucose and C_6 sugars.

The outstanding result of this investigation is the feasibility of a one pot *self*-sustainable hydrogenolysis starting from cellulose not pretreated, leading a liquid phase mainly constituted by ethanol (58.4-68.7%). This process is performable under neutral conditions, without any further addition of acid or basic substance in order to enhance the conversion.

The role of the bimetallic ensemble of palladium and iron present on the catalytic surface is the main responsible for the peculiar reactivity observed. Such evidence has been demonstrated through the comparison of the reactivity of the bimetallic catalyst Pd/Fe$_3$O$_4$ with two benchmark catalysts (Pd/C and Fe$_3$O$_4$).

The last part of the research concerns the possibility to use, instead of molecular hydrogen, other hydrogen-donor (H-donor) molecules to convert the cellulose into short chain alcohols. In particular, the present investigation was focused also on the reactivity of limonene and 2-propanol as H-donor substrates.

Pd-based catalysts (Pd/C and Pd/Fe$_3$O$_4$) have been confirmed very active towards the dehydrogenation of limonene into p-cymene, enabling to obtain

full conversion of a bulk solution of limonene, with a ca. 70% selectivity into p-cymene.

Moreover, the Pd/Fe_3O_4 catalyst is able to perform, at the same time, the dehydrogenation of limonene into p-cymene and the de-polymerization of the cellulose. Indeed, when a biphasic mixture of limonene and water (50% vol) is used to convert microcrystalline cellulose, at 240°C it is possible to obtain from each phase a high added value product: (i) p-cymene (ca. 70%) from the organic phase and (ii) ethanol (ca. 56%) from the aqueous phase.

When a 4% wt of microcrystalline cellulose is put into a bulk limonene organic phase, in presence of the bimetallic Pd/Fe_3O_4 catalyst, the highest conversion of cellulose (67%) was reached even though it was difficult to clarify the nature of the involved transformations.

Several evidences have been highlighted from the application of 2-propanol.

First of all, 2-propanol enables to convert completely sorbitol in a solution containing mainly 1,2-propanediol and ethanol. Therefore, 2-propanol acts as H-donor molecule with sorbitol. The presence of 2-propanol increases the selectivity into C_3 products, while the presence of water favors the C_2 alcohol formation.

2-Propanol can act as H-donor molecule for the conversion of cellulose, only in presence of water. The preliminary results obtained, highlighted that when the reaction is performed with 2-propanol, the conversion level is lower, but the selectivity into C_3 products becomes higher.

In any case, the presence of water has revealed its crucial importance to enable the cellulose hydrolysis and in general a successful conversion into valuable products. Therefore, 2-propanol may be a hydrogen source for the cellulose, only in presence of water. In analogy with sorbitol, using cellulose as starting molecule, the prevailing formation of C_3 products in presence of higher amounts of 2-propanol can be observed.

Other activities

SCIENTIFIC PRODUCTION

Reverse chronological order

B. Gumina, F. Mauriello, C. Espro, S. Galvagno, P.J.C. Hausoul, R. Palkovits
Conversion of cellulose by using sustainable H-donor molecules, promoted by Pd/Fe₃O₄ catalyst
Manuscript in preparation

B. Gumina, C. Espro, S. Galvagno, R. Pietropaolo, F. Mauriello
Bio-ethanol production from unpretreated cellulose under neutral *self*-sustainable hydrolysis/hydrogenolysis conditions promoted by the heterogeneous Pd/Fe₃O₄ catalyst (Communication)
Angewandte Chemie Int. Ed. **2018**, *Manuscript submitted*

C. Espro, **B. Gumina**, T. Szumelda, E. Paone, F. Mauriello
Catalytic transfer hydrogenolysis as an effective tool for the reductive upgrading of cellulose, hemicellulose, lignin and their derived platform molecules *(Review)*
Catalysts **2018**, *8* (8), 313 DOI: 10.3390/catal8080313

B. Gumina, F. Mauriello, R. Pietropaolo, S. Galvagno, C. Espro
Hydrogenolysis of sorbitol into valuable C3-C2 alcohols at low H₂ pressure promoted by the heterogeneous Pd/Fe₃O₄ catalyst *(Full paper)*
Molecular Catalysis **2018**, *446*, 152-160 DOI: 10.1016/j.mcat.2017.12.038

C. Espro, **B. Gumina**, E. Paone, F. Mauriello

Upgrading lignocellulosic biomasses: Hydrogenolysis of platform derived molecules promoted by heterogeneous Pd-Fe catalysts *(Review)*
 Catalysts **2017**, *7*(3), 78 **DOI: 10.3390/catal7030078**

F. Mauriello, A. Vinci, C. Espro, **B. Gumina**, M.G. Musolino, R. Pietropaolo

Hydrogenolysis vs. aqueous phase reforming (APR) of glycerol promoted by a heterogeneous Pd/Fe catalyst *(Full paper)*
Catalysis Science & Technology **2015**, *5*, 4466-4473 **DOI: 10.1039/c5cy00656b**

SCIENTIFIC PRODUCTION 1ST PAGE

Reverse chronological order

catalysts

MDPI

Catalytic Transfer Hydrogenolysis as an Effective Tool for the Reductive Upgrading of Cellulose, Hemicellulose, Lignin, and Their Derived Molecules

Claudia Espro [1], Bianca Gumina [1], Tomasz Szumelda [2], Emilia Paone [3] and Francesco Mauriello [3,*]

1 Dipartimento di Ingegneria, Università di Messina, Contrada di Dio–Vill. S. Agata, I-98166 Messina, Italy; espro@unime.it (C.E.); bianca.gumina@unime.it (B.G.)
2 Jerzy Haber Institute of Catalysis and Surface Chemistry, Polish Academy of Sciences, Niezapominajek 8, 30-239 Krakow, Poland; ncszumel@cyf-kr.edu.pl
3 Dipartimento DICEAM, Università Mediterranea di Reggio Calabria, Loc. Feo di Vito, I-89122 Reggio Calabria, Italy; emilia.paone@unirc.it
* Correspondence: francesco.mauriello@unirc.it; Tel.: +39-0965-169-2278

check for updates

Abstract: Lignocellulosic biomasses have a tremendous potential to cover the future demand of bio-based chemicals and materials, breaking down our historical dependence on petroleum resources. The development of green chemical technologies, together with the appropriate eco-politics, can make a decisive contribution to a cheap and effective conversion of lignocellulosic feedstocks into sustainable and renewable chemical building blocks. In this regard, the use of an indirect H-source for reducing the oxygen content in lignocellulosic biomasses and in their derived platform molecules is receiving increasing attention. In this contribution we highlight recent advances in the transfer hydrogenolysis of cellulose, hemicellulose, lignin, and of their derived model molecules promoted by heterogeneous catalysts for the sustainable production of biofuels and biochemicals.

Keywords: lignocellulosic biomasses; H-donor molecules; hydrogenolysis; catalytic transfer hydrogenolysis reactions; heterogeneous catalysis; cellulose; hemicellulose; lignin; glycerol; polyols; furfural; levulinic acid; aromatic ethers

1. Introduction

The hegemony of fossil resources is declining by now. In the last few decades, industrial chemistry has accepted the challenge for the sustainable production of chemicals and energy by using renewable biomasses as starting supplies [1]. Moreover, the changes in consumer attitudes towards "green" products, as well as government initiatives for sustainable development programs and regulations, are surely the key driving factors for the development of the bio-based chemical industries and refineries [2–6].

While many criticisms have been raised towards the first generation of bio-energies and biofuels since they are in direct competition with human and animal food, reducing the land availability [7], we have recently achieved significant progress in the production of chemical building blocks and intermediates from lignocellulosic wastes and residues [8–20]. This is because their use in the chemical industry presents several advantages including: (i) the production of less toxic by-products and lower environmental risks, (ii) the reduction of CO_2 emissions, (iii) a minor dependence on fossil resources and/or foreign commodities, and (iv) the use of indigenous raw materials that can add value in many agriculture products or processes.

Hydrogenolysis of sorbitol into valuable C3-C2 alcohols at low H_2 pressure promoted by the heterogeneous Pd/Fe$_3$O$_4$ catalyst

Bianca Gumina[a], Francesco Mauriello[b,*], Rosario Pietropaolo[b], Signorino Galvagno[a], Claudia Espro[a,*]

[a] Dipartimento di Ingegneria, Università di Messina, Contrada di Dio–Vill. S. Agata, I-98166 Messina, Italy
[b] Dipartimento DICEAM, Università Mediterranea di Reggio Calabria, Loc. Feo di Vito, I-89122 Reggio Calabria, Italy

ABSTRACT

The hydrogenolysis of sorbitol and various C5-C3 polyols (xylitol; erythritol; 1,2- 1,4- and 2,3-butandiol; 1,2-propandiol; glycerol) have been investigated at low molecular hydrogen pressure (5 bar) by using Pd/Fe$_3$O$_4$, as heterogeneous catalyst and water as the reaction medium. Catalytic experiments show that the carbon chain of polyols is initially shortened through dehydrogenation/decarbonylation and dehydrogenation/retro-aldol mechanisms followed by a series of cascade reactions that include dehydrogenation/decarbonylation and dehydration/hydrogenation processes. At 240 °C, sorbitol is fully converted into lower alcohols with ethanol being the main reaction product in liquid phase.

© 2017 Elsevier B.V. All rights reserved.

1. Introduction

In the last decade, a growing attention has been devoted to the production and the utilization of bio-sugars and bio-alcohols obtainable from renewable cellulose, hemicellulose and lignin (the main fractions of lignocellulosic biomasses) [1,2]. To this regard, cellulose and hemicellulose derived sorbitol (C6 polyol), xylitol (C5 polyol) and glycerol (C3 polyol) have been inserted in the list of top 12 biomass-based building blocks [3–5] representing key renewable resources for modern biorefineries.

With a global market expected to overcome 2.3 Mt/year, sorbitol is attracting intense industrial and research interests [6,7]. At present, it is mainly produced by hydrogenation of glucose [5,6,8] (easily obtained by the hydrolysis of cellulose [9–15]) and largely used in pharmaceutical, food and cosmetic industries [16]. Moreover, it has been proposed as building block for production

of biofuels, chemicals [17–19] and renewable hydrogen (through aqueous-phase reforming reactions–APR) [17,20–24]. Xylitol (C5 polyol) is commonly produced by catalytic hydrogenation of xylose as well as from the hydrogenation of hemicellulose and it is widely applied as sweetener and inhibitor for the development of bacteria in foods [16,25]. Erythritol (C4 polyol) is the main starting substrate for the synthesis of butanediols (BDOs), that are widely employed as precursors of polyester resins, polyurethanes and polymers such as polybutylene-terephthalate (PBT) [16,25]. Glycerol (C3 polyol) is cheaply available in continuously growing quantities, being the main by-product in bio-diesel production. The selective hydrogenolysis of glycerol can lead to 1,2-propanediol (1,2-PDO), that is a useful compound in several industrial fields [4]. The shortest polyol is ethylene glycol (EG, C2 polyol), which is typically used as antifreeze agent and as a precursor of polyesters, such as polyethylene terephthalate (PET) and polyethylene-naphthalate (PEN). Catalytic epoxidation of ethylene is presently the main technology applied in the production of EG, although industrial processes to obtain it directly from cellulose are in continuous development [1]. Among others, a valuable desirable product from

* Corresponding authors.
E-mail addresses: francesco.mauriello@unirc.it (F. Mauriello),
claudia.espro@unime.it (C. Espro).

Upgrading Lignocellulosic Biomasses: Hydrogenolysis of Platform Derived Molecules Promoted by Heterogeneous Pd-Fe Catalysts

Claudia Espro [1], Bianca Gumina [1], Emilia Paone [2] and Francesco Mauriello [2,*]

[1] Dipartimento di Ingegneria, Università di Messina, Contrada di Dio Vill. S. Agata, I-98166 Messina, Italy; espro@unime.it (C.E.); bianca.gumina@unime.it (B.G.)

[2] Dipartimento DICEAM, Università Mediterranea di Reggio Calabria, Loc. Feo di Vito, I-89122 Reggio Calabria, Italy; emilia.paone@unirc.it

* Correspondence: francesco.mauriello@unirc.it; Tel.: +39-0965-1692278

Abstract: This review provides an overview of heterogeneous bimetallic Pd-Fe catalysts in the C–C and C–O cleavage of platform molecules such as C2–C6 polyols, furfural, phenol derivatives and aromatic ethers that are all easily obtainable from renewable cellulose, hemicellulose and lignin (the major components of lignocellulosic biomasses). The interaction between palladium and iron affords bimetallic Pd-Fe sites (ensemble or alloy) that were found to be very active in several sustainable reactions including hydrogenolysis, catalytic transfer hydrogenolysis (CTH) and aqueous phase reforming (APR) that will be highlighted. This contribution concentrates also on the different synthetic strategies (incipient wetness impregnation, deposition-precipitaion, co-precipitaion) adopted for the preparation of heterogeneous Pd-Fe systems as well as on the main characterization techniques used (XRD, TEM, H_2-TPR, XPS and EXAFS) in order to elucidate the key factors that influence the unique catalytic performances observed.

Keywords: heterogeneous catalysis; palladium; iron; iron oxides; bimetallic catalysts; cellulose; polyols; hemicellulose; furfural; lignin; phenol derivatives; aromatic ethers; hydrogenolysis; hydrodeoxygenation (HDO); catalytic transfer hydrogenolysis (CTH); aqueous phase reforming (APR)

1. Introduction

Modern chemical industry is facing the big challenge of overcoming its historical dependence on fossil resources by reconciling the economic recovery with the protection of environment and the reduction of greenhouse gas emissions. At the 21st United Nations Climate Change Conference (COP21), 195 nations agreed on a global action plan aimed to limit the global warming below 2 °C above pre-industrial levels. The "Paris Agreement" comes into force on the 4th November 2016 and is expected to be a new course in the global climate effort [1].

To achieve this ambitious goal, several countries are releasing new green economy strategies. USA have launched the "National Bioeconomy Blueprint Program" addressing five strategic objectives able to generate economic growth and to meet societal needs [2]. Accordingly, the EU has set a "Bioeconomy Strategy and Action Plan" [3–5] identifying, under the Framework Programme for Research and Innovation in Europe—Horizon 2020, seven priority challenges in research and innovation that can have a tangible effect on everyday life [6]. Asian countries, also due to their high growth rate of population, will be decisive for the development of sustainable biotechnologies, bio-industries and bio-refineries [7–9]. With the world population approaching about 9.6 billion by 2050 and limited natural reserves, the use of renewable resources is therefore essential for the sustainable supply of

Catalysis Science & Technology

ROYAL SOCIETY OF CHEMISTRY

PAPER

Hydrogenolysis *vs.* aqueous phase reforming (APR) of glycerol promoted by a heterogeneous Pd/Fe catalyst†

Francesco Mauriello,*[a] Alessandro Vinci,[a] Claudia Espro,[b] Bianca Gumina,[b] Maria Grazia Musolino[a] and Rosario Pietropaolo[a]

The hydrogenolysis and the aqueous phase reforming of glycerol have been investigated under mild reaction conditions, using water as the reaction medium and Pd/Fe as the catalyst. The experiments, in the presence of added H_2 or under inert atmosphere, clearly show that the dehydration/hydrogenation route is the key step in the case of C–O bond cleavage (hydrogenolysis) while dehydrogenation is a prerequisite for C–C bond breaking (APR), with the latter favoured at higher reaction temperatures. The temperature dependence of the C–C and C–O bond rupture is discussed by taking into account the bond energies involved in the competitive hydrogenolysis and APR reactions. Finally, the Pd/Fe catalyst was also tested in the hydrogenolysis and APR of ethylene glycol in the same temperature range, with the aim of clarifying the selective cleavage of C–O and C–C bonds in biomass derived C_2–C_3 polyols.

Introduction

Growing attention has been gained on the use of renewable biomass for bulk chemical production.[1,2]

Glycerol, the main byproduct from the production of biodiesel, is one of the top 12 building block chemicals largely used as bio-feedstocks for the production of chemical products.[3,4] Due to the worldwide expansion of biofuels, at present the production of glycerol has reached over 2 million tonnes that consistently enter the market every year.[5] This unique situation has made glycerol attractive as a renewable starting material for the synthesis of valuable chemicals.

The conversion of biomass into chemicals and fuels commonly implies oxygen removal. In this context, the selective hydrogenolysis of glycerol has gained more and more attention, leading to the formation of propylene diols, ethylene glycol and propanols.[6,7] Considerable research effort has been directed towards the conversion of glycerol into 1,2-propanediol (1,2-PDO), which is a high demand chemical, largely used in the production of unsaturated polyester resins, functional fluids, food products, cosmetics and pharmaceuticals.[8] Currently, the industrial production of 1,2-propanediol mainly occurs through the route of propylene oxide hydration. Therefore, glycerol hydrogenolysis to 1,2-propanediol represents a sustainable alternative process that would assist both the environmental benefits and economic viability of biodiesel manufacture.

At the same time, the production of hydrogen through the aqueous-phase reforming (APR) of biomass-derived polyols is considered as a promising catalytic process.[9–14] Glycerol is an interesting starting substrate for "bio"-hydrogen production since the related process becomes spontaneous at much lower temperature than that generally used today for H_2 manufacture from CH_4. An ideal catalyst for H_2 production from glycerol needs to be very active both for C–C bond breaking as well as in promoting the water gas shift (WGS) reaction thus reducing the CO content.

Furthermore, H_2 – generated *in situ* by the aqueous phase reforming of glycerol – has been successfully used for the conversion of glycerol to 1,2-PDO, representing an interesting alternative to the direct use of molecular hydrogen.[15–18]

Hydrogenolysis and APR reactions involve the breaking of C–C, C–H, C–O and O–H bonds, therefore glycerol can also be considered as a model compound for fundamental studies involving the selective cleavage of chemical bonds of biomass derived substrates.

Heterogeneous palladium catalysts were found to be poorly efficient for the hydrogenolysis of biomass derived polyols.[6,7] However, in past years, the coprecipitated Pd/Fe catalyst has been deeply investigated[19–26] for its superior performance in several catalytic reactions including the hydrogenolysis[20,21] and the transfer hydrogenolysis (CTH) of glycerol using 2-propanol as the reaction solvent,[22,23] as well as

[a] *Dipartimento DICEAM, Università Mediterranea di Reggio Calabria, Loc. Feo di Vito, I-89122 Reggio Calabria, Italy. E-mail: francesco.mauriello@unirc.it; Tel: (+39) 09651692278*
[b] *Dipartimento DIECII, Università di Messina, Contrada di Dio, 1 - Vill. S. Agata, I-98166 Messina, Italy*
† Electronic supplementary information (ESI) available. See DOI: 10.1039/c5cy00656b

ATTENDANCE AT CONFERENCES

Reverse chronological order

XI National Congress AICIng
Bologna, Italy
9th – 12nd September **2018**
Oral Speech
Conversione della cellulosa mediante utilizzo di molecole 'H-donor'
B. Gumina

255th American Chemical Society National Meeting
New Orleans, USA
18th - 22nd March **2018**
Oral Speech
Sustainable bio-ethanol production from crystalline cellulose promoted by Pd/Fe$_3$O$_4$ catalyst
B. Gumina, F. Mauriello, C. Espro, R. Pietropaolo and S. Galvagno

13rd Europacat Congress on Catalysis
Florence, Italy
27th - 31st August **2017**
Poster
Sustainable Bio-Ethanol production from Crystalline Cellulose promoted by the Pd/Fe$_3$O$_4$ catalyst
B. Gumina, F. Mauriello, C. Espro, S. Galvagno and R. Pietropaolo

VII National Workshop AICIng
Milan, Italy
12nd - 13rd June **2017**
Oral Speech
Bio-Ethanol production from the Crystalline Cellulose promoted by the heterogeneous Pd/Fe$_3$O$_4$ catalyst
B. Gumina, F. Mauriello, C. Espro, S. Galvagno and R. Pietropaolo

X National Congress AICIng
Udine, Italy
11st - 14th September **2016**
Oral Speech
Conversione del sorbitolo in prodotti ad alto valore aggiunto in condizioni blande mediante catalizzatore bimetallico Pd/Fe
B. Gumina, F. Mauriello, C. Espro, S. Galvagno and R. Pietropaolo

International Congress on Catalysis (ICC)
Beijing, China
3rd - 8th July **2016**
Poster
Conversion of biomass derived sorbitol into high value products under mild reaction conditions promoted by bimetallic Pd/Fe catalysts
 B. Gumina, F. Mauriello, C. Espro, S. Galvagno and R. Pietropaolo

SCICASI Congress
Catanzaro, Italy
3rd – 4th December **2015**
Oral Speech
Conversion of sorbitol biomass derived under mild reaction conditions promoted by Pd/Fe catalyst
B. Gumina, F. Mauriello, C. Espro, S. Galvagno and R. Pietropaolo

AWARDS

VII National Workshop AICIng
Milan, Italy, 12nd - 13rd June **2017**
Awarded as one of the best scientific oral speech
Bio-Ethanol production from the Crystalline
Cellulose promoted by the heterogeneous Pd/Fe$_3$O$_4$
catalyst
B. Gumina, F. Mauriello, C. Espro, S. Galvagno and
R. Pietropaolo

ATTENDANCE AT DOCTORAL SCHOOLS

1st International School of Process Chemistry
Gargnano (BS), Italy
26th - 29th March **2017**

3rd SINCHEM Doctorate Winter School
Bologna, Italy
15th - 17th February **2016**

EUROPEAN MOBILITY

Visiting PhD student for one year (1st May 2017 - 30th April 2018), under the scientific supervision of **Prof. R. Palkovits** at the '*Institut für Technische und Makromolekulare Chemie*' (ITMC) of the RWTH Aachen University, Germany.